

**DESIGN OF AN AIR COOLED REFRIGERATION SYSTEM
OPERATING AT VARYING CONDENSING PRESSURE.**

Michael Sigalas

**A Thesis
in
The Faculty
of
Engineering**

**Presented in Partial Fulfillment of the Requirements
for the degree of Master of Engineering at
Concordia University
Montreal, Quebec, Canada**

April 1979

© Michael Sigalas, 1979

ABSTRACT

DESIGN OF AN AIR COOLED REFRIGERATION SYSTEM OPERATING AT VARYING CONDENSING PRESSURE.

MICHAEL SIGALAS

Contrary to current industrial practice a modified air-cooled outdoor refrigeration system was designed to operate at varying condensing pressures. It allowed the condensing pressure to drop proportionally with the ambient outdoor temperature until some point at which any further reduction in condensing pressure would result in a reduction of refrigeration capacity and or poor expansion valve control.

Tests of the modified system revealed that as the condensing pressure was lowered, the refrigeration capacity increased, the power consumption decreased and the coefficient of performance increased. When conditions dictated control of condensing pressure, the condensing pressure control system acted to stabilize that pressure although the ambient temperature continued to fall.

Equations developed to predict refrigeration capacity, power consumption and coefficient of performance showed very close correlation with experimental data and represent a great improvement over equations used presently. Their use makes prediction of system performance with a variety of refrigerants possible.

ACKNOWLEDGEMENTS

The author wishes to express his gratitude and deep appreciation to his supervisors, Dr. S. Lin and Dr. G.D. Xistris. In addition the author is deeply indebted to Messrs. John Elliot and Tom Dugdale for their technical assistance.

Special thanks are also due to Prestcold (North America) Ltd. for providing equipment used for the experiment, and Penn-Johnson Controls Co. for building the prototype controls used.

TABLE OF CONTENTS

	<u>PAGE</u>
Abstract	1
List of Figures	11
Nomenclature	vi
Chapter 1. Introduction	1
Chapter 2. Modified outdoor air-cooled refrigeration system design	5
2.1 The expansion valve problem	6
2.2 Condensing pressure control system	11
Chapter 3. Theoretical analysis	18
3.1 Reciprocating compressor performance	18
3.1.1 Compressor volumetric efficiency	20
3.1.2 Compression efficiency	24
3.1.3 System coefficient of performance	30
3.2 Computer program predicting system performance	31
Chapter 4. Experimental set-up and test procedure	34
4.1 Modified Refrigeration system	35
4.2 Chamber cooling system	41
4.3 Test procedure	43
Chapter 5. Data reduction and discussion	54
Chapter 6. Conclusions	64
References	67
Appendix <u>I</u> Computer program listing	86
Appendix <u>II</u> Modified refrigeration system	104
Appendix <u>III</u> Chamber cooling system design	110

LIST OF FIGURES

<u>FIGURE</u>		<u>PAGE</u>
1	T-S diagram of ideal refrigeration cycle	70
2	Basic component arrangement of actual refrigeration cycle	70
3	Ideal refrigeration cycle at high and low condensing pressure	71
4	Cross-section of typical thermostatic expansion valve	72
5	Schematic diagram of thermostatic expansion valve operation	72
6	Balanced port thermostatic expansion valve schematic	73
7	Differential pressure control schematic diagram	73
8	Conventional refrigeration system using condensing pressure control valve	74
9	Conventional condensing pressure control valve	74
10	Modified condensing pressure control valve	75
11	P-V diagram of ideal vapor compression cycle	76
12	Indicator diagram of refrigeration compressor	76
13	Overall layout of experimental set-up	77
14	Modified refrigeration test system schematic	78
15	Chamber cooling system schematic	79
16	Experimental and theoretical refrigeration capacity curves	80
17	Experimental and theoretical power consumption	81
18	Experimental and theoretical coefficient of performance	82

PAGE

19	Theoretical volumetric and compression efficiencies	83
20	Modified test system pressure recording	84
21	Modified test system pressure recording	85
22	Modified test system pressure recording	86

APPENDIX

A1	Test unit watt meter connection	109
A2	Wiring diagram of modified test system	110
A3	Chamber cooling system compressor-condenser balancing; system 2	112
A4	Chamber cooling system compressor-condenser-evaporator balancing; system 2	113
A5	Chamber cooling system operation envelope; system 2	114
A6	Chamber cooling system compressor-condenser balancing; system 1	115
A7	Chamber cooling system compressor-condenser-evaporator balancing; system 1	116
A8	Chamber cooling system operation envelope; system 1	117
A9	Wiring schematic of chamber cooling system	118

NOMENCLATURE

A_o	area of expansion valve orifice, ft^2 , (cm^2)
A	compressor valve port area, ft^2 , (cm^2)
A_s	expansion valve orifice for summer operation or suction valve port area, ft^2 , (cm^2)
A_w	expansion valve orifice for winter operation, ft^2 , (cm^2)
A_d	discharge valve port area, ft^2 , (cm^2)
b_p	brake power
C	clearance volume ratio
C_{eff}	effective clearance volume ratio
C_d	discharge coefficient
COP	coefficient of performance
F	force, lbf , (Nt)
G_d	drag coefficient
G_1, G_2	constants
g_c	conversion constant
h	enthalpy, Btu/lbm , (Joules/Kg)

k	spring coefficient
K_1, K_2, K	constants in compression efficiency equation
L	length on indicator card representing compressor swept volume, ft, (cm).
L_2	length on indicator card representing compressor discharge volume, ft, (cm)
\dot{m}	mass flow rate through expansion valve, lbm/hr , (Kg/hr)
m_g	mass induced during suction, lbm , (kg)
m_c	clearance volume mass, lbm , (kg)
MEP	mean effective pressure
n	polytropic exponent of compression and expansion process
P	pressure, lb_f/ft^2 , (Pa)
P_D	pressure difference to overcome valve drag force, lb_f/ft^2 , (Pa)
P_t	pressure difference to overcome valve throttling pressure drop, lb_f/ft^2 , (Pa)
q	volume flow rate, ft^3/hr , (cm^3/hr)
Q_{9-8}	refrigeration capacity, Btu/hr , (Joules/hr)

R_c	compression ratio
R_o	compression ratio obtained from blanked suction test
T	temperature, $^{\circ}\text{F}$, ($^{\circ}\text{C}$)
thp	theoretical power
v	specific volume, ft^3/lbm , (cm^3/Kg)
V	volume, ft^3 , (cm^3)
V_{ind}	volume of vapor induced to compressor, ft^3 , (cm^3)
V_s	compressor cylinder swept volume, ft^3 , (cm^3)
V_c	clearance volume, ft^3 , (cm^3)
V	velocity, ft/hr , (m/hr)
W	work, ft-lb , (Nt-m)
W_{TOT}	total work for the ideal compression cycle, ft-lb , (Nt-m)
W_{in}	electrical power input to compressor motor, watts
W_{2-1}	electrical power input to produce Q_{g-g} , watts
α	number of discharge valve ports
β	number of suction valve ports

ρ density, lbm/ft^3 , (kg/cm^3)

η_{vol} volumetric efficiency

η_c compression efficiency

η_{mech} mechanical efficiency

η_{mot} motor efficiency

CHAPTER I

INTRODUCTION

Refrigeration is a term used to denote the maintenance of a body at a temperature lower than that of its surroundings. To maintain or produce the low temperature, it is necessary to transfer heat from the cold body or refrigerated space. A refrigerator is a device employed to accomplish this effect by the expenditure of external energy in the form of work or heat or both. For the refrigerator to operate continuously, it must reject heat to an external sink, usually the atmosphere.

The basic cycle for a mechanical refrigeration system is the ideal vapor compression cycle illustrated in Figure 1. A typical equipment arrangement that may be used to carry out the processes defined by the cycle is depicted in Figure 2. Referring to Figure 1, it is apparent that there are only two pressure levels in this system, friction loss being ignored. Vapor is compressed from p_L at 1 to p_H at 2; condensed liquid at 3 is throttled with no work output from p_H to p_L at 4. The existence of the two pressure levels allows evaporation of the refrigerant at a low temperature, and condensation of the same fluid at a higher temperature. Heat must be transferred to the refrigerant to produce the evaporation, and it is in this low-pressure heat exchanger where the refrigeration effect is achieved. This heat is transferred from a secondary fluid which passes through the evaporator (usually air, water or secondary coolants). The cooling medium passing through the condenser, carries away the sum of the heat energy absorbed by the refrigerant in the evaporator and the contribution of the work of

compression supplied in the compressor.

Forty-five percent of refrigeration systems using air as the secondary fluid in the condensation process are outdoor units, that is, the condenser is located outdoors [1]. Heat transfer theory dictates that the refrigerant must be condensed at a temperature higher than the ambient temperature. Therefore, during the summer the system is forced to work at relatively high compression ratios. As the ambient temperature falls in the winter, the system will condense at a lower temperature. To prevent the condensing pressure from dropping in direct proportion to the ambient temperature, various forms of controls have been developed. The philosophy behind their mandatory use being that without sufficiently high condensing pressure during low ambient temperature operation, the system can experience both running-cycle and off-cycle problems [2, 3]. The terms 'running cycle' and 'off cycle' are employed by the refrigeration industry to denote whether the compressor is running or not. Two running-cycle problems of prime concern are:

- (1) Since the pressure differential across the thermostatic expansion valve port affects the rate of refrigerant flow through it, low condensing pressure generally causes insufficient refrigerant to be fed to the evaporator drastically decreasing the capacity of the system [2].
- (2) Any system using hot gas for defrost or compressor capacity control, must have a high condensing pressure to operate properly. In either case, failure to have sufficient condensing pressure will result in low suction pressure and or iced evaporator coils [3].

The primary off-cycle problem is the possible inability to get the system starting if the refrigerant has migrated to the condenser. Migration is the off-cycle mass transfer of refrigerant from a higher temperature point of the system to a lower temperature point. The evaporator pressure may not build up to the cut-in point of the low pressure control and the compressor cannot start even though refrigeration is required. Even if the evaporator pressure builds up to the cut-in setting, compressor cycling could result. This is because the thermostatic expansion valve may not open to feed sufficient refrigerant to prevent the evaporating pressure from dropping and when the evaporation pressure reaches the cut-out setting the compressor will stop [2].

There are three methods of preventing the condensing pressure from dropping when the ambient temperature decreases:

- (1) Cycling the condenser fan (s) on and off;
- (2) Varying the speed of the condenser fan motor to change the air flow passing through the condenser;
- (3) Reducing the available heat exchange surface by flooding a portion of the condenser tubes with liquid refrigerant.

The last method is considered to be the most reliable and best suited for low ambient temperatures.

Figure 3 illustrates that as the condensing pressure drops, the compression ratio decreases, the refrigeration effect (Btu/lb) in the evaporator increases, and the power consumption decreases. Therefore, if a system is able to operate satisfactorily at low condensing pressure, its coefficient of performance and equipment life will increase.

The objectives of this thesis are:

- (1) To design an outdoor aircooled refrigeration system that operates at varying ambient temperature conditions by allowing the condensing pressure to drop as the ambient temperature falls;
- (2) To study experimentally the advantages and limitations of such a system;
- (3) To predict analytically the performance of the system and compare to experimental results.

CHAPTER 2

MODIFIED OUTDOOR AIR-COOLED REFRIGERATION SYSTEM DESIGN

The advantages of increased capacity, reduced power consumption and increased equipment life materialize when the condensing pressure is allowed to drop in proportion to the ambient temperature. However, at reduced condensing pressures and consequently reduced compression ratios, a number of conditions not met by the conventional refrigeration system must be satisfied by the modified system as follows:

- (1) At a fixed evaporating pressure, supply a constant refrigerant mass flow to the evaporator, independent of the pressure difference across the expansion valve;
- (2) Allow the condensing pressure to drop to some minimum value beyond which any further reduction will result in loss of capacity or poor expansion valve control. Maintain this minimum pressure as ambient temperature continues to fall;
- (3) Control room relative humidity by varying the heat transfer capacity of the evaporator coil as the system capacity changes. Thus, balance the evaporator coil to the remainder of the system at all times so that the temperature difference between room and evaporating temperature remains constant.

2.1 THE EXPANSION VALVE PROBLEM

Flow through the expansion valve is proportional to the pressure difference across it and the area of the orifice through which expansion takes place. Expansion valve performance is described [4] by:

$$\Delta P = \frac{\rho q^2}{2C_d^2 A_o^2 g_c} \quad (2.1)$$

where ρ = density of inlet fluid

q = volume flow rate through the orifice

C_d = discharge coefficient

A_o = area of expansion orifice

g_c = conversion constant

If the mass flow rate is to remain constant as the pressure drop across the expansion valve orifice is reduced, then the orifice area A_o must increase.

First consider the conventional thermostatic expansion valve illustrated in Figure 4. Figure 5 shows that the operation of the expansion valve is determined by three fundamental pressures:

- (1) Bulb pressure P_1 acts on one side of the diaphragm and creates an opening force;
- (2) Evaporator pressure P_2 , supplied through the external equalizing tube, acts on the opposite side of the diaphragm and tends to close the valve;
- (3) Spring pressure P_3 , which also assists in the closing action, is applied to the pin carrier and is transmitted through push rods to a buffer plate on the evaporator side of the diaphragm.

When the valve is modulating, bulb pressure is balanced by the evaporator pressure plus the spring pressure.

$$P_1 = P_2 + P_3 \quad (2.2)$$

When the same refrigerant is used in both the thermostatic bulb element and refrigeration system, each will exert the same pressure if their temperatures are identical. After evaporation of the liquid refrigerant in the evaporator the suction gas is superheated; however, the evaporator pressure (neglecting pressure drop in the evaporator) is unchanged. The expansion valve bulb, which is located at the evaporator outlet, senses the temperature of this superheated vapor. Since it contains a saturated liquid vapor mixture, its temperature and pressure increase to the saturated conditions at the superheated vapor temperature. This higher bulb pressure acting on the top (bulb side) of the diaphragm is greater than the opposing evaporator pressure plus spring pressure, causing the valve pin to be moved away from the seat. The valve is opened until the spring pressure, combined with the evaporator pressure, is sufficient to balance the bulb pressure. Figure 5 is a curve of closing force versus bulb temperature showing the relation of closing force, opening force, and superheat. If the valve does not feed enough refrigerant, the evaporator pressure drops or the bulb temperature is increased or both and the valve opens, admitting more refrigerant until the three pressures are again in balance. Conversely, if the valve feeds too much refrigerant, the bulb temperature is decreased, or the evaporator pressure increases or both and the valve tends to close until the three pressures are again in balance. With an increase in evaporator load, the liquid refrigerant evaporates at a faster rate and increases the evaporator pressure. The higher evaporator pressure results in a higher evaporator temperature

and a correspondingly higher bulb temperature. The additional evaporator pressure acts on the bottom of the diaphragm while the additional bulb pressure acts on the top. Thus, the two opposing pressure increases on the diaphragm, cancel out each other and the valve adjusts easily to the new load condition with a negligible change in superheat range. However, when the load varies drastically, the valve pin is already in a partially closed position about which it must still be able to modulate to control the superheat. As this partially closed position comes closer to the fully closed position and the valve attempts to modulate, the amplitude of the modulation is increased considerably and the valve is said to hunt [5]. At this point the control has reached a state of instability.

Testing has shown that this instability usually occurs at approximately 30% of the valve's rated capacity [6] and is caused primarily by high expansion valve inlet pressure acting on the top portion of the valve pin. Although this pressure is acting on a very small area, it results in a force opposing the spring and evaporator pressures. Since expansion valves in conventional systems are operated at fixed pressure differences across them, this force is balanced by providing a stronger spring to oppose it. As the condensing pressure decreases, the force acting on the valve pin is also decreased and, an imbalance is now created by the portion of the spring force originally designed to balance the entering liquid pressure force at high condensing pressure [9].

In the modified system, the condensing pressure will be allowed to drop proportionally with the ambient temperature thus reducing the pressure differential across the valve. Figure 3 depicts two refrigeration

cycles, one operating at high condensing pressure (summer operation: 1-2-3-4-5-6-7-8-9-1) and the other at low condensing pressure (winter operation: 1-2'-3'-4'-5'-6'-7'-8'-9-1). Thus for maximum increase in system capacity the mass flow rate must remain constant at low and high condensing pressures.

Using equation (2.1),

$$\dot{m}_6^2 = \frac{(P_6 - P_8)(2C_d^2) A_s^2 g_c}{v_6} \quad \text{for summer operation} \quad (2.3)$$

$$\dot{m}_{6'}^2 = \frac{(P_{6'} - P_{8'})(2C_d^2) A_w^2 g_c}{v_{6'}} \quad \text{for winter operation} \quad (2.4)$$

Designing for maximum capacity increase, the mass flow rate at the two condition must be equal.

$$\dot{m}_6^2 = \dot{m}_{6'}^2 = \frac{(P_6 - P_8)(2C_d^2) A_s^2 g}{v_6} = \frac{(P_{6'} - P_{8'})(2C_d^2) A_w^2 g}{v_{6'}} \quad (2.5)$$

thus

$$A_w^2 = \frac{(P_6 - P_8)}{(P_{6'} - P_{8'})} \frac{\rho_6}{\rho_{6'}} A_s^2 \quad (2.6)$$

therefore

$$A_w = \sqrt{\frac{(P_6 - P_8)}{(P_{6'} - P_{8'})} \left(\frac{\rho_6}{\rho_{6'}}\right)} A_s \quad (2.7)$$

From Eq. (2.7), the expansion valve throttling port at the winter condition must be larger than the corresponding port at the summer condition by

$$\sqrt{\frac{\Delta P_s}{\Delta P_w} \left(\frac{\rho_s}{\rho_w}\right)}$$

where the subscripts s and w refer to summer and winter conditions respectively.

If the expansion valve for the modified system is selected to satisfy the winter condition, it will be oversized in the summer when the maximum capacity of the system is reduced and the orifice size of the valve must be smaller. A conventional valve can, in most cases, modulate at that maximum load summer condition, but as the load is lowered, the expansion valve will attempt to modulate closer towards the closing position to reduce the refrigerant flow rate and the valve will enter its unstable zone and begin hunting. Several trial installations by the author have shown that conventional expansion valves used in a system where the condensing pressure is allowed to drop with the ambient temperature become erratic in operation at low load summer conditions.

The valve required, in this type of a system must have exceptional stability with the capability of modulating without "hunting" at a very low percentage of its rated capacity.

An expansion valve with these features has recently been introduced on the market. It is a fully-balanced port valve with the capability of modulating down to 5% of its rated capacity [8]. It represents a basic change in the design approach for thermostatic expansion valves. Figure 6 illustrates a schematic cross-section of the outlet chamber of the balanced port valve. The three forces P_1 , P_2 and P_3 act in the same manner as the conventional expansion valve discussed earlier.

Force P_4 is exerted by the entering liquid pressure acting in the opening direction. However, the same liquid pressure is transmitted to the underside of the piston seal and also acts in a closing direction. The area of the main port is equal to the area of the piston chamber

bore, and as a result, these forces cancel and the piston position is independent of entering liquid pressure. Since the piston is independent of entering liquid pressure, excellent control stability can be expected at considerably less than design pressure differential across the valve port [10].

In summary, the thermostatic expansion valve utilized in the modified system must be:

- (1) a fully-balanced port valve with the ability to successfully modulate at a very low percentage of its rated capacity;
- (2) selected so that its orifice permits the summer design mass flow rate at the winter lowest pressure differential across it.

2.2 CONDENSING PRESSURE CONTROL SYSTEM

The modified aircooled outdoor refrigeration system will allow the condensing pressure to drop proportionally with the ambient temperature. Figure 3 shows a modified system refrigeration cycle in summer and winter operation. For the purposes of discussion, the summer cycle will be considered first. Subcooled liquid leaves the condenser at 5 and, after sustaining pressure loss and heat gain (or further subcooling, depending on the temperature of the surroundings through which the liquid line passes), it enters the thermostatic expansion valve at 6. Proper expansion valve operation depends on saturated or subcooled liquid supply. It is obvious that if point 6 enters the wet vapor region on

the P-h diagram, loss of refrigeration capacity and poor expansion valve control will result. In conclusion, point 6 can only be allowed to drop to the saturated liquid line. From the control point of view, this is extremely difficult to achieve and therefore, a minimum differential pressure will be maintained between points 6 and 7.

Figure 3 shows that as the condensing pressure drops and approaches the evaporating pressure, point 8 at the outlet of the expansion valve may move to the subcooled liquid region. A portion of the evaporator will be used to saturate the liquid refrigerant before evaporation takes place. Again, loss of evaporator capacity will result. This condition will be prevented if a positive difference in pressure between points 7 and 8 exists. Two controls will monitor the difference in pressure between points 6-7 and 7-8, and when either one reaches a minimum set difference in pressure, the condensing pressure must be controlled as the ambient temperature continues to fall.

In designing the control, the pressure at points 6 and 8 can easily be sensed through a capillary tube connected at the inlet and outlet of the expansion valve respectively. However, the state at point 7 occurs during the expansion process and, as such, cannot be measured directly. States 6 and 7 always exist at the same temperature. By sensing the temperature at the inlet of the expansion valve with a bulb partially filled with liquid refrigerant, the saturated pressure of the refrigerant at that temperature will be exerted on the diaphragm, as shown in figure 7. When the refrigerant in the bulb is the same as that in the system, the pressure in the bulb will be that of point 7. For accurate control it is imperative that the liquid vapor interface of the bulb-diaphragm

assembly be located in the bulb under all operating conditions.

Figure 7 illustrates the schematic diagram of the differential pressure control. The bulb senses the temperature of the subcooled liquid refrigerant entering the expansion valve and exerts a pressure, P_7 , on the diaphragm equal to the saturated pressure at the liquid temperature. The resulting force F_7 acts on one side of the fulcrum. Pressure P_6 at the entrance of the expansion valve is applied through a capillary tube to the adjacent diaphragm and creates a second force F_6 at the other side of the fulcrum. A third force F_s , opposing F_6 , is generated by a spring.

The force diagram on figure 7 shows that when $F_6 > F_7 + F_s$, the angular position of the lever is such that contact is not made at the switch. As the liquid entering the expansion valve approaches saturation $F_6 = F_7 + F_s$ and the lever closes the contacts of the electrical switch. A similar control with the bulb located at the entrance of the expansion valve and the capillary tube at the outlet will monitor the pressure difference between P_7 and P_8 of figure 3.

As was previously stated, when either one of the differential pressure controls, measuring the difference in pressure between states 6-7 and 7-8, reaches its minimum set pressure differential, the condensing pressure must be prevented from dropping further as the ambient temperature continued to fall. To understand the method employed to accomplish this, it is important to describe the condensing pressure control valve presently used in the majority of conventional air cooled systems in which the condenser is located in the outdoor environments.

Figure 8 depicts a conventional refrigeration system using a condensing pressure control valve. During high ambient temperature conditions, liquid refrigerant from the condenser enters port C and leaves through port R to the liquid receiver. When the discharge pressure drops below the valve setting, the valve modulates to permit discharge gas to enter port B. Metering discharge gas into the liquid refrigerant produces a higher pressure at the condenser outlet, thus reducing the flow and allowing the level of condensed liquid refrigerant to rise in the condenser. The flooding of the condenser with liquid refrigerant reduces the available heat exchange surface area and increases the operating temperature difference between ambient and condensing temperatures.

The condensing pressure control valve illustrated in detail in Figure 9, is a three way modulating valve. The push rod is an independent piece which is fixed neither at the diaphragm nor at the valve disc. The dome on the top portion of the control makes up a closed system with the diaphragm and is pressurized with nitrogen at a fixed pressure, P_c . This pressure causes the diaphragm to exert a force F_c on the push rod attempting to open the discharge gas port and bypass discharge gas to the receiver through the liquid line. The discharge gas pressure, P_d , opposes the dome pressure through a passage providing pressure on the underside of the diaphragm. This pressure creates a force F_d opposing F_c . A spring force F_s is also exerted on the valve disc in a direction acting to close the discharge gas port.

When the discharge pressure, P_d , is higher than the dome pressure

P_c , the resulting net force $F_c - F_d$ acts towards the inside of the dome so that no force is exerted on the push rod. In this condition, the spring force is the only force acting on the valve disc and provides a closing force. The spring force acting on the disc when the discharge valve port is closed is F_{sc} and the position of the valve disc is referenced as $x = 0$, where x is the travel of the disc.

When the discharge pressure, P_d , falls below the dome pressure, P_c , as the condensing pressure drops due to a lower ambient temperature, a net force $F_c - F_d$ is transmitted by the push rod to the valve disc and opposes the spring force F_{sc} . The expression $(F_c - F_d) - F_{sc} > 0$ describes the operation of the control until the force difference $F_c - F_d = F_{sc}$ and the valve disc is balanced and ready to open. It is still in the position $x = 0$.

As the ambient temperature falls further and the condensing pressure falls proportionally, the force difference $F_c - F_d$ increases and overcomes the spring force F_{sc} and begins to open the discharge gas valve port. The valve disc moves to a new position, $x = x_1$, where the spring force $F_s = F_{sc} + kx$ can balance the force difference $F_c - F_d$. The expression that describes the control from the point that the forces on the valve disc are balanced and its position is still $x = 0$ (that is, the valve disc is ready to open) is $(F_c - F_d) - F_{sc} = kx$. It is obvious that as the force difference $F_c - F_d$ increases, the valve disc will open to a new position away from discharge gas valve seat in order to balance the forces.

Figure 10 illustrates the head pressure control valve used in the

modified refrigeration systems where the condensing pressure is allowed to drop with the ambient temperature. The point at which the condensing pressure must be controlled is variable and depends on the amount of liquid subcooling and pressure drop in the liquid line.

Therefore, a condensing pressure control with a fixed control pressure cannot be used.

The dome-diaphragm assembly consists of a closed system with the capillary line and bulb, and is charged with liquid refrigerant. As in the case of the differential pressure control bulb, the liquid vapor interface must be located in the bulb under all operating conditions. When the modified refrigeration system is operating at varying condensing pressures, and neither one of the differential pressure controls used to monitor the pressure difference between states 6-7 and 7-8 of Figure 3 has made contact, the condensing pressure control of Figure 10 is inoperative. That is, the discharge gas port is closed. The bulb senses the ambient temperature and exerts a pressure on diaphragm equal to the saturated pressure of the refrigerant at the ambient temperature. Since the condensing pressure is higher than the ambient temperature, the discharge pressure acting on the opposite side of the diaphragm higher and the net pressure differential acts towards the inside of the dome. No force is exerted on the push rod and the spring force keeps the valve disc closed against the discharge gas port.

When either one of the differential pressure controls senses its minimum setting, the electrical contact is closed and power is supplied to the heater wrapped around the head pressure control bulb. The vapor

pressure in the bulb is increased as a result of the heat input, and when the resulting force is sufficient to overcome the discharge pressure force and the spring force, the valve disc begins to open the discharge gas port and the condensing pressure is increased. This increase in condensing pressure is caused by the differential pressure controls and the electrical contact that initiated the control action will open cutting power to the heater and the cycle will be repeated.

CHAPTER 3

THEORETICAL ANALYSIS

Equations used to date to predict compressor performance have been developed for the ideal compression cycle and reflect great discrepancies from the performance of the actual compressor [9,10]. The complexity of the compression, expansion, suction and delivery processes of the actual compressor makes a purely theoretical analysis extremely difficult. It is not within the objectives of the thesis to carry out such an analysis, but rather to find equations that allow for closer prediction of volumetric efficiency, system capacity, compression efficiency and power consumption. This is done by utilizing data which are available from compressor manufacturers or can be easily obtained from an installed system.

3.1 RECIPROCATING COMPRESSOR PERFORMANCE

Consider the ideal compression cycle assuming that:

- (1) The compression and expansion processes are polytropic and, for convenience, the same polytropic exponent is used;
- (2) The suction and delivery processes occur at constant pressure and temperature.

Figure 11 is a pressure volume diagram of the ideal cycle of a reciprocating compressor with clearance volume. The total work of the cycle is the sum of the work values for each individual process. For each process:

$$W = \int P dV \quad (3.1)$$

In accord with assumption 2, processes 4-1 and 2-3 are constant pressure processes; therefore the work can be expressed as:

$$W_{4-1} = \int_4^1 P dV \quad (3.2)$$

$$= P_1(V_1 - V_4) \quad (3.3)$$

and $W_{2-3} = P_2(V_3 - V_2) \quad (3.4)$

Assumption 1 states that for processes 1-2 and 3-4, $PV^n = c$. The work for process 1-2 is represented by:

$$W_{1-2} = \int_1^2 P dV = \int_1^2 \frac{c}{V^n} dV \quad (3.5)$$

$$= P_1 V_1^n \int_1^2 \frac{1}{V^n} dV \quad (3.6)$$

and for process 3-4, by:

$$W_{3-4} = P_3 V_3^n \int_3^4 \frac{1}{V^n} dV \quad (3.7)$$

The total work for the ideal compression cycle is expressed by:

$$W_{TOT} = P_1 V_1^n \int_1^2 \frac{1}{V^n} dV + P_2(V_3 - V_2) + P_3 V_3^n \int_3^4 \frac{1}{V^n} dV + P_1(V_1 - V_4) \quad (3.8)$$

$$= \frac{P_2 V_2 - P_1 V_1}{1 - n} + P_2(V_3 - V_2) + \frac{P_4 V_4 - P_3 V_3}{1 - n} + P_1(V_1 - V_4) \quad (3.9)$$

Assumption 2 states that:

$$P_1 = P_4 \quad ; \quad T_1 = T_4 \quad (3.10)$$

$$P_2 = P_3 \quad ; \quad T_2 = T_3 \quad (3.11)$$

Substituting equations (3.10) and (3.11) into equation (3.9) gives the following expression:

$$W_{TOT} = \frac{P_2(V_2-V_3)}{1-n} - P_2(V_2-V_3) - \frac{P_1(V_1-V_4)}{1-n} + P_1(V_1-V_4) \quad (3.12)$$

$$= \frac{n}{1-n} [P_2(V_2-V_3) - P_1(V_1-V_4)] \quad (3.13)$$

Figure 11 shows that

$$V_1 - V_4 = m_g v_1 \text{ and } V_2 - V_3 = m_g v_2 \quad (3.14)$$

where m_g is the amount of gas drawn in per cycle from 4-1 at T_1 and P_1 and discharged from 2-3 at T_2 and P_2 . Substituting equation (3.14) into equation (3.13) yields the expression for the total work:

$$W_{TOT} = m_g \frac{n}{n-1} [P_2 v_2 - P_1 v_1] \quad (3.15)$$

The work per pound of gas compressed in the ideal compression cycle is expressed as:

$$W_c = \frac{n}{n-1} P_1 v_1 \left[\frac{P_2 v_2}{P_1 v_1} - 1 \right] \quad (3.16)$$

or

$$W_c = \frac{n}{n-1} P_1 v_1 \left[\left(\frac{P_2}{P_1} \right)^{n-1/n} - 1 \right] \quad (3.17)$$

3.1.1 COMPRESSOR VOLUMETRIC EFFICIENCY

By definition, volumetric efficiency is the ratio of the volume of gas induced per revolution to the swept volume per revolution.

$$\eta_{vol} = \frac{V_{ind}}{V_s} \quad (3.18)$$

Continuing to make reference to the ideal compression cycle of Figure 11, the induced volume into the compressor is expressed by:

$$V_{ind} = (m_c + m_g) v_1 - m_c v_4 \quad (3.19)$$

The compression and expansion processes have been assumed to be polytropic; therefore

$$p_1 v_1^n = C_1 = p_2 v_2^n \quad \text{and} \quad p_3 v_3^n = C_2 = p_4 v_4^n \quad (3.20)$$

The clearance volume V_c , corresponding to V_3 on the pressure volume diagram is expressed by:

$$V_c = m_c v_4 R_c^{-1/n} \quad (3.21)$$

where R_c is the compression ratio and is defined as:

$$R_c = \frac{p_3}{p_4} \quad (3.22)$$

Therefore

$$m_c v_4 = \frac{V_c}{R_c^{-1/n}} = V_c R_c^{1/n} \quad (3.23)$$

Combining equations (3.23), (3.19) and (3.18) yields the following expression for volumetric efficiency:

$$\eta_{vol} = \frac{(m_c + m_g) v_1 - V_c R_c^{1/n}}{V_s} \quad (3.24)$$

$$= \frac{(m_c + m_g) v_1}{V_s} - \frac{V_c}{V_s} R_c^{1/n} \quad (3.25)$$

The clearance volume ratio, C , is defined as:

$$C = \frac{V_c}{V_s} \quad (3.26)$$

where V_c and V_s are the clearance volume and swept volume of the compressor respectively. Furthermore, figure 11 illustrates that

$$V_1 = V_s + V_c \quad \text{and} \quad V_1 = (m_c + m_g) v_1 \quad (3.27)$$

which, when combined with equations (3.26) and (3.24), yield the equation for the volumetric efficiency of the ideal compression cycle.

$$\eta_{vol} = \frac{V_s + V_c}{V_s} - C R_c^{1/n} \quad (3.28)$$

$$\eta_{vol} = 1 - C(R_c^{1/n} - 1) \quad (3.29)$$

The efficiency obtained from the equation above gives values considerably higher than can be expected [4]. The actual compressor experiences losses in efficiency from:

- (1) piston leakage,
- (2) valve leakage,
- (3) throttling effects
- and (4) oil entrainment.

The highest percentage of loss is contributed by valve leakage and piston leakage. High speed photography of refrigeration compressor valve movement [5] has shown that the valves (usually the reed type) reach a state of undulation and at high compression ratios the valve actually never closes tight against its seat. The complexity of this problem makes analytical prediction difficult.

To allow for these losses in efficiency, an effective clearance volume ratio, C_{eff} , can be found for use with equation (3.29) by using pumping data available from compressor manufacturers, or easily attainable on an installed system. This effective clearance volume ratio is assumed to be constant throughout the operating range of the compressor. The simplest test that provides the required data is the blanked suction test. In this test, the compressor suction valve is closed and the compressor is allowed to pull a vacuum. By recording the minimum suction pressure attained by the compressor and the discharge pressure at that condition, the compression ratio R_0 , at which the volumetric efficiency is equal to zero, can be evaluated as follows:

$$\eta_{vol} = 0 = 1 - C_{eff}(R_0^{1/n} - 1) \quad (3.30)$$

where $R_0 = \frac{\text{Absolute Discharge Pressure (blanked suction test)}}{\text{Absolute Suction Pressure (blanked suction test)}}$

and $R_c = R_0$ when $\eta_{vol} = 0$

It follows, then, that the effective clearance volume ratio, C_{eff} , is expressed by:

$$C_{eff} = \frac{1}{R_0^{1/n} - 1} \quad (3.31)$$

Substituting equation (3.31) for the clearance volume ratio in equation (3.29) yields the expression for volumetric efficiency with allowance for losses,

$$\eta_{vol} = 1 - \frac{(R_c^{1/n} - 1)}{(R_0^{1/n} - 1)} \quad (3.32)$$

3.1.2 COMPRESSION EFFICIENCY

To identify the factors which influence compression efficiency, a standard indicator may be employed. The indicator recreates a diagram of events in a refrigeration compressor cylinder. The diagram, known as an indicator card, will be used to investigate compression efficiency. Compression efficiency is defined as:

$$\eta_c = \frac{\text{theoretical power}}{\text{indicated power}} \quad (3.33)$$

S.R. Hirsch [6] has suggested that compression efficiency can be obtained from the indicator diagram by considering the several areas of the actual indicator diagram illustrated in Figure 12.

$$\eta_c = \frac{\text{area abcd}}{\text{area abcd} + \text{area adk} + \text{area bkc}} \quad (3.34)$$

Area abcd reflects the useful work done between P_1 and P_2 and can be considered as the theoretical power. The total area of the diagrams (area abcd + area adk + area bkc) represents the actual compression work.

The work required to force the gas through the discharge and suction valves is represented by areas bkc and adk respectively.

Dividing each term of equation (3.34) by L , the length of the indicator diagram representing the swept volume of the compressor results in:

$$\eta_c = \frac{\frac{\text{area abcd}}{L}}{\frac{\text{area abcd}}{L} + \frac{\text{area adk}}{L} + \frac{\text{area bkc}}{L}} \quad (3.35)$$

For the ideal compression cycle, the area of the useful work in the pressure volume diagram divided by the swept volume yields the mean effective pressure (MEP). Therefore,

$$MEP = \frac{\text{area } abcd}{L} = \frac{\frac{n}{n-1} P_a [R_c^{n-1/n} - 1]}{V_a} \quad (3.36)$$

The compression efficiency equation is simply expressed by:

$$\eta_c = \frac{MEP}{MEP + \frac{\text{area } adk}{L} + \frac{\text{area } bkc}{L}} \quad (3.37)$$

To investigate the work areas adk and bkc , the following assumptions are made:

- (1) The work areas adk and bkc are assumed to be equivalent to rectangular areas;
- (2) The length of the rectangular area depicting the suction valve work adk is equal to the length L of the indicator diagram representing the swept volume;
- (3) Neglecting the effect of clearance volume, the length L_2 on the indicator diagram follows the relation

$$L_2 = R_c^{-1/n} L.$$

From assumptions 1 and 3 above, it follows that:

$$\frac{\text{area } bkc}{L} = \frac{\text{area } bgkc}{L} = \frac{\text{area } bgkc}{L_2 R_c^{1/n}} = \frac{\Delta P_2}{R_c^{1/n}} \quad (3.38)$$

where $\Delta P_2 = \frac{\text{area } bgkc}{L_2}$ and represents the pressure to be overcome by compressor during discharge. Similarly, from assumptions 1 and 2 results the expression:

$$\frac{\text{area adk}}{L} = \frac{\text{area amnf}}{L} = \Delta P_1 \quad (3.39)$$

where ΔP_1 is the pressure differential required to permit flow in the compressor cylinder during the suction process. Substituting equations (3.38) and (3.39) into equation (3.37) results in an equation that permits the use of fluid mechanics to evaluate the effect of pressure losses on compression efficiency,

$$\eta_c = \frac{\text{MEP}}{\text{MEP} + \Delta P_1 + \Delta P_2 / R^{1/n}} \quad (3.40)$$

3.1.2.1 VALVE EFFECT ON COMPRESSION EFFICIENCY

Consider the valve, whether poppet or reed, as a flat plate extending into the gas stream. A drag force is exerted on the valve and has the form [12]:

$$F = \frac{1}{2} G_D \rho \bar{V}^2 A \quad (3.42)$$

where

G_D = drag coefficient

ρ = density

\bar{V} = velocity of gas stream

A = projected area of valve perpendicular to stream

The differential in pressure required to overcome this drag force can be expressed as:

$$\Delta P_D = \frac{1}{2} \rho G_D \bar{V}^2 \quad (3.42)$$

An additional pressure differential to be overcome is experienced from the throttling of the gas as it is forced through the valve port.

This pressure differential is given by [12]:

$$\Delta P_t = \frac{\rho q^2}{2C_d^2 A_o^2 g_c} \quad (3.43)$$

From the definition of volumetric efficiency, the induced flow rate is:

$$q = V_s n_c S_c n_v \quad \text{where} \quad \begin{array}{l} n_c = \text{number of cylinders} \\ S_c = \text{compressor speed} \end{array} \quad (3.44)$$

Substituting equation (3.44) into equation (3.43) yields the expression for the pressure differential to be overcome due to throttling as:

$$\Delta P_t = \frac{\rho V_s^2 n_v^2}{2C_d^2 A_o^2 g_c} \quad (3.45)$$

At both the suction and the discharge valves the pressure differential to be overcome is comprised of a component due to the drag and a component due to throttling. As shown in figure 12, ΔP_1 , is the pressure difference at the suction valve and, ΔP_2 , is that at the discharge valve:

$$\Delta P_1 = \Delta P_{D1} + \Delta P_{t1} \quad (3.46)$$

$$\Delta P_2 = \Delta P_{D2} + \Delta P_{t2} \quad (3.47)$$

Combining equations (3.46), (3.45) and (3.42) yields an equation describing the pressure difference required at the suction valve to permit flow:

$$\Delta P_1 = G_1 \rho_a \bar{V}_a^2 + \frac{G_2 \rho_a n_v^2}{A_s^2} \quad (3.48)$$

where

$$G_1 = \frac{G_D}{2}; \quad G_2 = \frac{V_s^2 S_c^2 n_c^2}{2C_d^2 g_c}; \quad \bar{V}_a = \frac{V_s n_v}{\theta A_s} \quad (3.49)$$

β = number of suction ports

A_s = suction port area

Substituting equation (3.49) into equation (3.48), and rearranging expression (3.51) is derived:

$$\Delta P_1 = \rho_a \eta_v^2 \left[\frac{G_1 V_s^2}{\beta^2 A_s^2} + \frac{G_2}{A_s^2} \right] \quad (3.50)$$

$$= K_1 \rho_a \eta_v^2 \quad (3.51)$$

where

$$K_1 = \frac{G_1 V_s^2}{\beta^2 A_s^2} + \frac{G_2}{A_s^2} \quad (3.52)$$

Similarly, the expression describing the pressure to be overcome at the discharge valve is,

$$\Delta P_2 = K_2 \rho_b \eta_v^2 \quad (3.53)$$

and from the assumption that the compression process is polytropic and follows the expression $Pv^n = c$, it can be reduced to:

$$\Delta P_2 = K_2 \rho_a R_c^{1/n} \eta_v^2 \quad (3.54)$$

where

$$K_2 = \frac{G_1 V_s^2}{\alpha^2 A_d^2} + \frac{G_2}{A_d^2} \quad (3.55)$$

α = number of discharge ports

A_d = discharge port area

Using equations (3.51), (3.54) and (3.40), the compression efficiency is found from:

$$\eta_c = \frac{\text{MEP}}{\text{MEP} + K_1 \rho_a \eta_v^2 + K_2 \rho_a \eta_v^2} \quad (3.56)$$

Substituting equation (3.36) for the mean effective pressure into equation (3.56)

$$\eta_c = \frac{\frac{n}{n-1} P_1 [R_c^{n-1/n} - 1]}{\frac{n}{n-1} P_1 [R_c^{n-1/n} - 1] + K_3 \rho_a \eta_v^2} \quad (3.57)$$

Where $K_3 = K_1 + K_2$

The compression process has been assumed to be described by $P_1 \rho_a^{-n} = c$.

Therefore,

$$\eta_c = \frac{\frac{n}{n-1} P_1 [R_c^{n-1/n} - 1]}{\frac{n}{n-1} P_1 [R_c^{n-1/n} - 1] + K_3 \left(\frac{P_1}{c}\right)^{1/n} \eta_v^2} \quad (3.58)$$

Dividing the numerator and denominator of equation (3.58) by P_1 yields the final expression for the compression efficiency:

$$\eta_c = \frac{\frac{n}{n-1} [R_c^{n-1/n} - 1]}{\frac{n}{n-1} [R_c^{n-1/n} - 1] + K P_1^{1-n/n} \eta_v^2} \quad (3.59)$$

where $K = K_3 C^{-1/n}$

The brakepower of the compressor is expressed [4] by:

$$\text{bp} = \frac{\text{thp} \cdot \eta_v}{\eta_c \eta_{\text{mech}}} = W_{\text{in}} \eta_{\text{mot}} \quad (3.60)$$

where

thp = theoretical power

W_{in} = power input

η_{mech} = mechanical efficiency

η_{mot} = motor efficiency

Rearranging equation (3.60), the compression efficiency is described by:

$$\eta_c = \frac{\text{thp } \eta_v}{W_{in} \eta_{mech} \eta_{mot}} \quad (3.61)$$

To calculate the compression efficiency at any condition of operation using equation (3.59), the constant K must be evaluated. When the power consumption at a condition is known, equation (3.61) is used to calculate the compression efficiency at that condition. Substituting this value into equation (3.59), the constant K may be found.

3.1.3 SYSTEM COEFFICIENT OF PERFORMANCE

The coefficient of performance of the Rankine refrigeration cycle is defined as the ratio of system refrigeration effect to the power input used to create that effect. Referring to the P-h diagram of the cycle depicted in figure 3, and realizing that the greatest portion of superheat ($T_1 - T_g$) occurs outside the evaporator:

$$\text{COP} = \frac{Q_{g-8}}{W_{2-1}} \quad (3.62)$$

The refrigeration capacity during the evaporation process 9-8 is described by:

$$Q_{9-8} = V_{ind} \rho_1 (h_9 - h_8) = V_s \rho_1 \eta_v (h_9 - h_8) \quad (3.63)$$

From equations (3.60) and (3.17) it is seen that the power input to the compressor can be expressed as:

$$W_{in} = \frac{\frac{n}{n-1} P_1 V_1 [R_c^{n-1/n} - 1] \eta_v}{\eta_c \eta_{mech} \eta_{mot}} \quad (3.64)$$

Substituting equations (3.63) and (3.64) into equation (3.62), the expression for the coefficient of performance is found as

$$\text{COP} = \frac{V_s \rho_1 (h_g - h_f) \eta_c \eta_{\text{mech}} \eta_{\text{mot}}}{\frac{n}{n-1} P_1 V_1 [R_c^{n-1/n} - 1]} \quad (3.65)$$

3.2 COMPUTER PROGRAM CALCULATING SYSTEM PERFORMANCE

The equations to calculate volumetric efficiency, compression efficiency, refrigeration capacity, power consumption and coefficient of performance have all been developed in previous sections. Computer programs have been written to calculate the thermodynamic properties of refrigerants 12, 22, 502. For flexibility, thermodynamic property function programs and subroutine programs have been written which can be easily incorporated into computer programs where values for the thermodynamic properties are required. These subroutines, originally presented by Kartsonnes and Erth [13], used property equations supplied by "Freon" Products Laboratory, E.I. duPont de Nemours and Company [14]. The constants in the thermodynamic equations which represent the refrigerants under consideration have been published in references [15, 16, 17].

The subprograms presented have been successfully used and produce consistently accurate results. The calculated thermodynamic properties for R-12 and R-22 agree exactly with the published data in the ASHRAE HANDBOOK OF FUNDAMENTALS - 1977. The equations used to calculate the thermodynamic properties of refrigerant 502 have been published by Martin and Downing [17].

The calculation of the thermodynamic properties is subdivided into five subprograms for programming flexibility. Each subprogram represents a basic building block from which future programs may be written.

All of the programs are written in Fortran.

The listing of the program in Appendix I shows that at the beginning of each subprogram, the purpose of the program is presented, followed by a description of the input and output parameters. Numerous comment cards, which are designated by a "C" in column one, are dispersed throughout each program to indicate the function of the cards following. By means of these comment cards and a basic knowledge of Fortran, the program listings can be read in order to follow the method of calculation employed in each subprogram.

The subprograms SPVOL and TSAT are function subprograms, whereas the subprograms SATPRP, VAPOR and SPHT are subroutine subprograms. SPVOL is written as a function subprogram because specific volume and hence, density of vapor refrigerant as a function of pressure and temperature is frequently required in refrigeration calculations; TSAT is also a function subprogram because the saturation temperature corresponding to a given pressure is frequently desired. Subprograms SPVOL, VAPOR and SPHT use function subprogram TSAT to check the validity of the input pressure and temperature combination. Thus, when either SPVOL or TSAT is used in the main program ENECON, it is treated as a function in the same manner as the Fortran mathematical functions.

The following table provides a guide to usage of the subprograms. The required property and its corresponding Fortran name are listed, along with the required input parameters and the necessary subprograms for execution.

The thermodynamic property subprograms have been employed in the main program ENECON to predict the performance of the refrigeration system.

Property Required FORTRAN Name	Required Input Parameters	Subprograms Used for Execution
Saturation temp. - TSAT	NR, PSAT	TSAT
Saturation press. - PSAT	NR, TF	SATPRP, SPVOL, TSAT
Spec. vol. sat. liq. - VF	NR, TF	SATPRP, SPOL, TSAT
Spec. vol. sat. vap. - VG	NR, TF	SATPRP, SPOL, TSAT
Enth. sat. liq. - HF	NR, TF	SATPRP, SPVOL, TSAT
Latent enth. vap. - HFG	NR, TF	SATPRP, SPVOL, TSAT
Enth. sat. vap. - HG	NR, TF	SATPRP, SPVOL, TSAT
Entropy sat. liq. - SF	NR, TF	SATPRP, SPVOL, TSAT
Entropy sat. vap. - SG	NR, TF	SATPRP, SPVOL, TSAT
Spec. vol. liq. - SVOL	NR, TF, PPSIA	SPVOL, TSAT
Spec. vol. vap. - VVAP	NR, TF, PPSIA	VAPOR, SPVOL, TSAT
Enth. vap. - HVAP	NR, TF, PPSIA	VAPOR, SPVOL, TSAT
Entropy vap. - SVAP	NR, TF, PPSIA	VAPOR, SPVOL, TSAT
Spec. ht cons. vol. - CV	NR, TF, PPSIA	VAPOR, SPVOL, TSAT
Spec. ht cons. press. - CP	NR, TF, PPSIA	SPHT, SPVOL, TSAT
Spec. ht ratio - GAMMA	NR, TF, PPSIA	SPHT, SPVOL, TSAT
Sonic velocity - SONIC	NR, TF, PPSIA	SPHT, SPVOL, TSAT

NR = refrigerated number (12, 22 or 502)

TF = temperature (°F)

PPSIA = pressure (psia)

PSAT = saturation pressure (psia)

CHAPTER 4

EXPERIMENTAL SET-UP AND TEST PROCEDURE

To evaluate the performance of the aircooled refrigeration system at varying condensing pressures, a chamber where the temperature can be controlled to simulate outdoor conditions was built. For purposes of clarity the experimental set-up used will be described in two sections. One specifying the modified refrigeration system to be tested and the other describing the system used to control the temperature in the chamber.

Figure 13 depicts a block layout diagram identifying the location of the two systems in relation to the chamber. The refrigeration system used to control the temperature in the chamber is located outside the chamber while only the evaporators and air handler being located inside. The modified system is similar in design to commercial outdoor air-cooled systems. That is the complete system is designed as a package called condensing unit comprised of compressor, condenser, receiver, condensing pressure control valve, filters, moisture indicator, solenoid valve, suction accumulator, hand shut-off valves and electrical control panel. This portion of the system is located usually on the roof and is connected through piping to the expansion valve and evaporator located somewhere in the building remote from the condensing unit. In a similar fashion, the condensing unit of the modified system to be tested is located inside the temperature control chamber and the thermostatic expansion valve, differential pressure controls and evaporator are located outside.

4.1 MODIFIED REFRIGERATION SYSTEM

Figure 14 illustrates the modified refrigeration test system and a list of system components. Components of primary concern are discussed and items such as hand shut-off valves and regulating valves are mentioned only as to their relation to the test procedure.

The compressor used is a semihermetic compressor, manufactured by Prestcold (North America) Ltd., whose specifications are shown in table 1 of Appendix II. Low ambient temperature operation required that it is equipped with a crankcase heater to assist in starting and to boil off refrigerant from the crankcase lubricating oil during the off-cycle.

The condenser has been selected to operate at a smaller than usual temperature differential between ambient temperature and condensing temperature. This is because the heat of condensation of the modified refrigeration system tested is rejected into the chamber and it becomes the load for the chamber cooling system. By reducing this temperature difference, any condensing temperature of the test unit can be controlled by a chamber temperature higher from the one possible with a condenser operating at a normal (larger) temperature difference. This permits the chamber cooling system to operate at a correspondingly higher evaporating temperature where its capacity is increased and can offset the load more easily.

The condensing pressure control valve described in detail in Chapter 2 has been modified from a conventional condensing pressure control (also described in Chapter 2) manufactured by Alco Valve Co.

The dome is equipped with fittings to accept a pressure transducer. The refrigerant in the dome is the same as that of the system (R-12).

Components such as liquid refrigerant filter-drier (item 13) suction filter (item-18) and suction accumulator (item 19) have all been selected for minimum pressure drop through them. The filters and moisture indicator are obvious in their function and will not be discussed. The pump down solenoid valve is a very important component and should be installed in all refrigeration systems. During normal operation the valve is always open. When the compressor is running and a safety failure condition occurs such as high discharge pressure, low suction pressure or thermal overload the compressor is stopped immediately by the corresponding control. However when the load of a refrigeration system is satisfied, the compressor is stopped indirectly by the initiation of the pump-down cycle. As the operating control (usually a thermostat or a low pressure control) senses that the load is satisfied the pump down solenoid is deenergized closing the liquid line feeding the expansion valve. The compressor continues to operate until the suction pressure drops sufficiently to trip the low pressure safety control. The effect of the pump down cycle is to collect all the refrigerant in the liquid receiver prior to stopping the compressor and as a result eliminate the problem of migration during the off-cycle and also permit an easier start of the compressor. The wiring diagram of the test unit, illustrated in figure A2 of Appendix II, shows the method in which the pump down solenoid is wired in relation to the other system electrical components.

The suction accumulator (item 19) is also an extremely important device especially in outdoor systems. Its function is to prevent liquid refrigerant and oil from returning to the suction of the compressor in large particle form that could cause valve damage. This is achieved by first collecting the liquid refrigerant and oil in its reservoir and then metering it through an orifice to the suction gas stream in a finely atomized form that can be tolerated by the compressor.

Item 28 of figure 14 is a safety pressure control (referred to as dual pressure control) used to stop the compressor in the event of excessive discharge pressure or low suction pressure. The low pressure section of the control is also used to terminate the pump down cycle. Item 29 is a suction pressure control which is used as the operating control. In the test system the suction pressure control contact is wired in series with the pump down solenoid valve coil and is used to initiate the pump down cycle.

The two differential pressure controls (item 14 and 15) are prototypes built by Penn-Johnson Control Co. [19], according to the design requirements described in Chapter 2. The refrigerant in the bulb is R-12 and the minimum pressure differential that can be consistently monitored is 7 psi (48.23 kpa). Test results of the differential pressure control provided by Penn-Johnson Controls Co. are shown in table 2 Appendix II.

The balanced port expansion valve described in detail in Chapter 2 is a commercially available valve manufactured by Sporlan Valve Co. Since the introduction of the balanced port thermostatic expansion valve by Sporlan many manufacturers have also developed similar valves. The principle of operation used by all manufacturers is identical and the only differences are minor ones to overcome patent restrictions.

The evaporator used is a chiller manufactured by Standard Refrigeration Co. It is a tube-in-tube multipass heat exchanger whose specifications are shown in table 3 of Appendix II. It is located outside the test chamber and is insulated with eight inches (20.3 cm) of polypropylene foam. The secondary coolant is ethylene glycol mixed with water to a 50% concentration by weight. The glycol is drawn from the reservoir by the pump and after passing through the chiller it goes to a steam-glycol heat exchanger where its temperature is increased to the original temperature entering the chiller. From the steam-glycol heat exchanger the glycol is returned to the reservoir.

The aircooled subcooler (item 11) is used to increase the amount of subcooling to simulate the condition of having subcooled liquid after the expansion valve at low compression ratios. During normal operation hand shut off valves 10 and 12 are closed and valve 9 is open. To activate the subcooling circuit, valve 9 is closed and valves 10 and 12 are opened.

Pressure transducers were used to measure the condensing pressure, dome pressure of the condensing pressure control, pressure

at the inlet of the expansion valve and pressure at the outlet of the expansion valve. The locations of the transducers are shown in figure 14 as TR1 to TR4. The output from the transducers after being amplified was inputted to a strip chart recorder. The transducers were calibrated using a digital voltmeter and a known pressure gauge accurate to .1 psi (.689 Kpa).

Using the barometric pressure the two transducers measuring the pressure entering and leaving the thermostatic expansion valve have been calibrated to measure absolute pressure, while the transducers measuring dome pressure of the condensing pressure control and condensing pressure have been calibrated to measure gauge pressure.

A multi channel digital thermometer using copper-constantan thermocouple wire was used to record temperatures throughout the system. The location of these thermocouples is shown in figure 14, as T1 to T7. Each thermocouple was inserted into a 5 mm diameter well protruding 5 mm into the refrigerant tubing of the system. All thermocouple wells were filled with Dow Corning 340 heat sink compound manufactured specifically for this purpose. The digital thermometer used has an accuracy of .2°F (.1°C).

Two watt meters connected as shown in figure A1 of Appendix II were used to measure the power input to the compressor.

Prior to operation, the modified outdoor aircooled refrigeration system was evacuated and charged with refrigerant 12 using the following procedure. The suction and discharge service valves were closed opening their evacuation ports. A vacuum pump was connected to

both suction and discharge evacuation ports through high vacuum hoses. The vacuum pump was operated until a pressure of 1.5 mm of Hg. absolute was reached. The vacuum pump was stopped and refrigerant 12 was injected into the system through the liquid line filter drier until the system pressure increased above atmospheric pressure. This procedure of evacuating and charging was repeated a second time. Then the compressor suction and discharge service valves were opened and the entire system was evacuated to 0.5 mm of Hg. absolute pressure. Refrigerant 12 was again injected into the system to bring the system pressure above atmospheric conditions, before the vacuum pump was disconnected. Using a gauge manifold, the system was vapor charged through the suction service valve until the sight glass of the moisture indicator showed bubble free liquid passing through it.

4.2 CHAMBER COOLING SYSTEM

To simulate the outdoor ambient temperature conditions a chamber in which the test unit was to be located was built. The refrigeration system used to control the temperature in the chamber will be described in detail below. The wide variation in temperature to be controlled makes a flooded evaporator type system ideal; however the cost of such a system is very high and as a result a refrigeration system with direct expansion evaporator coils was built.

The 12 ft. x 10 ft. x 7 ft. (3.6m x 3.0 m x 2.1m) chamber was built by Fabian Inc. It is of panelized construction with panels made of a wooden frame enclosed by sheet steel in which 8 inches (20.3cm) of polypropylene foam insulation is used.

In explaining the operation of the refrigeration system used to control the chamber temperature the design involved in obtaining the temperature range of operation will be discussed. In every refrigeration system the three basic components involved must be balanced in order to operate at a particular condition are compressor, condenser and evaporator. Since the system will be working at a wide spectrum of conditions the compressor used is an open type compressor which is direct driven by a motor. This motor has been slightly oversized to eliminate the use of crankcase pressure regulating devices to assist in starting after each defrost cycle. The compressor is a six cylinder compressor, manufactured by Prestcold (North America) Ltd. with special valve covers equipped with hydraulically operated cylinder unloading devices. The term cylinder unloading refers to the action of the unloading mechanism to close the suction port so that no vapor

refrigerant enters the cylinder during the suction stroke. The compressor of the chamber cooling system is operated with either two cylinders in operation (33% of maximum capacity) or four cylinders (66% of maximum capacity). Two cylinders are always unloaded. The condenser is a water cooled condenser that has been selected to result in low condensing pressures. Two evaporators are used to satisfy a maximum range of operation. Each evaporator is used correspondingly with the compressor operating at 33% capacity and 66% capacity. For reference, system 1 will refer to the compressor operating at 66% capacity using evaporator 1 and system 2 will refer to the compressor operating at 33% with evaporator 2.

Figure A3 of Appendix III is a plot of the compressor performance curves superimposed on the condenser performance curves for system 2. The compressor curves are refrigeration capacity versus condensing temperature at constant evaporating temperatures. For each evaporating temperature there are two curves. The one on top is the heat of condensation at that evaporating temperature while the one on the bottom is the refrigeration capacity at that evaporating temperature. The condenser curves are condenser capacity versus condensing temperature at constant water flow rate. The dotted line of figure A3 shows that at 3 (gall/min) water flow rate and plus 10°F. evaporating temperature the unit will condense at approximately 112°F (the intersection of the heat of condensation curve at plus 10°F evaporating temperature and the condenser curve of 3 gall/min.) The system capacity at that condition is found by dropping a vertical line from the point of intersection to the capacity curve of + 10°F (-12.2°C) evaporating temperature. At this point of intersection the compressor and the condenser are said to be balanced. By evaluating all these points of

balance the compressor-condenser curves of figure A4 Appendix III have been plotted at constant water flow rate. Now by superimposing the capacity curves of the evaporator to be used, the points at which compressor-condenser-evaporator are balanced are found. Figure A5 of Appendix III shows figure A4 with an envelope of operating conditions. Note that the three components still balance outside this envelope, but the condensing temperature is above 120°F (48.9°C). Chamber temperatures of -10°F to $+40^{\circ}\text{F}$ (-23.3°C to 4.44°C) are possible with system two, while the condensing temperature is below 120°F .

A similar series of curves for system one are plotted in figure A6, A7 and A8 of Appendix III. Chamber temperatures of -10°F to -26°F are possible with system 1. By examining both sets of curves it can be seen that a single water flow rate of 3 Gall/min is required to balance the system for the whole evaporating temperature range.

Figure 15 illustrates the chamber cooling system schematic and list of components. The compressor (item 1) discharges vapor refrigerant to the oil separator (item 2). The function of the oil separator is to separate the lubrication oil from the discharge gas stream and return it to the compressor. In this case the separated oil is returned to the compressor crankcase through the suction accumulator to be discussed later. The oil from the oil separator to the suction accumulator passes through a solenoid valve (item 24) which when the compressor is off, is deenergized and oil is not returned. Three minutes after the compressor starts it energizes and begins to return oil to the suction accumulator. The purpose for this is to allow enough time until the temperature of the oil separator increases and boils off any excess liquid refrigerant

that may have condensed in the oil separator during the off cycle. From the oil separator the discharge gas passes through a muffler (item 3) whose function is to dampen out discharge gas stream pulsation and reduce the vibration in the refrigerant lines. From the muffler two paths are available. The one leading to the two way valves 16 and 20 does not permit any flow because both hot gas defrost valves (item 16 and item 20) are closed in that direction when the system is in the refrigeration mode. Thus the discharge gas passes through solenoid valve 4 and goes to the reevaporator storage reservoir 5. Item 5 is a reservoir filled with ethylene glycol at a concentration of 50% by weight. There are two individual heat exchange circuits inside the reservoir. One through which the discharge gas passes to be desuperheated and increase the glycol temperature in the process, and the other through which liquid refrigerant in the defrost cycle is evaporated before returning to the compressor. From the reevaporator reservoir desuperheated vapor refrigerant goes to the water cooled condenser (item 8) where it is condensed and enters the auxiliary liquid refrigerant receiver 7. From the receiver it passes through a filter-drier (item) and a moisture indicator (item 9) before it enters the heat exchanger circuit of the suction accumulator. The purpose of this is to insure that liquid refrigerant is boiled off from the accumulator reservoir so that only oil remains to be returned to the crankcase of the compressor. Hand shut off valve (10) is only used to isolate the liquid line if servicing is required. From this point two circuits are available depending on the temperature required to be controlled. Evaporator 1 (item 15) is used when the compressor is operating with 4 cylinders (i.e. 66% capacity) and evaporator 2 when operating with 2 cylinders (i.e. 33% capacity).

Depending on the system required, one of the two solenoid valves 11 or 12 is energized to open and allow liquid refrigerant to flow to the thermostatic expansion valve 13 or 17 depending on the system. The thermostatic expansion valves used are of the balanced port type previously described in chapter 2. This type of thermostatic expansion valve is necessary due to the very wide evaporating temperature range of operation. The capacity of the system at -40°F (-40°C) evaporating temperature is only a fraction of the capacity at 15°F (-9.4°C) and as a result the valve will be oversized at low evaporating temperatures. Therefore the valve used has to be able to modulate at a small percentage of its rated capacity and as discussed in Chapter 2 the balanced port expansion valve is designed precisely for that purpose. The solenoid valves 28 and 29 on the lines branching from the inlet of the refrigerant distributors 14 and 18 are closed during the refrigeration cycle and open only during the defrost cycle.

From the expansion valve the wet-vapor passes through refrigerant distributor 14 or 18 to the evaporators. The refrigerant distributor is an essential device for systems using multi circuit evaporators. This is because by weight the wet-vapor is predominantly liquid, but the vapor occupies the greater volume. The liquid and vapor tend to move at different velocities and separate into two layers, with the heavier liquid to the bottom. When a distributor is not used, some of the evaporator circuits may receive the greatest share of liquid. The other circuits, accepting a concentrated share of the vapor, are relatively inactive and the total effective evaporator area is reduced. From the evaporator slightly superheated gas goes to hot gas defrost gas valves 16 or 18. During the refrigeration mode the valve coil is deenergized

and gas is permitted to flow to check valve 21. From check valve 21 suction gas passes through suction filter 22 and then enters suction accumulator 23. As has already been mentioned the function of the suction accumulator is to prevent liquid refrigerant and oil from entering the compressor in large particle form, that may damage compressor valves. This is achieved by collecting the oil and liquid refrigerant in its reservoir and then metering it through an orifice to the suction gas stream in a finely atomized form. In this system the oil return line from the oil separator is connected to the suction accumulator inlet so that oil is returned to the crankcase through the accumulator. To boil off any excess liquid refrigerant from the accumulator oil-refrigerant mixture, a heat exchanger circuit is provided in the accumulator reservoir. As shown in Figure 15 liquid refrigerant passes through the accumulator heat exchanger to accomplish this feat. Suction gas is prevented from going to the reevaporator suction line by check valve 25. From the suction accumulator the suction gas stream enters the compressor and the cycle is completed.

As can be seen from Figures A3 to A8 of Appendix III the chamber cooling system evaporates below 32°F (0°C) throughout the operating temperature range. Therefore frost will build up on the evaporator coils and during operation they will have to be defrosted. Electric heat defrost methods are the simplest in operation but result in large room temperature increases during the defrost cycle. Thus the chamber cooling system has been designed with a hot gas defrost system which results in the smallest room temperature increases possible. Since the system operates at various evaporating temperatures, suction pressure can not be used to initiate the defrost cycle as is usually done on conventional

demand defrost systems. Similarly since humidity in the chamber will not be controlled it also can not be used to initiate the defrost cycle. The system used is an experimental system soon to be released on the market manufactured by Cusco Electronics Ltd. in Montreal, Canada. This system uses a photocell as the sensing device to actually measure the amount of ice built up on the evaporator coil. The sensor is located on a fin of the coil and emits light through a perforation on a plate which becomes an extension of the evaporator coil fin. When this perforation is filled in by ice built up, light does not pass through and a switch is closed to initiate the defrost cycle. Two such sensors are used, one on each evaporator coil.

To understand the defrost cycle assume that the evaporator defrost sensor has just initiated the defrost cycle for system 1. Solenoid valve 4 has closed and discharge gas is diverted to hot gas defrost valve 16 which has been energized by the defrost cycle to close the suction passage and allow discharge gas to pass through it to the outlet of evaporator 1. Note that hot gas defrost valve 20 is still deenergized and no discharge gas can pass to evaporator 2. Discharge gas condenses in evaporator 1 and in so doing rejects heat to the ice on the evaporator and begins to melt it. Refrigerant at the outlet of the evaporator may not be fully condensed because the evaporator fan is stopped when the defrost cycle is initiated and as a result the capacity of the evaporator to act as a condenser is reduced. Thus liquid-vapor mixture passes through solenoid 28 which has been energized by the defrost initiation (solenoid 29 is still closed) to the water cooled condenser 27 where it is fully condensed. Liquid refrigerant from the condenser outlet enters the thermostatic expansion

valve and it then passes through the reevaporator circuit of reservoir 5 where it exchanges heat with the glycol which has been heated by discharge gas during the refrigeration mode. In evaporating, the glycol temperature is reduced until the defrost cycle is completed. From the reevaporator outlet superheated gas enters the suction accumulator through check valve 25. From the suction accumulator the gas enters the compressor suction to complete the cycle. Note that suction gas can not back feed to evaporator 1 or evaporator 2 due to check valve 21. When the ice on the evaporator coil is melted the perforation on the sensor will open and the defrost cycle will be terminated, and system will enter the refrigeration mode by energizing solenoids 4 and 11 and deenergizing solenoids 28 and 16. In a similar fashion evaporator 2 is defrosted when its sensor initiates the defrost cycle.

4.3 TEST PROCEDURE

The purpose of the experiment is to evaluate the performance of the modified refrigeration system at varying condensing temperatures and investigate its advantages and limitations. Data to be used for the theoretical prediction of system performance are also obtained.

The blanked suction test was performed first, this test is very simply performed on any installed system. With the test refrigeration system in operation for a period of fifteen to twenty minutes the setting of the suction pressure safety control was set at its minimum. If this minimum setting is above the expected vacuum pressure attainable by the compressor it may be disconnected electrically. The suction service valve was closed and the compressor was allowed to run until the suction pressure measured at the suction gallery port of the valve plate had stabilized to some minimum value. This minimum vacuum pressure and the corresponding discharge pressure (measured at the discharge gallery port of the compressor valve plate) were recorded.

These two data have been used to evaluate the compression ratio at which the volumetric efficiency is equal to zero and subsequently calculate the effective clearance volume of the compressor. Based on this effective clearance volume, the theoretical volumetric efficiency and refrigeration capacity of the compressor have been evaluated. The results are discussed in the following chapter.

The second part of the experiment involved the evaluation of performance of the modified air cooled refrigeration system at different evaporating and condensing temperatures. The procedure used to obtain

these conditions is described below making reference to Figure 14.

With the compressor in operation, the glycol flow rate was selected by adjusting valves 22 and 23 to permit glycol collection in a container in a reasonable amount of time and also to produce an initial temperature drop through the evaporator of approximately 10°F (5.5°C). By shutting valve 25 and opening valve 24 glycol was collected in a container and using a stop watch the time required to collect the glycol was recorded. The weight of the glycol collected was also recorded.

As the glycol was being continuously cooled the evaporating temperature of the test system gradually dropped, when it reached 40°F (4.4 °C), the steam valve 27 was opened until the evaporating temperature stabilized. This is explained by the realization that with every cycle the glycol temperature entering the evaporator is reduced and in order for the system to satisfy the load it must evaporate at a lower temperature. The glycol temperature entering the evaporator at a particular condition is prevented from dropping any further by supplying heat to the glycol returning to the reservoir. When the heat supplied is the same as the heat extracted, at the evaporator, the glycol entering temperature and as a result the refrigeration system evaporating temperature will stabilize.

For the first series of tests this evaporating temperature was held constant and the condensing temperature was varied. The first condensing temperature to be controlled was that of 130°F (54.4 °C). This was achieved by physically restricting air flow through a portion of the

the condenser until the condensing temperature measured at T5 was 130°F (54.4°C). However in increasing the condensing temperature the evaporating temperature increased above 40°F (4.4 °C) and the steam rate had to be reduced until the evaporating temperature was stabilized again at 40°F (4.4°C). With evaporating temperature and condensing temperature stabilized at the desired condition, the following data were taken:

- 1) T1 - Glycol inlet temperature to evaporator
- 2) T2 - Glycol outlet temperature from evaporator
- 3) T3 - Temperature of liquid refrigerant entering the expansion valve
- 4) T4 - Refrigerant temperature leaving the expansion valve
- 5) T5 - Condensing temperature
- 6) TR1 - Pressure of liquid refrigerant entering expansion valve
- 7) TR2 - Pressure of refrigerant leaving expansion valve
- 8) TR3 - Condensing pressure
- 9) Power input to Compressor.

To obtain the condition of 40°F (4.4°C) evaporating temperature and 110°F (43.3°C) condensing temperature, a portion of the restriction on the condenser face area was removed until the condensing temperature dropped to 110°F (43.3°C). Consequently the evaporating pressure dropped and the steam rate was increased until the evaporating temperature stabilized again at 40°F (4.4°C). Data points 1 to 9 previously mentioned were recorded.

The two conditions at 90°F (32.2°C) and 70°F (21.1°C) presented difficulty from the fact that the chamber cooling system had to be used to lower and maintain the chamber temperature to levels resulting in

the above condensing temperatures. As stated in the previous section the chamber cooling system can control temperatures from 26°F to 45°F (-3.3°C to 7.2°C) while compressor, condenser, and evaporator are balanced. To operate the modified system at condensing temperatures of 90°F and 70°F the chamber temperature had to be reduced to approximately 75°F and 55°F respectively. These two points are outside the operation envelopes of the cooling system and as such continuous operation at these conditions is not recommended as far as compressor life is concerned. However adequate care in designing the system permits operation in those conditions provided the system is continuously monitored.

Continuing with the test procedure the chamber thermostat was set at some value considerably lower than the chamber temperature to be maintained. As the chamber temperature was being reduced the condensing temperature of the test unit began dropping. When the condensing temperature reached 90°F (32.2°C) the thermostat setting was increased until its contacts opened and the chamber cooling system entered the pump down cycle and stopped. At that condition the thermostat setting was at the correct point so that the chamber temperature modulated above the condition resulting to a condensing temperature on the test unit of 90°F (32.2°C). Since the chamber ambient temperature fluctuated as its cooling system went on and off the test unit condensing temperature also fluctuated proportionally. In every instance the chamber thermostat was adjusted until the test unit condensing temperature modulated about 90°F (32.2°C). Again as in previous situations where the condensing temperature of the test unit was reduced, its evaporating temperature dropped and the steam rate to the steam/glycol heat exchanger had to be increased

until the evaporating temperature stabilized again the 40°F (4.4°C) condition. Again readings 1 to 9 were recorded. The procedure of this paragraph was repeated to obtain readings at lower condensing temperatures.

Having completed the tests at 40°F (4.4°C) evaporating temperatures the complete procedure was repeated for evaporating temperatures of 30°F, 20°F, 10°F, 0°F, -10°F (-12°C, -6.67°C, -17.77°C, -23.3°C).

The series of tests described below were used to evaluate the performance of the condensing pressure control system. The first was the simulation of the condition where, the pressure differential, between the pressure of the liquid refrigerant entering the expansion valve and the saturated liquid refrigerant at that temperature, is below the minimum setting of the differential pressure control used to monitor that difference. Heat was supplied through heaters to the liquid refrigerant entering the expansion valve until the differential control closed its contacts and supplied heat to the condensing pressure control bulb heater.

The second was the simulation of the condition where the difference in pressure, between the saturated pressure of the liquid refrigerant entering the expansion valve and the pressure at the outlet of the expansion valve, is below the minimum setting of the differential control used to monitor that difference. The subcooler (item 11) of figure 14 was activated by closing valve 9 and opening valves 10 and 12. This ensured that the first condition mentioned above would not reoccur. The condensing temperature was then lowered, by lowering the chamber temperature until the second differential control closed its contacts and energized the heater. The results of this test are discussed in the following chapter.

CHAPTER 5

DATA REDUCTION AND DISCUSSION

As can be seen from Figures 16, 17 and 18, experimental and theoretical values have been evaluated and plotted for refrigeration capacity, power consumption, and coefficient of performance. Theoretical prediction of volumetric efficiency and compression efficiency has been plotted on Figure 19.

In discussing the method in which test data have been obtained Figure 3 will be used. To evaluate the capacity of the modified refrigeration test system resulting from the test described in chapter 4, first the amount of heat transferred from the glycol to the evaporating refrigerant in the chiller is found by

$$Q = \dot{m}_g C_{pg} \Delta t_g \quad (5-1)$$

where \dot{m}_g = glycol flow rate through the chiller

C_{pg} = specific heat of glycol

Δt_g = temperature difference of glycol between entering and leaving conditions from the chiller.

The mass flow rate of the glycol through the chiller is that found by dividing the weight of the glycol collected, by the time it was collected in. The specific heat of glycol has been obtained from data published in ASHRAE HANDBOOK OF FUNDAMENTALS [18] and has been evaluated at the mean temperature of the glycol entering and leaving the chiller. The glycol temperature difference entering and leaving the chiller is taken directly from the test data.

To be able to compare experimental and theoretical data the capacity has to be evaluated at zero degrees subcooling at the entrance of the expansion valve. As has been already discussed this was not the case in the actual experiment and thus the contribution of the amount of subcooling to the total heat transferred from the glycol in the chiller has to be subtracted. This was done by first evaluating the refrigerant flow rate by

$$\dot{m}_R = \frac{Q}{h_g - h_6} \quad (5-2)$$

where Q = total heat transferred from glycol in the chiller as evaluated by equation (5-1)

h_g = enthalpy of saturated refrigerant vapor at suction pressure and temperature

h_6 = enthalpy of subcooled refrigerant entering the expansion valve.

Having found the refrigerant mass flow rate the refrigeration capacity of the modified aircooled outdoor refrigeration test system at zero subcooling is found by,

$$Q_{rt} = \dot{m}_R (h_g - h_{10}) \quad (5-3)$$

where \dot{m}_R = refrigerant mass flow rate

h_{10} = enthalpy of saturated liquid refrigerant evaluated at the pressure entering the expansion valve.

The capacity of the modified refrigeration test system at zero subcooling is plotted on Figure 16 versus condensing pressure at constant evaporating temperatures. On the same graph the theoretical capacity

is plotted as calculated from equation (3.63). The equation used to calculate the volumetric efficiency was equation (3.32) where R_0 has been found from the blanked suction test, described in chapter 4. Equation (3.63) shows the capacity of the system as evaluated with $T_{10} - T_8$ of subcooling. The theoretical data have all been evaluated at zero subcooling by using $(h_9 - h_{10})$ instead of $(h_9 - h_8)$ in equation 3.63.

The experimental data curve of figure 16 clearly shows that as the condensing pressure drops the refrigeration capacity of the system increases. Note that under certain conditions the capacity of the system increased by as much as 90%. However, the system will operate at these conditions a very small percentage of the year, and the effective capacity increase will result from the average yearly ambient temperature of the area where the system is located. From the theoretical data plotted on the same graph it is seen that the equation for volumetric efficiency permitted calculation of the system capacity with results which are close to the experimental. The average percent difference between experimental and theoretical is $\pm 5\%$.

Figure 17 illustrates good agreement between the experimental and the theoretical power consumption curves. The theoretical power consumption has been calculated using equations (3.61), (3.17) and (3.59). The constant K in equation (3.59) has been evaluated by using the power consumption from one of the test points. Again it is seen that the power consumption decreases as the condensing pressure decreases.

An increase in capacity combined with a decrease in power consumption as the condensing pressure is decreased results in an

increase in coefficient of performance. This is depicted in figure 18 when both experimental and theoretical coefficient of performance curves are shown. The experimental coefficient of performance has been evaluated by dividing the experimental refrigeration capacity by the experimental power consumption and conversion constant (to convert electrical power units to thermal units). The theoretical COP has been calculated using equation (3.65). Again the correlation between experimental and theoretical data is very good.

The theoretical volumetric efficiency curve of Figure 19 shows that the volumetric efficiency is a function of the compression ratio only and increases with a decrease in condensing pressure. The compression efficiency curve of Figure 19 illustrates that a condensing pressure decrease results in a corresponding compression efficiency decrease. Examining equation (3.59) shows that, for a fixed evaporating pressure (p_1), a decrease in condensing pressure and consequently compression ratio causes the term $\frac{n}{n-1} (R_c \frac{n-1}{n} - 1)$ to decrease while $KP^{\frac{1-n}{n}}$ increases due to the volumetric efficiency increase. The constant K in equation (3.59) is partly comprised of two other constants, K_1 and K_2 described by equations (3.52) and (3.55) respectively. It is seen that in order to increase the compression efficiency the value of K and consequently of K_1 and K_2 must be kept as small as possible. It follows then that large suction and discharge valve port areas will increase compression efficiency.

The benefits of the modified aircooled refrigeration system operating at varying condensing pressures has been verified by the experimental results of refrigeration capacity, power consumption and coefficient of performance already discussed. To examine the

operation of the condensing pressure control system the two conditions under which the system will control the condensing pressure, even if the ambient temperature continues to fall, have been simulated. Figure 20 shows a strip chart recording of the operation of the system. The pressure on strip 2 is the pressure inside the dome of the condensing pressure control. Strip 3 shows the pressure at the inlet of the expansion valve and strip 4 the pressure at the outlet of the expansion valve. The chart motion is as indicated by the arrow. While the system was operating normally, heat was supplied to the liquid line feeding the expansion valve, to decrease the amount of subcooling until the differential control measuring the pressure difference between points 6 and 7 of figure 3 sensed its minimum value and closed its electrical contacts. At this point the condensing pressure had to be controlled. The closing of the differential control contacts energized the condensing pressure control bulb heater and the pressure in the dome increased causing the control to bypass discharge gas to the liquid refrigerant and increase the condensing pressure. Note that as the bulb pressure increases so that the liquid refrigerant pressure entering the expansion valve. As soon as this pressure begins to increase the pressure difference between points 6 and 7 of figure 3 is increased and the differential control contacts open to cut power to the bulb heater. The dome pressure and condensing pressure start falling until the differential control senses the same condition and energizes the heater to repeat the cycle. After the second cycle the chamber temperature was decreased without affecting the ability of the condensing pressure control system to operate properly. As predicted by the design, the condensing pressure was prevented from dropping

although the ambient temperature was continuing to fall.

To test the operation of the second differential pressure control, the supply of heat to the liquid refrigerant was removed allowing the condensing pressure to fall with the ambient temperature.

Both the dome pressure of the condensing pressure control and the liquid refrigerant pressure entering the expansion valve dropped as shown in Figure 21. To prevent the differential control measuring $P_6 - P_7$ from initiating control of condensing pressure, the air cooled subcooling circuit was put into operation. This ensured that the difference in pressure between points 6 and 7 of Figure 3 was above the minimum setting of the differential control. The ambient temperature was then lowered until the second differential control measuring the difference in pressure between point 7 and 8 of Figure 3 closed its contact and energized the condensing pressure control bulb heater to control the condensing pressure. Figure 22 shows that the condensing pressure control system periodically increased the condensing pressure by supplying heat to the bulb and increasing the dome pressure of the condensing pressure control. Comparing Figures 20 and 22 it is seen that the amplitude of the condensing pressure modulation is much higher in Figure 20 than figure 22. This is explained by the fact that at higher ambient temperatures more heat is supplied to the bulb by the heater than at low ambient temperatures. An arrangement that will minimize the heat loss of the bulb heater to the atmosphere will permit a smaller heater to be used that will create the same amount of condensing pressure modulation at high and low ambient temperatures. Insulation of the bulb heater resulted in a small amplitude condensing pressure modulation with a high occurrence of heater turnouts.

Numerous tests revealed that the modified condensing pressure control system operates according to the intended design. When the liquid refrigerant pressure at the entrance of the expansion valve approaches the saturated liquid pressure at the entrance temperature one of the differential pressure controls initiates condensing pressure control. This always ensures that the liquid refrigerant entering the expansion valve is subcooled.

Similarly when the saturated liquid refrigerant pressure at the temperature entering the expansion valve approaches the evaporating pressure the second differential pressure control initiates the condensing pressure control action. This ensures that the condition where subcooled liquid exist at the outlet of the expansion valve never occurs.

Figures 20 to 22 show that the thermostatic expansion valve modulates to control the amount of superheat of the refrigerant vapor at the outlet of the evaporator. According to valve specifications this modulation has an amplitude of 3 psi (20.67 Kpa) when selected properly. In this experiment the modulation amplitude has been consistantly 5 psi (34.45 Kpa). All attempts to reduce this amplitude were fruitless leading to the conclusion that excessive friction between the piston seal and the piston chamber was present, causing the valve to overshoot with every adjustment (see Figure 6). This is substantiated by the fact that this amplitude of modulation was present under all operating conditions. At low compression ratios illustrated in figure 22 the balanced port expansion valve is operating at rated conditions which means that the amplitude of modulation is at

its minimum. At high compression ratios depicted in Figure 20 the expansion orifice required is smaller than that at low compression ratios and the expansion valve is now oversized. If the increased amplitude of modulation occurring at low compression ratios was an indication of slight hunting this amplitude of modulation at high compression ratios would increase as the valve entered its zone of instability. As has been already shown the amplitude at the two conditions is identical, indicating proper expansion valve operation and identifying friction as the cause of higher amplitude of expansion valve modulation.

The increase in refrigeration capacity, decrease in power consumption and consequent increase in power consumption at low compression ratios have all been shown in Figure 16 to 18. Although the advantages of the modified outdoor aircooled refrigeration system are considerable, its use has to be limited to certain applications.

Applications such as storage rooms where the product in the winter time enters at a lower temperature than the summer, the load in the winter is considerably smaller. At the same time the capacity of the modified system can be higher by as much as 50% to 80% depending on the operating conditions. These two factors will cause the system to operate in very short cycles, and although shorter running time at reduced power consumption seems very attractive the life of the compressor may be compromised. In addition, a large number of short operating cycles may result in higher operating costs based on peak power pay schedules. Thus unless the excess capacity available under low ambient temperature conditions is utilized the operating savings may be minimal if any.

An ideal application for the modified refrigeration system is blast freezers where a product's temperature is reduced to a certain value and then it is placed in storage. Blast freezers are designed to lower the product temperature in a certain time limit. When the capacity of the system increases the freezing time is lowered and production is increased. Multiple compressor systems are another example of ideal application. In such systems multiple compressors are used to satisfy a constant load. In the winter a number of compressors may be shut down and still satisfy the load. The advantages are obvious when it is considered that less compressors are used at a reduced power consumption to satisfy the same load.

Applications where humidity control is essential are only possible with the modified system under certain conditions. The evaporator is selected for the maximum capacity condition (winter) at a certain temperature difference between room and evaporating temperature. When the capacity of the system is reduced in the summer the evaporator is oversized and in order to balance with the compressor and condenser the temperature difference between room and evaporating temperature is decreased. This variation in temperature difference causes a change in relative humidity in the room. Relative humidity will remain constant only if the change in evaporator capacity is achieved by reducing the air flow through the evaporator or its heat transfer surface area while the difference between room and evaporating temperature remains constant.

Hot gas defrost and capacity control systems are not possible with the modified refrigeration system operating at varying condensing

pressures. Low discharge gas temperatures at low compression ratios are inadequate to create enough heat transfer for defrost. Capacity control using discharge gas is also made difficult due to the large volumes of vapor required to offset small percentages of refrigeration capacity.

CHAPTER 6

CONCLUSIONS

A modified outdoor air cooled refrigeration system was designed to operate at varying condensing pressures overcoming problems usually associated with conventional outdoor refrigeration systems operating at low ambient temperature conditions. Modifications to the conventional refrigeration system were implemented to the expansion device and the condensing pressure control system. A chamber temperature control system was built to simulate ambient temperature conditions resulting in varying condensing pressures.

Detailed testing of the modified air cooled refrigeration system indicates the following:

- 1) as the ambient temperature of the chamber was reduced the test system condensing pressure fell proportionally and as a result the system capacity increased, the power consumption decreased and the coefficient of performance increased.
- 2) the balanced port expansion valve permitted full refrigerant flow at reduced pressure differentials across its expansion orifice. This allowed the refrigeration capacity to increase as the operating compression ratio was decreased. Caution must be used in selecting the expansion valve for the maximum

expected capacity at the lowest expected differential pressure across it.

- 3) in accordance with the design, the condensing pressure control system detected the point at which any further reduction in condensing pressure would result in a refrigeration capacity reduction and or poor expansion valve control and acted to prevent the condensing pressure from dropping further although the ambient temperature continued to fall. Differential pressure controls with a smaller minimum pressure differential setting will permit the refrigeration system to approach optimum operating condition at low ambient temperature situations without inducing loss in capacity or poor expansion valve control.
- 4) an arrangement to minimize heat loss to the atmosphere from the condensing pressure control bulb heater should be found to permit a minimum condensing pressure increase as the heater is energized.
- 5) the increase in refrigeration capacity at low condensing pressure should be utilized against an additional load instead of being used to reduce the system operating time. When the modified system is applied to a fixed refrigeration load the system operating time will be reduced in proportion to the increase in refrigeration capacity as the ambient temperature

drops. The compressor will operate in shorter cycles, drastically reducing its life and perhaps offsetting power consumption savings due to the increased number of starts when the peak power drawn is high. The advantages of the system should be employed in satisfying increased refrigeration loads at reduced power consumption.

- 6) during the winter when the advantages of the system materialize the compressor will also be operating at a reduced compression ratio which will increase the expected life of the compressor.
- 7) humidity control is not possible with the modified refrigeration system unless auxiliary controls are used to vary the evaporator fan speed to maintain a constant temperature difference between room and evaporating temperatures of the system as its refrigeration capacity changes.
- 8) hot gas defrost systems and capacity control systems using discharge gas are not possible with the modified system since a high discharge gas temperature is essential for their operation. At low compression ratios the discharge gas temperature is too low to permit proper operation of these systems.

Equations developed to predict refrigeration capacity power consumption and coefficient of performance showed very close correlation with experimental data and represent an improvement

over equations used presently. Their use makes prediction of system performance with a variety of refrigerants possible. Further work is obtaining data for the polytropic exponent of compression and expansion processes for the common refrigerants will permit a more detailed analysis of compressor performance.

REFERENCES

1. Ashrae Journal, Refrigeration Unit Market Breakdown, Sept. 1973.
2. Sporlan Valve Co., Bulletin No. 90-30, Condensing Pressure Control Valves, February 1973.
3. Alco Valve Co., Bulletin No. 15.71T, Condensing Pressure Control Valves, January 1971.
4. Sheerer J.L., Murphy A.T. and Richardson H.H., Introduction to System Dynamics, Addison-Wesley Publishing Co., 1967.
5. Stoeker W.F., Stability of an Evaporator-Expansion valve Control Loop, Ashrae Transaction, Vol. 72, Part II, P.1V.3.1, 1966.
6. Sporlan Valve Co., Bulletin No. 10-10, Thermostatic Expansion Valves for Refrigeration and Air Conditioning, August 1975.
7. Robert Neidermeir, Sporlan Valve Co., Private Conversation, April 1976.
8. Sporlan Valve Co., Internal Bulletin No. F210-40-15, August 1972.

9. Ashrae Handbook, Equipment Volume, Compressors, Chapter 12, 1975.
10. Hirsh S.R., On the Relation of Compressor Theory to Performance, Ashrac Journal, July 1973.
11. Prestcold Ltd, Internal Film, High Speed Photographic Analysis of Refrigeration Compressor Valve Operation, Theale, England, 1978.
12. Streeter V.L., Fluid Mechanics; McGraw-Hill Co., Fourth Edition, 1966.
13. Kartsonnes G.T. and Erth R.A., Computer Calculation of the Thermodynamic Properties of Refrigerants 12,22,502, Proceedings of the Ashrae Annual Meeting, Volume 77, Part II, August 1971.
14. "Freon" Products Division, E.I. du Pont de Nemours and Co., Bulletins X-88F and X-88B1, Wilmington, Delaware 1969.
15. Martin J.J., Correlations and Equations Used in Calculating Thermodynamic Properties of Freon Refrigerants, Thermodynamic and Transport Properties of Gases, Liquids and Solids, ASME, New York, 1959.
16. "Freon" Products Division, E.I. du Pont de Nemours and Co., Freon Products Bulletin T-22, Wilmington, Delaware, 1966.

17. Martin J.J. and Dowing R.C., Thermodynamic Properties of Refrigerant 502, Ashrae Transactions, Vol. 76, Part II, 1970.
18. Ashrae Handbook, Fundamentals Volume, Secondary Coolants, Chapter 17, 1977.
19. Penn Johnson Controls Co., File No. S-2241-A13, Prototype Differential Pressure Controls for Prestcold North America Ltd, 2221 Camden Court, Oak Brook, Illinois 60521, 1979.

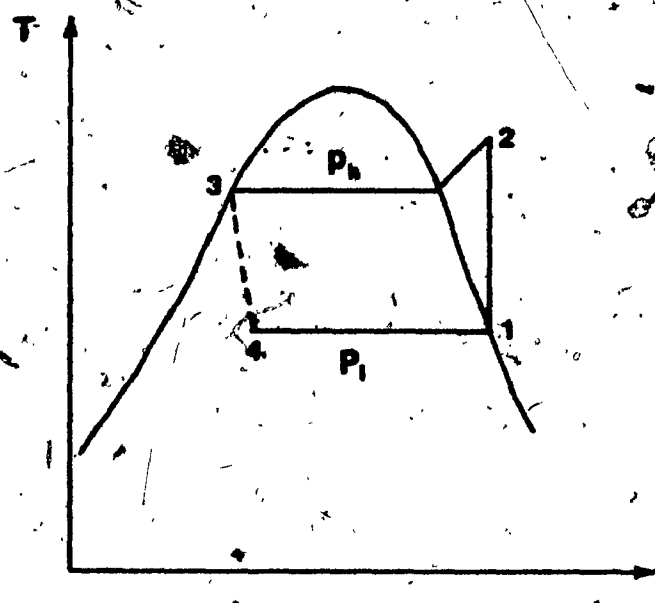


FIG.1 T-S diagram of ideal refrigeration cycle.

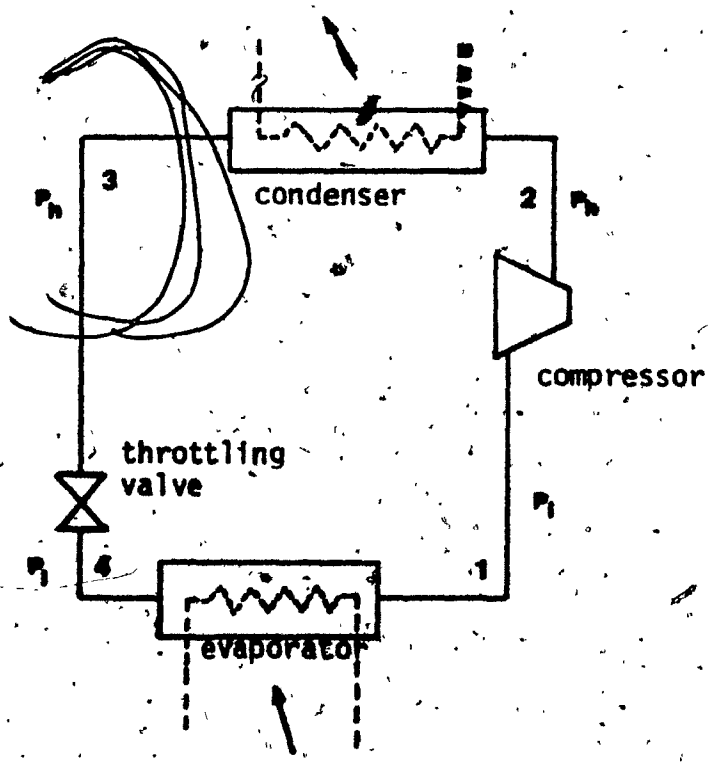


FIG.2 Basic component arrangement of actual refrigeration system.

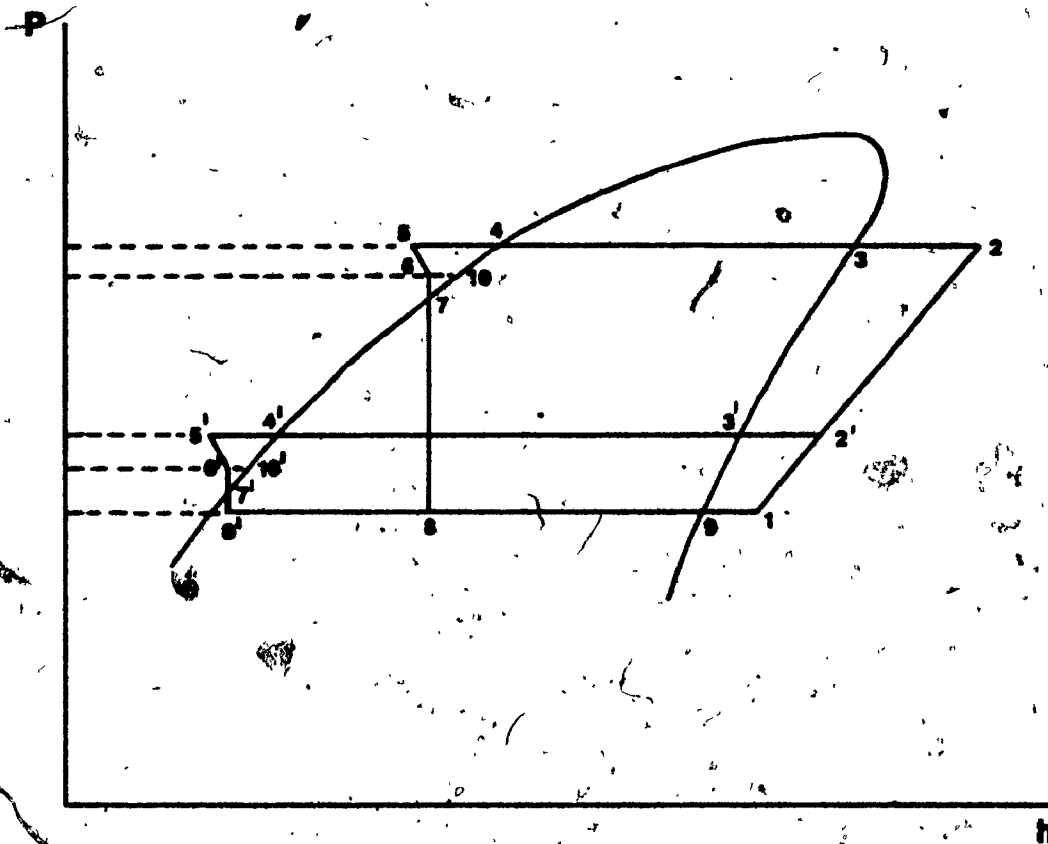


FIG. 3 Ideal refrigeration cycle at high and low condensing pressure.

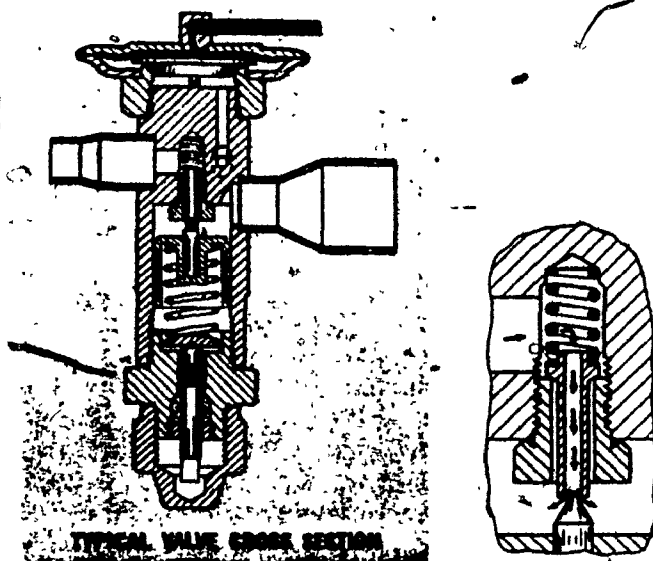


FIG 4. Cross section of typical thermostatic expansion valve
(courtesy of Sporlan Valve Co.)

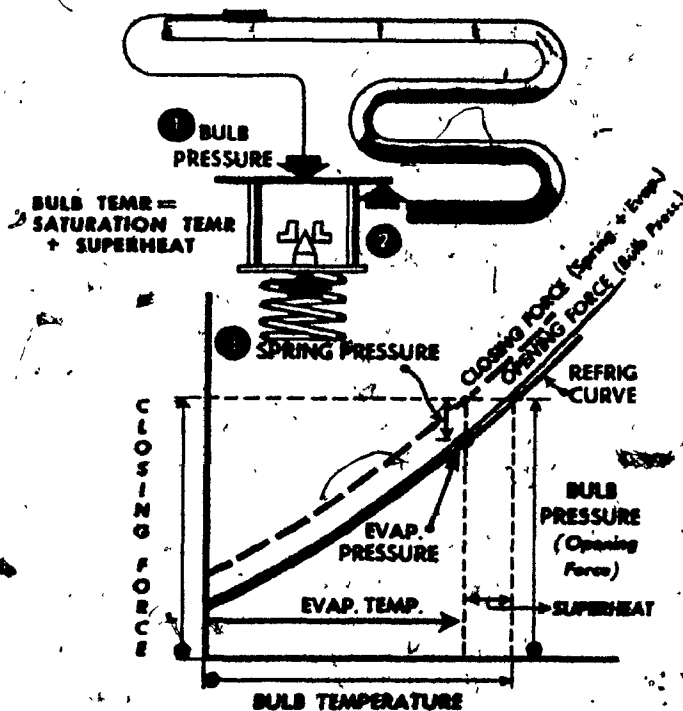


FIG 5. Schematic diagram of thermostatic expansion valve operation.
(courtesy of Sporlan Valve Co.)

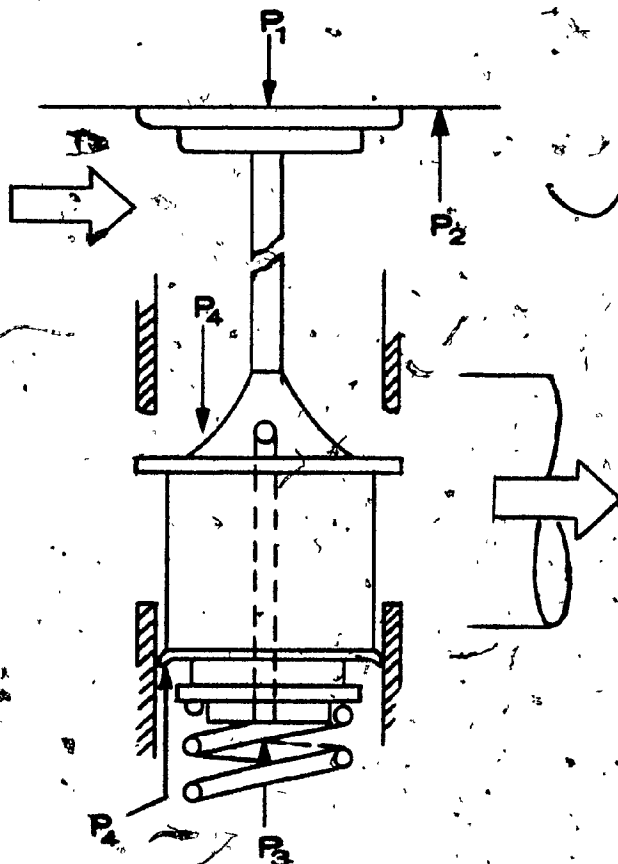


FIG 6 Balanced port thermostatic expansion valve schematic.
(Courtesy of Sportan Valve Company).

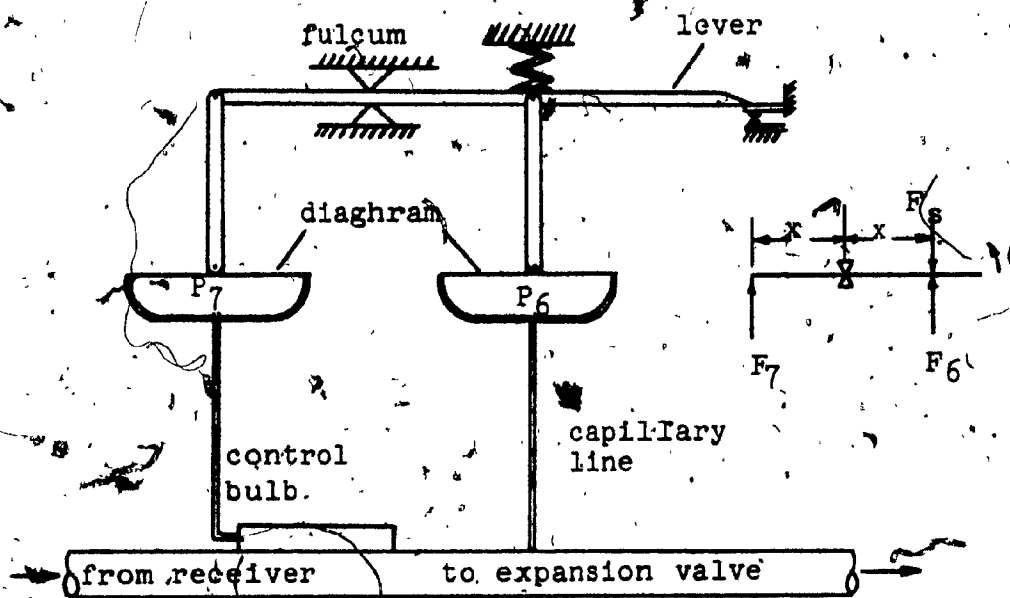


FIG 7 Differential pressure control schematic diagram.

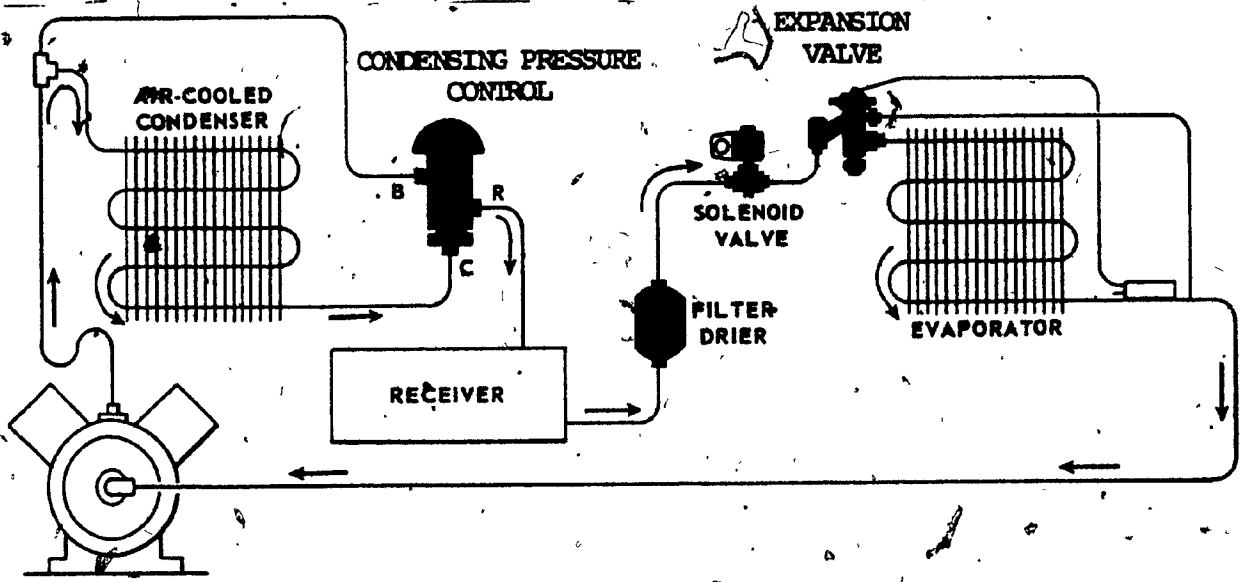


FIG 8 Conventional refrigeration system using condensing pressure control valve.

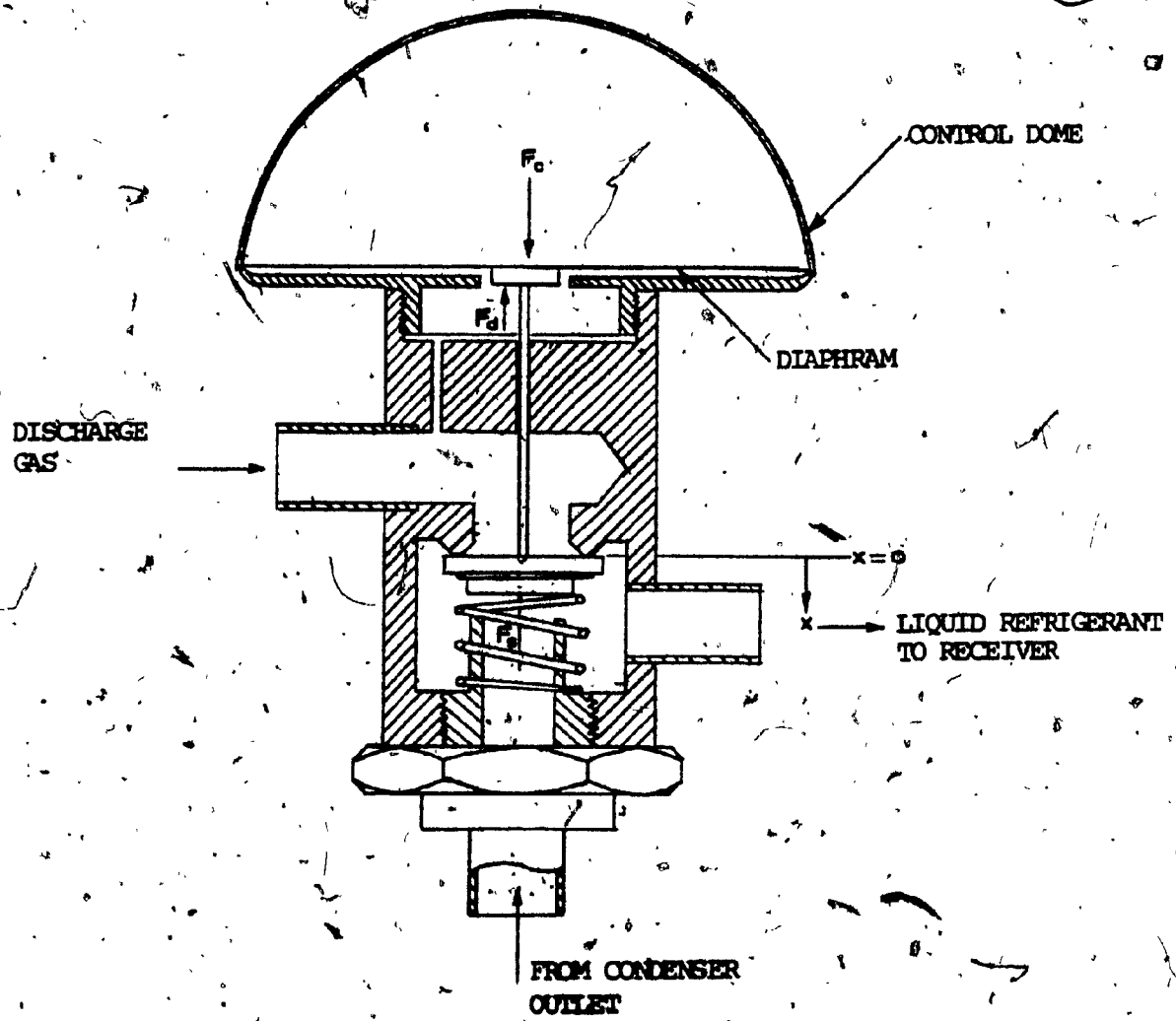


FIG 9 Conventional condensing pressure control valve.

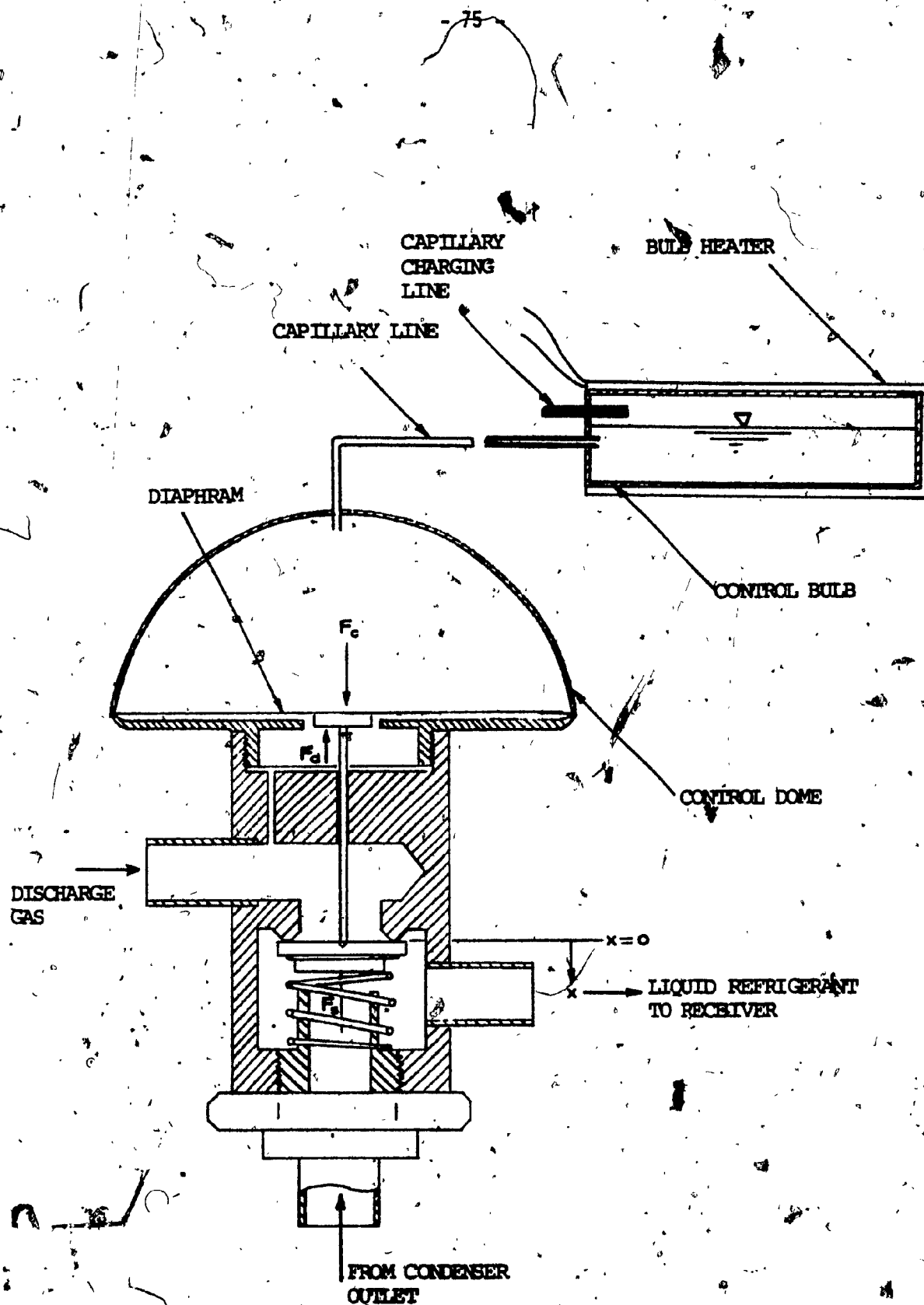


FIG 10 Modified condensing pressure control valve

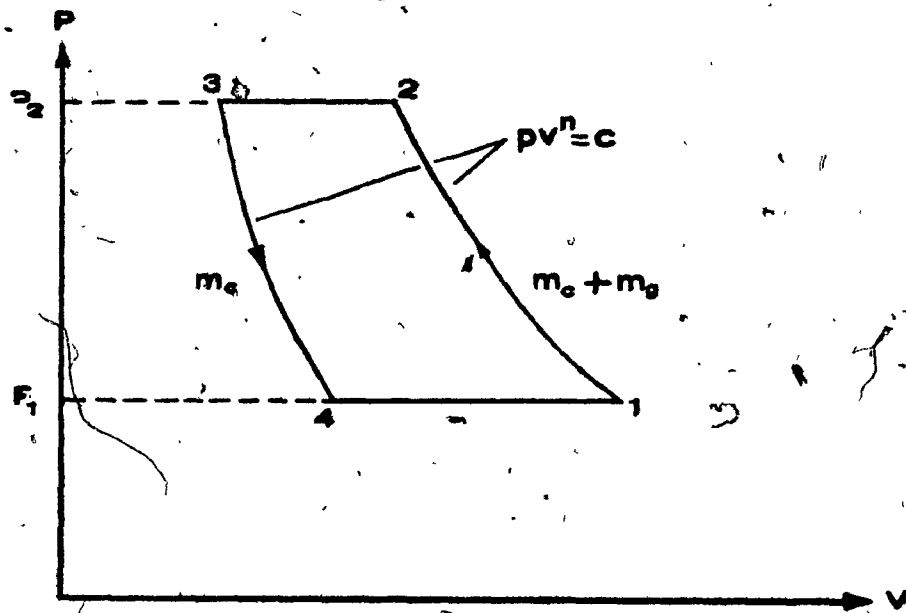


FIG 11 P-V diagram of ideal vapor compression cycle.

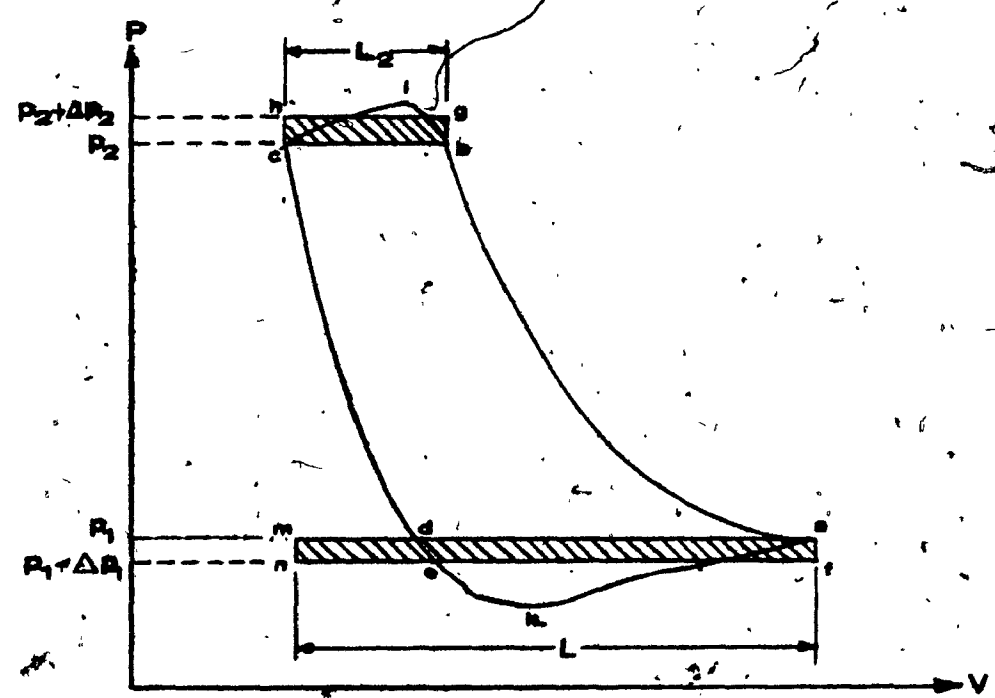


FIG 12 Indicator diagram of refrigeration compressor.

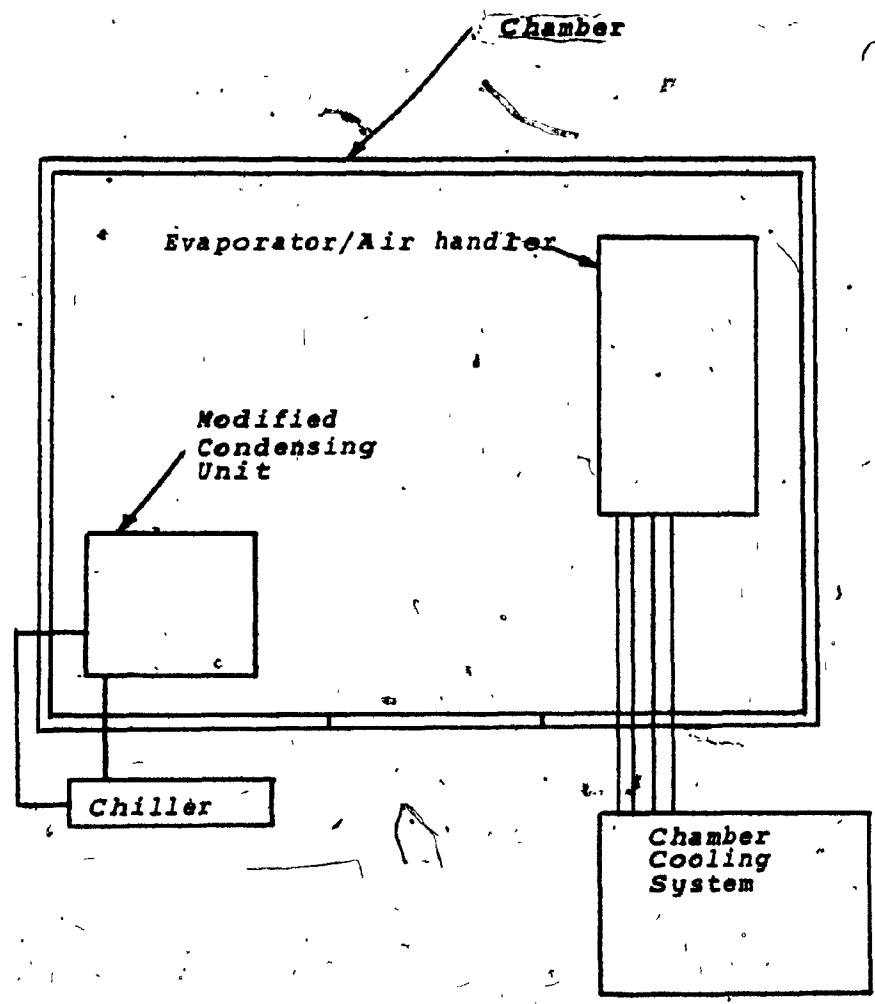
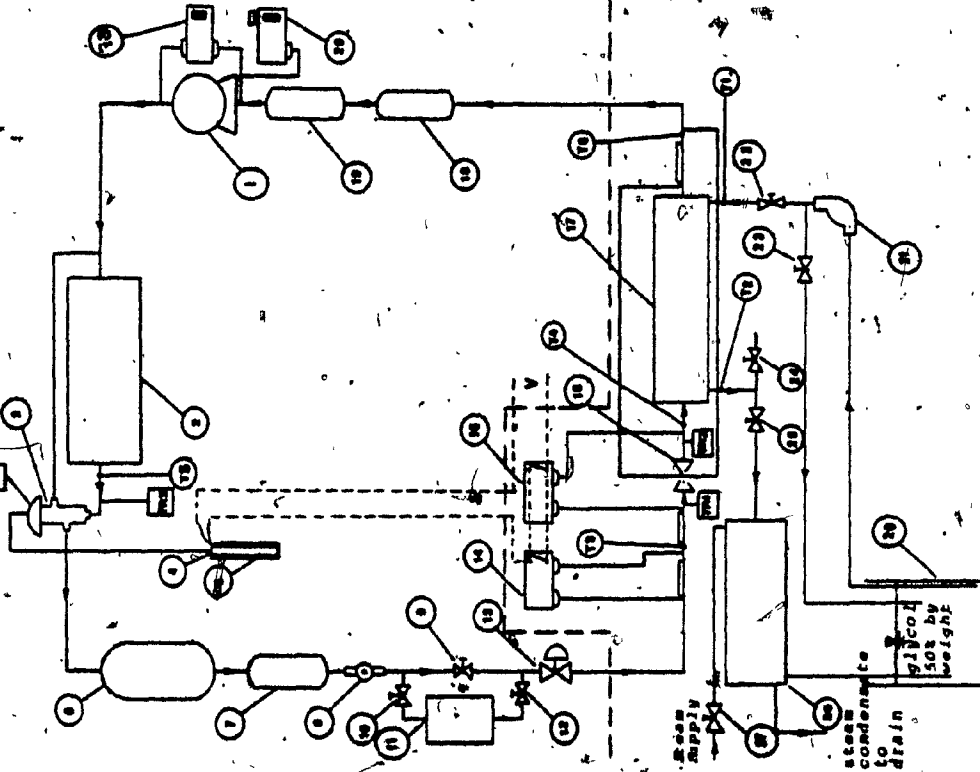


FIG. 13 Overall layout of experimental set-up



- 1 - Compressor
- 2 - Air cooled condenser
- 3 - Modified condenser-pressure control valve
- 4 - Condensing pressure control valve bulb
- 5 - Bulb heater
- 6 - Liquid refrigerant receiver
- 7 - Liquid refrigerant filter - drier
- 8 - Moisture indicator
- 9 - Hand shut-off valve
- 10 - Hand shut-off valve
- 11 - Air cooled liquid refrigerant subcooler
- 12 - Hand shut-off valve
- 13 - Pumpdown liquid line solenoid
- 14 - Differential pressure control
- 15 - Differential pressure control
- 16 - Balanced port expansion valve
- 17 - Evaporator - glycol chiller
- 18 - Section accumulator
- 19 - Section accumulator
- 20 - Glycol pump
- 21 - Hand regulating valve
- 22 - Hand shut-off valve
- 23 - Hand shut-off valve
- 24 - Hand shut-off valve
- 25 - Hand shut-off valve
- 26 - Steam - glycol heat exchanger
- 27 - Steam - regulating valve
- 28 - Discharge suction pressure safety control
- 29 - Suction pressure operating control
- 30 - Pressure transducer - liquid refrigerant leaving expansion valve
- 31 - Pressure transducer - liquid refrigerant leaving expansion valve
- 32 - Pressure transducer - condensing pressure at condenser outlet
- 33 - Pressure transducer - dome pressure of condensing pressure control
- 34 - Thermocouple - glycol inlet temperature to chiller
- 35 - Thermocouple - glycol outlet temperature from chiller
- 36 - Thermocouple - temperature entering expansion valve
- 37 - Thermocouple - temperature leaving expansion valve
- 38 - Thermocouple - condensing temperature
- 39 - Thermocouple - suction temperature at the expansion valve bulb

FIG. 14 Modified refrigeration test system schematic

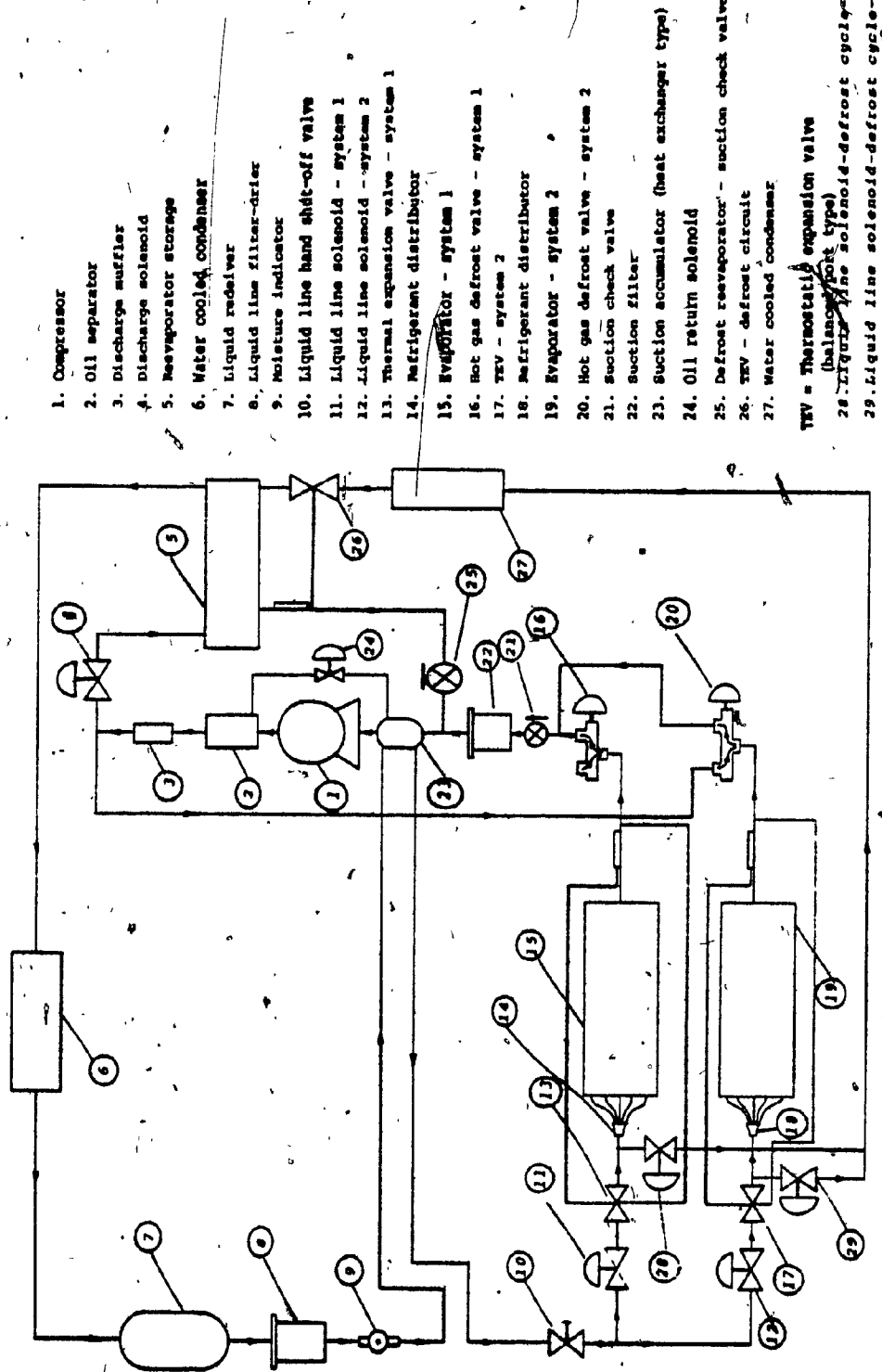


FIG. 15 Chamber cooling system schematic

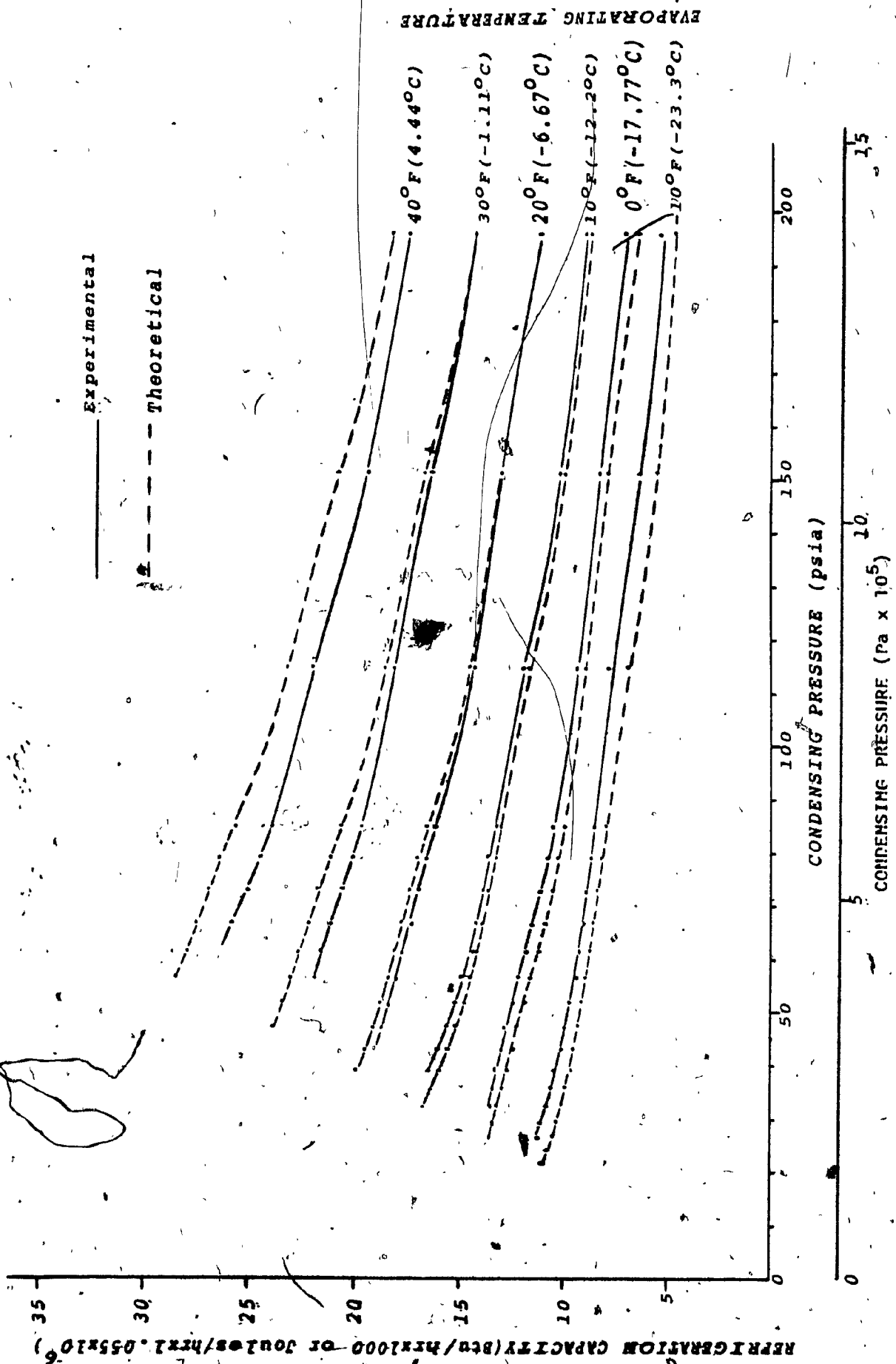


FIG. 16 Experimental and theoretical refrigeration capacity curves

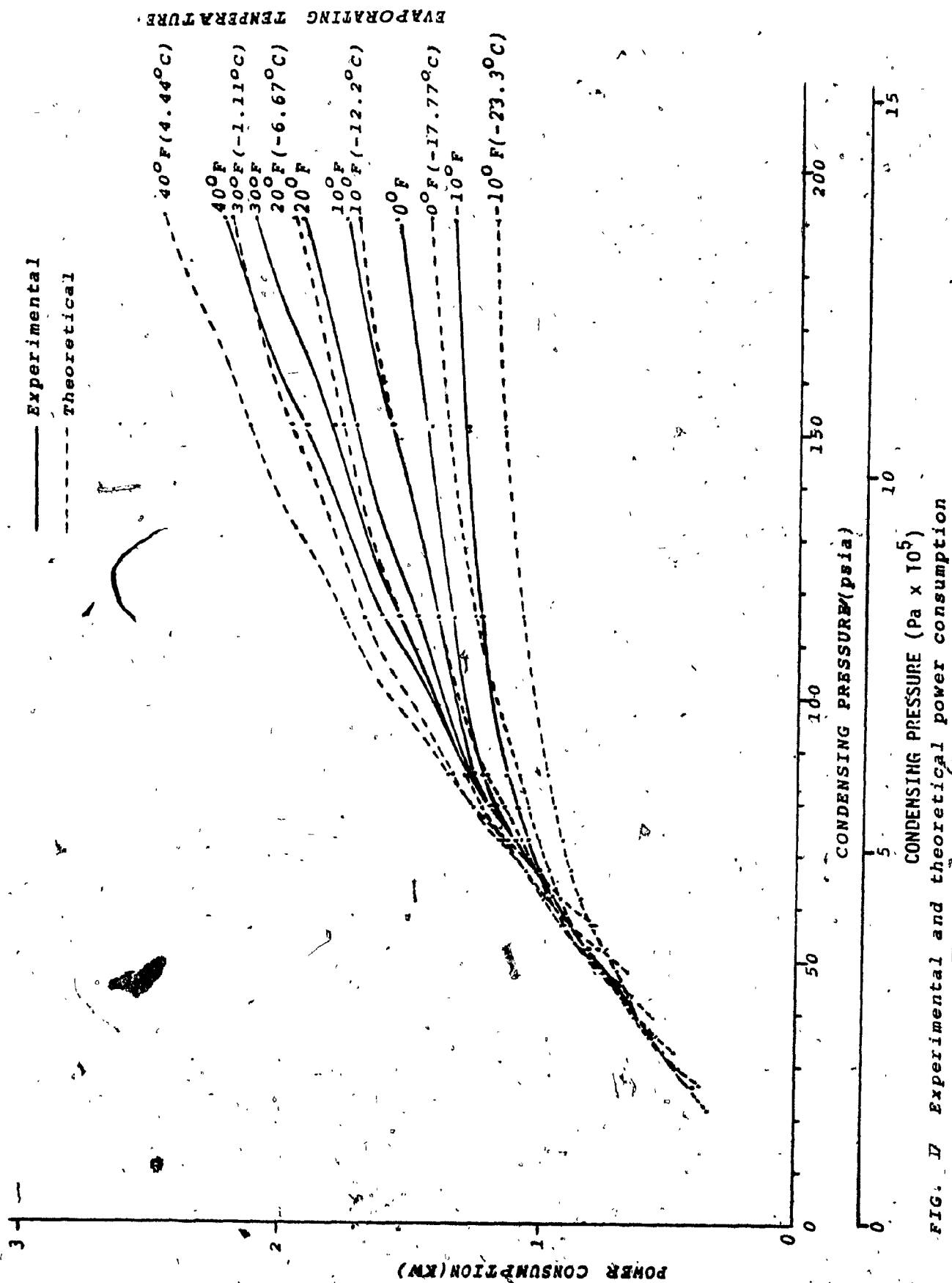


FIG. 17 Experimental and theoretical power consumption

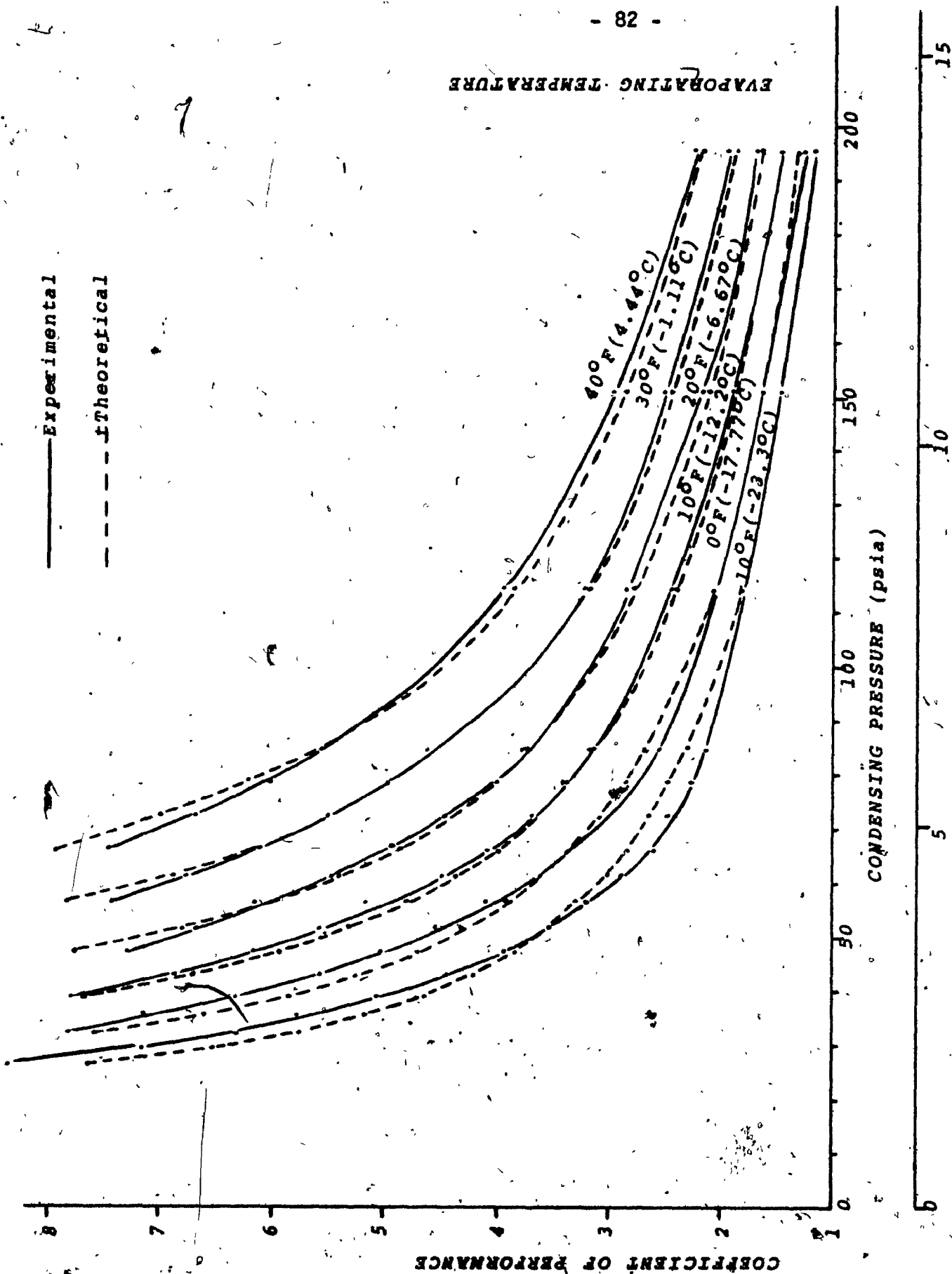


FIG. 18 Experimental and theoretical coefficient of performance

----- Volumetric efficiency
 ----- Compression efficiency

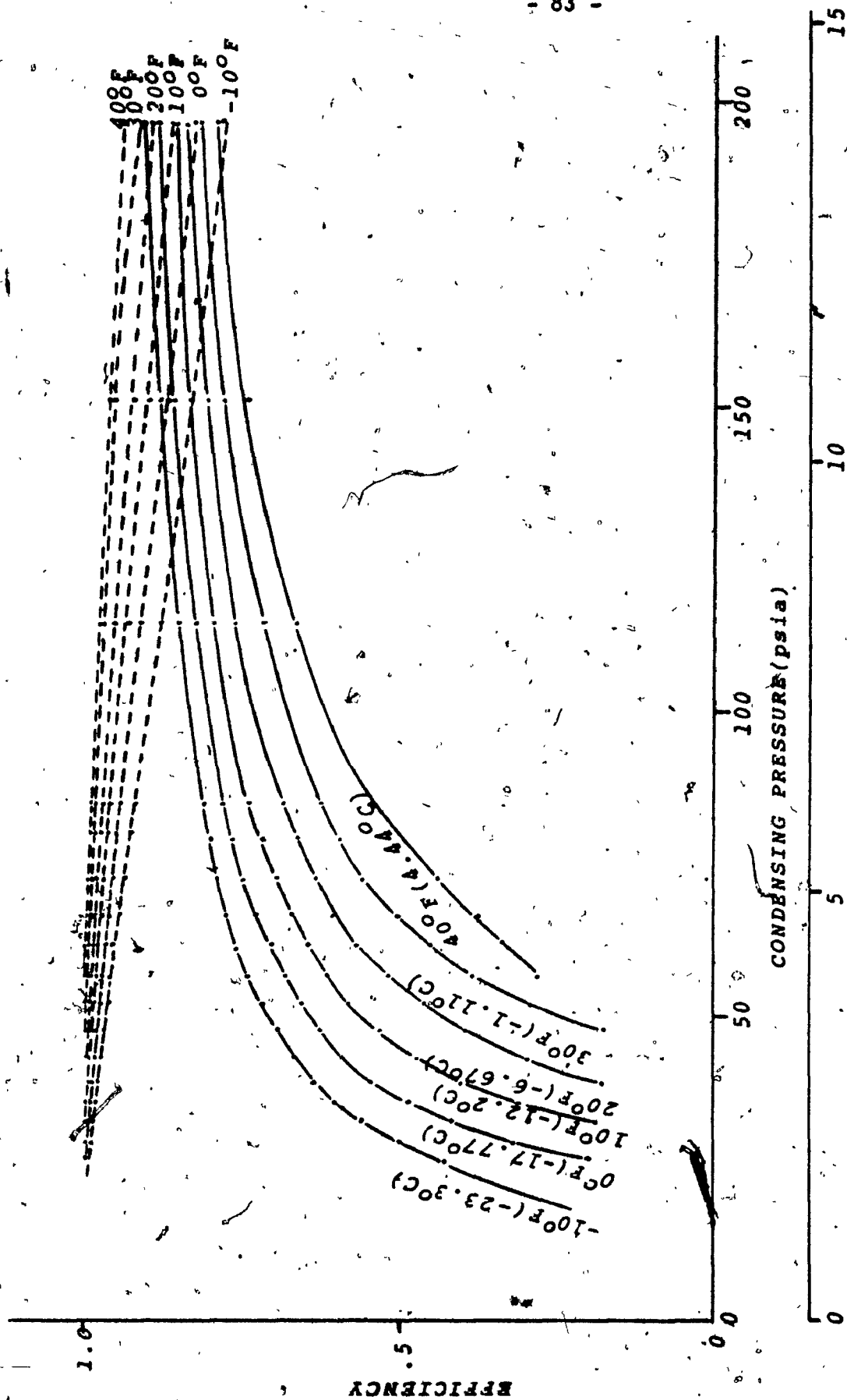


FIG. 19 Theoretical volumetric and compression efficiencies

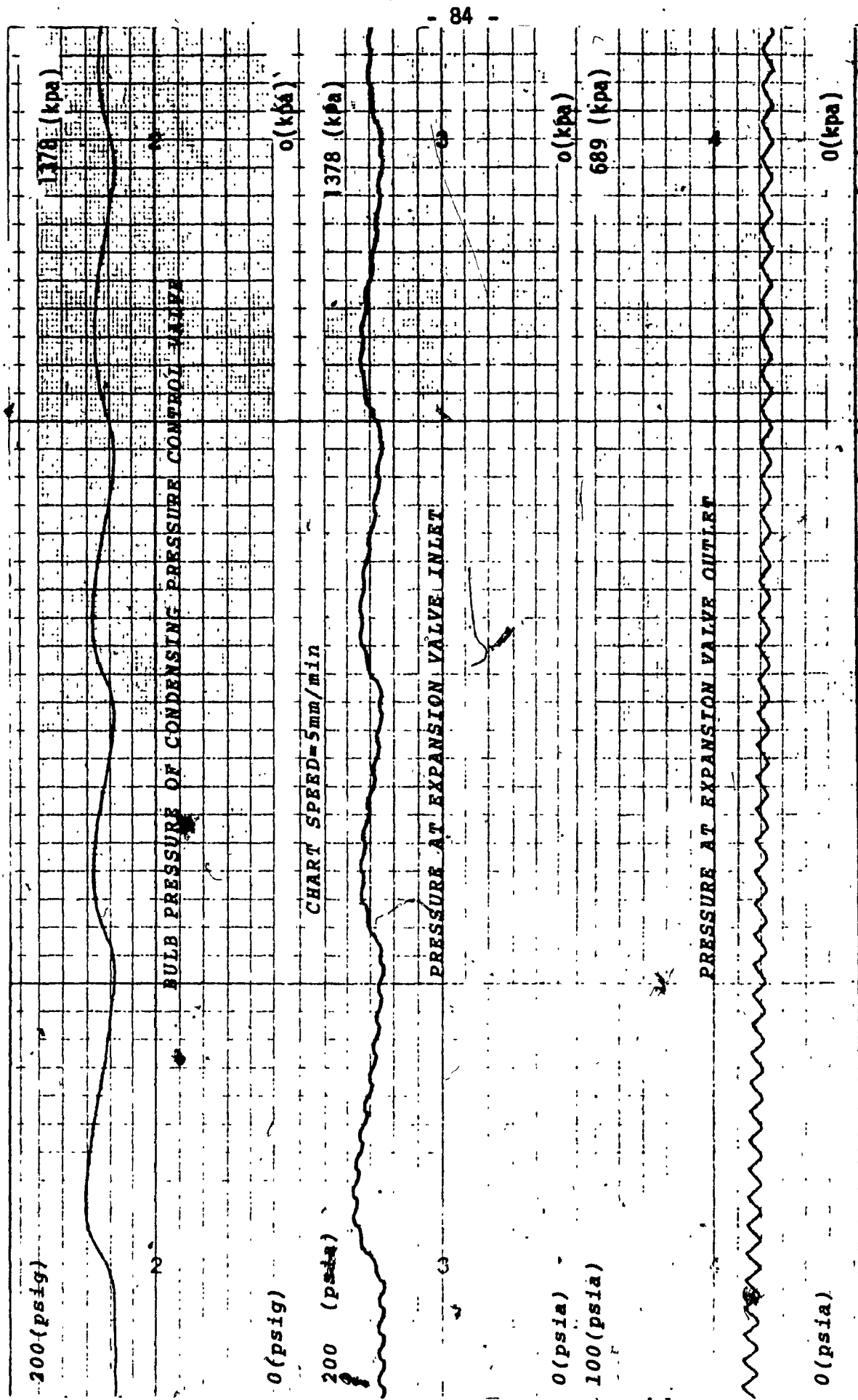


Fig. 20 Modified test system pressure recording.

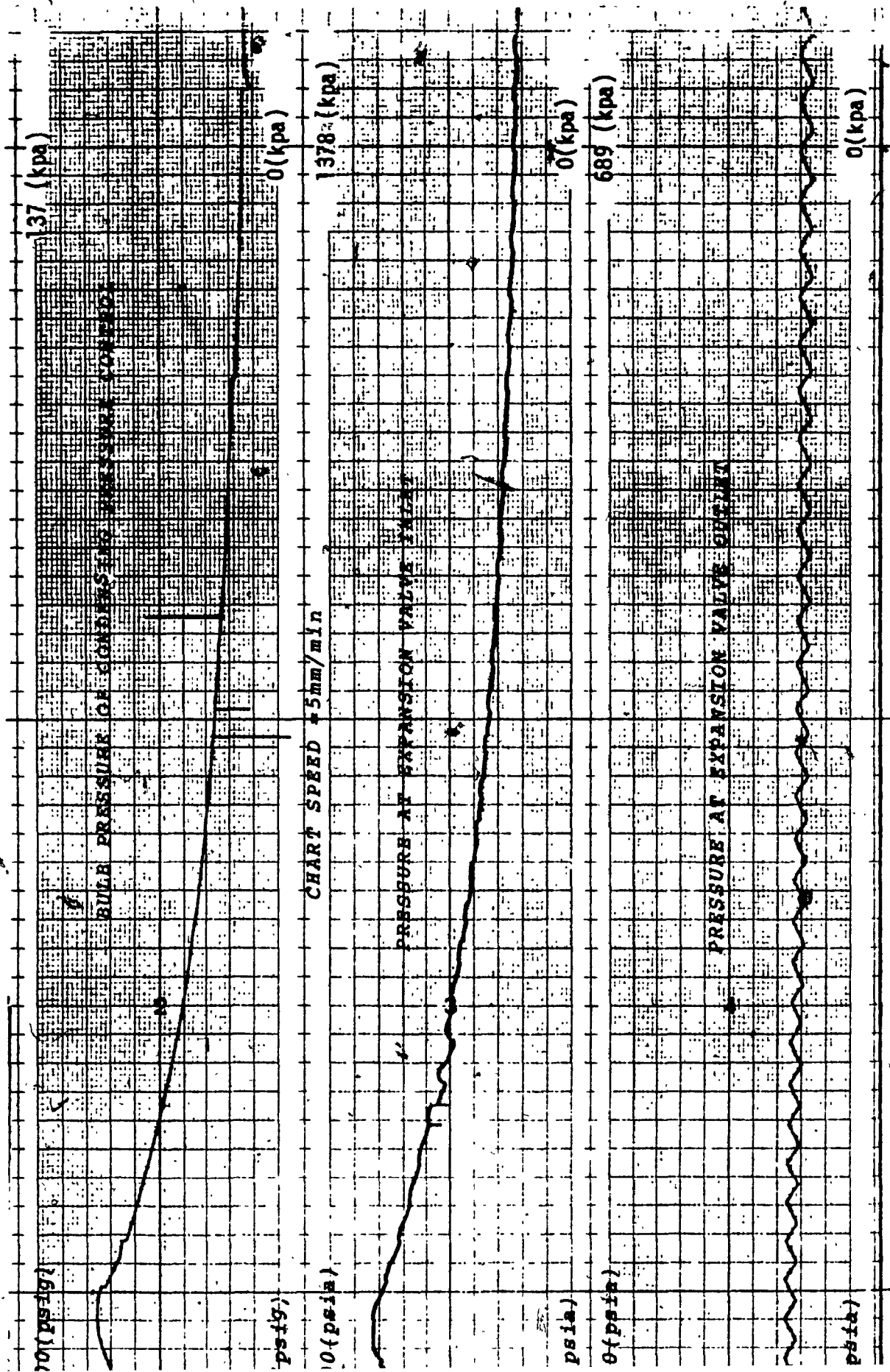


Fig. 21 Modified test system pressure recording.

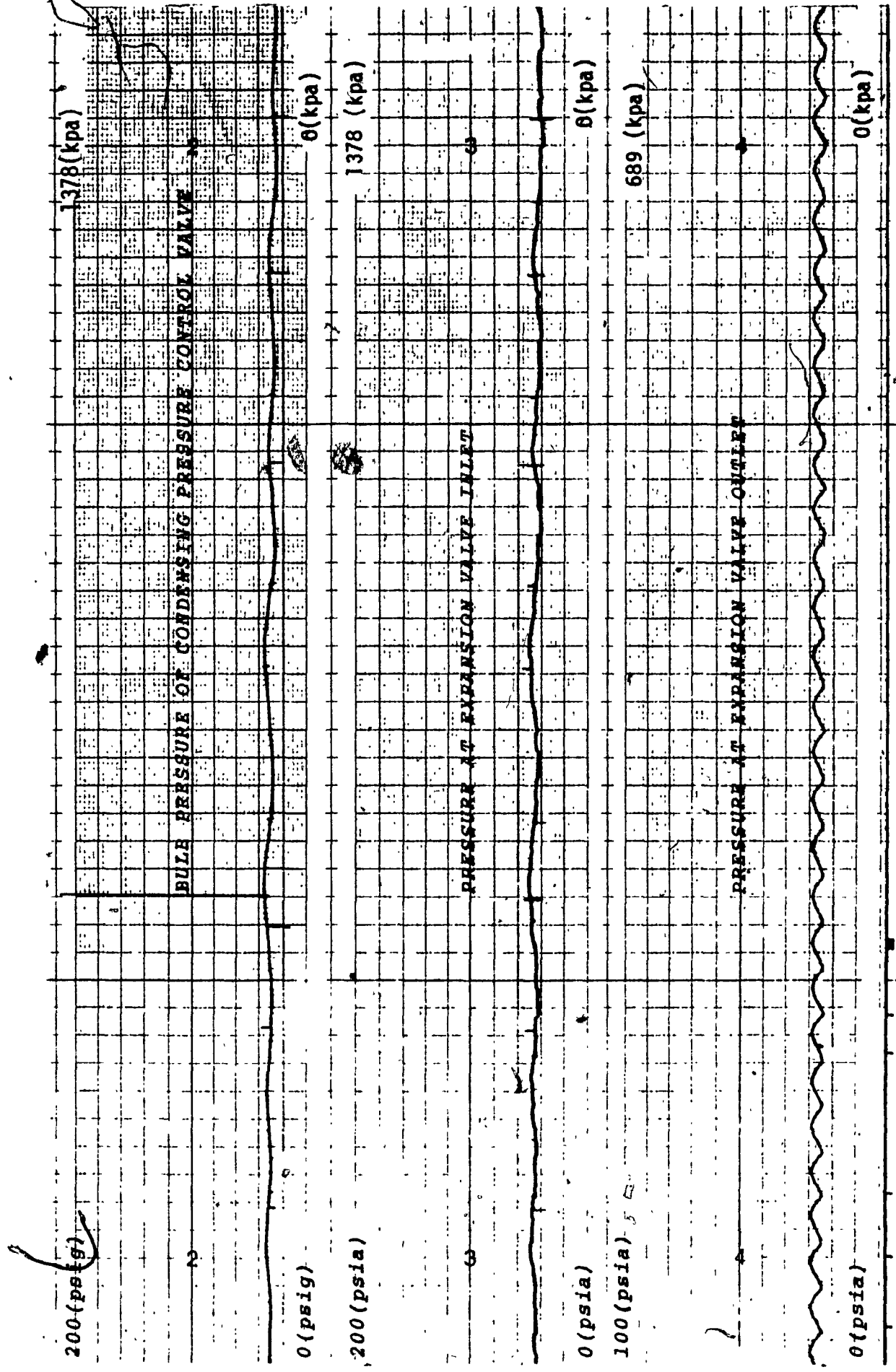


Fig. 22 Modified test system pressure recording.

APPENDIX I

COMPUTER PROGRAM LISTING.

PROGRAM FNECON 73/172 0PT=1 FIN 4.7-470 79/04/82. 18.47.06 PAGE 14

```

1  PROGRAM FNECON (INPUT,OUTPUT)
   DIMENSION OFA(40,3),DELTAH(60),PWR(60,3),R(60),HVOL(60),N(40)
   1,PVHC(60,3)
   DIMENSION SHR(40),HVOLC(40),QFAC(40)
   DIMENSION PFCO(60)
   DIMENSION COP(40),HC(60),PWIN(60)
   INTEGER RF,RFRS,PP,PN,CC
   REAL N,M
   REAL K
   REAL NI,N2
   REAL KKK
   REAL WPC1,WPC2,WPC,WPC2
   REAL K1,K2
   READ 1,NN,EP,CC
   1 FORMAT(13)
   PRINT 1,NN,EP,CC
   READ 4,VS,AS,AD,M,TS,DELTA1,DELTA2
   4 FORMAT(7F7,2)
   PRINT 4,VS,AS,AD,M,TS,DELTA1,DELTA2
   READ 5,PCRS,PFRS
   PRINT 5,PCRS,PFRS
   5 FORMAT(2F6,2)
   READ 10,((QEA(I,J),J=1,3),I=1,M)
   10 FORMAT(3F8,2)
   READ 7,RF,RFRS
   7 FORMAT(213)
   PRINT 7,RF,RFRS
   VS=COMPRESSOR SUPT VOLUME
   AS=SUCTION VALVE PORT AREA(SC.INCHES)
   AD=DISCHARGE VALVE PORT AREA(SC.INCHES)
   TS=AMOUNT OF SUPERHEAT TO COMPRESSOR
   DELTA1=PRESSURE DROP FROM EVAPORATOR INLET TO COMPRESSOR
   DELTA2=PRESSURE DROP FROM COMPRESSOR TO CONDENSER OUTLET
   PWR(1,3)=POWER INPUT FROM COMPRESSOR PERFORMANCE CHART(WATTS)
   PWR(1,2)=EVAPORATING TEMPERATURE (DEGREES F)
   PWR(1,1)=CONTENSING TEMPERATURE (DEGREES F)
   QEA(1,3)=EVAPORATOR FRICTION RATE ACTUAL(RTU/HRI)
   QEA(1,2)=EVAPORATING TEMPERATURE (DEGREES F)
   QEA(1,1)=CONDENSING TEMPERATURE (DEGREES F)
   RF=REFRIGERANT TO BE USED
   RFRS=REFRIGERANT USED IN BLANKED SUCTION TEST
   RORS=PCRS/PFRS
   RORS=COMPRESSION RATIO OBTAINED IN BLANKED SUCTION TEST
   TCRS=TSAT(RFRS,PCRS)
   TERS=TSAT(HCIS,PFRS)
   SCT=STABILIZED CVL INNER TEMP. AFTER EXPN. PRSS. IN A
   SCT=70.0
   CALL SPHT(HFRS,SCT,PFRS,CV,CP,CAPMA,SONIC)
   SHRUS=GAMMA
   CFFRS=1.0/((RORS**1.0/SHRUS))-1.0)
   IF (HFRS,EO,RF) GO TO 20
   CFFRS=EFFECTIVE CLEARANCE FROM BLANKED SUCTION TEST
   WITH REFRIGERANT USED IN BLANKED SUCTION TEST
   NR=NF
   CALL SPHT(INR,TFBS,PFRS,CV,CP,GAMMA,SONIC)
   SHPX=GAMMA
   RO=((CFFRS*1.0)/(CFFRS**SHRX))

```


115	PROGRAM FNECTN 73/172 OPT=1 NR=RF IF=QEA(1,2) CALL SATPRP(INR,TF,PSAT,VF,VG,HF,HFG,HG,SF,SG) H1SV=HG P1SV=PSAT P1=P1SV-DFLTAP1 C H1SV=ENTHALPY OF SATURATED VAPOR AT EVAPORATING TEMPERATURE C H2SL=ENTHALPY OF SATURATED LIQUID AT CONDENSING TEMPERATURE TFF=QEA(1,1) CALL SATPRP(INR,TFF,PSAT,VF,VG,HF,HFG,HG,SF,SG) P2SL=PSAT H2SL=HF P2=P2SL-DFLTAP2 DELTAH(1)=H1SV-H2SL TSFC=65.0 TSFC=SUPERHEATED GAS TEMPERATURE ENTERING COMPRESSOR CALL VAPOR(INR,TSEC,P1,VVAP,HVAP,SVAP) SVFC=VVAP DENSEC=1./SVFC HVOL=VOLUME TRIC EFFICIENCY HVOL(1)=ICA(1,3)*.961/(VS*DENSEC*DELTAH(1)) R(1)=(P2SL-DFLTAP2)/(P1SV-DFLTAP1) R=COMPRESSION RATIO PRINT 9,R(1),CLFF,HVOL(1) FORMAT(3F10.4) C=1.-HVOL(1)*CEFF IF(G.LT.0)GO TO 41 IF(R(1).LT.0)GO TO 41 IF(CEFF.LT.0)GO TO 41 A=ALOG(R(1)) B=ALOG(1.-HVOL(1)*CEFF) C=ALOG(CEFF) N(1)=A/(H-L) GO TO 51 41 N(1)=0. 51 NP=P2-P1 TTF=TSEC DO 102 J=1,10 K=J/10. AP=(K*NP-P1)/(K-.1)*DP*P1 PPP=P1*(K-.1)*NP CALL SPHT(INR,TTF,PPP,CV,CP,GAMMA,SONIC) SHRXX=GAMMA T2=GT*(RPP*(SHRXX-1.0)/SHRXX) TTF=T2-459.7 102 CONTINUE CALL VAPOR(INR,TTF,P2,VVAP,HVAP,SVAP) H2=HVAP CALL VAPOR(INR,TSEC,P1,VVAP,HVAP,SVAP) H1=HVAP COP(1)=DELTAH(1)/(H2-H1) CALL SPHT(INR,TSEC,P1,CV,CP,GAMMA,SONIC) XX=GAMMA
120	
125	
130	
135	
140	
145	
150	
155	
160	
165	
170	

	FUNCTION SPVOL	73/172	OPT=1	FIN 4.7.470	79704/02. 18.47.06	PAGE 2
60						
65						
70						
75						
80						
85						
90						
95						

ES43=3.4FS4
ES44=4.4FS4
FS45=5.4FS4

COMPUTE INITIAL ESTIMATE OF "M" FROM TOTAL GAS LAW
VN=1/(1+PPSIA)

ITER=0
COMPUTE "M" TO WITHIN 1.E-08 BY NEWTON ITERATION
1 ITER=ITER+1
IF (ITER.GT.30) GO TO 998

V=VN

V2=V**2
V3=V**3
V4=V**4
V5=V**5
V6=V**6

EMV=EXP(-ALPHA*(1+V**R(1)))

GO TO (2,3),1

2 F=FS1-FS2/V-E53/V2-E54/V3-E55/V4-FS6/V5-E57*EMV
FV=LS2/V2-E432/V3-FS43/V4-E554/V5-E565/V6-E57 *ALPHA(1)*EMV
GO TO 4

3 EM2V=EMV**2

F=FS1-FS2/V-E53/V2-E54/V3-E55/V4-FS6/V5-E57*EM2V/(FNAV*CPR(1))
1-12*CPR(1))/(FNAV*CPR(1))**2
4 VN=V-F/FV

IF (ABS((VN-V)/V).GT.1.E-08) GO TO 1

SPVOL=VN*H(1)

RETURN

PRINT FROM MESSAGE IF

NR NOT EQUAL TO 12,22,OR 502

IF IS LESS THAN OR EQUAL TO ZERO DEGREE R

IF IS LESS THAN 1FSAT CORRESPONDING TO PSAT-PPSIA

PPSIA IS LESS THAN OR EQUAL TO ZERO

4 MORE THAN 30 ITERATIONS ARE NEEDED

998 SPVOL=VN*R(1)

PRINT 9

RETURN

999 SPVOL=0

PRINT 9

9 FORMAT(37H ERROR IN CALLING SUBROUTINE -SPVOL)

RETURN

END

SURRECUTING SATPOP		73/172 OPT=1	FIN 4.74470	79/04/02 18.47.06	PAGE 2
60	C	1	3.32662E-04,2.25540PF-04,2.996802E-04,-2.413896F-07,		
		2	-6.509607F-08,-1.409043E-07,6.7236E-11,0.2.210AA1E-11,		
		3	0.0.0.0.0.0.257.341.64.058511/		
	C		ENTHALPY AND ENTROPY OF VAPOR CONSTANTS		
		DATA	X,Y/Z39.55655122,62.4009,35.308,-0.0165379361,-0.0453335,		
		1	-0.0744/		
	C		MICELLANEOUS CONSTANTS		
		DATA	TFRJ,LE10,LE10E/459.7,459.69,459.67,0.185053,2.307585093,		
		1	0.434294419/		
	C		ASSIGN "H" ACCORDING TO "NR"		
		I=0			
		IF (NR.EQ. 12) I=1			
		IF (NR.EQ. 22) I=2			
		IF (NR.EQ.502) I=3			
		IF (I.EQ.0) GO TO 999			
	C		CONVERT "H" TO "H" AND CHECK VALUE		
		T=TF+TFR(I)			
		IF (T.LE.0.0) GO TO 999			
	C		COMPARE T WITH TC(I)		
		IF (T.GT.TC(I)) GO TO 999			
	C		CALCULATE "PSAT"		
		GO TO (101,15,1)			
80		10	PSAT=10.0*(AVP(I)+RVP(I)/T+CVP(I)*ALOG10(T)+DVP(I)*T)		
		GO TO 12			
		11	PSAT=10.0*(AVP(I)+RVP(I)/T+CVP(I)*ALOG10(T)+DVP(I)*T+EVP(I)*		
		1	((FVP(I)-T)/T)*ALOG10(FVP(I)-T))		
	C		CALCULATE "VGM"		
		12	VG=SPVUL(MF,IF,PSAT)		
	C		CALCULATE "VFM"		
		GO TO (1,2,2)*I			
		1	TCM=TC(I)-T		
		VF=1.0/(AL(I)+RI(I)*TCM+CL(I)*TCM*(1./2.)*DL(I)*TCM*(1./3.)*			
		1	EL(I)*TCM*(2.))		
		GO TO 3			
		2	TRI=1.-T/TC(I)		
		VF=1.0/(AL(I)+RI(I)*TRI*(1./3.)*CL(I)*TRI*(2./3.)*DL(I)*TRI*(
		1	EL(I)*TRI*(4./3.))		
	C		CALCULATE "HFGM" BY CLAUSIUS CLAPIRON EQUATION		
		3	GO TO (31,32,32)*I		
		31	HFG=1000*(VFM-TR*PSAT)/TC(I)*RVP(I)+T+CVP(I)/T*E10+DVP(I)*T+J		
		GO TO 33			
		32	HFG=1000*(VFM-PSAT)/TC(I)*RVP(I)+T+CVP(I)/T*E10+DVP(I)*T-		
		1	EVPI(I)*E10*(FVP(I)*ALOG10(FVP(I)-T)/T)+J		
	C		SFG=HFG/T		
		33	CALCULATE "HGM" AND "HSCM"		
		T2=T+2			
		T3=T+3			
		T4=T+4			
		VR=VG-R(I)			
		VR2=2.*VR+2			
		VR3=3.*VR+3			
		VR4=4.*VR+4			
		KTDTC=K(I)*T/TC(I)			
		KTDTC=EXP(1-KTDTC)			
		HMAV=FXPL-ALPHA(I)*VG			
		H1=ACV(I)*1+NCV(I)*T2/2.*CCV(I)*T3/3.*DCV(I)*T4/4.-FCV(I)/T			
		H2=J+PSAT*VG			
105					
110					

SUBROUTINE SATPRP		73/172 OPT=1	FIN 4.7.470	79/84/02.18.47.06	PAGE 3
115		H3=A2(1)/VR.A3(1)/VR2.A4(1)/VR3.A5(1)/VR4 H4=C2(1)/VR.C3(1)/VR2.C4(1)/VR3.C5(1)/VR4 S1=ACV(1)*ALOG(1)*RCV(1)*I*CCV(1)*I2/2*DCV(1)/I2*YI2)			
120		S2=JPR(1)*A1*OG(VR) S3=R2(1)/VR.R3(1)/VR2.R4(1)/VR3.R5(1)/VR4 S4=H4 GO TO 16.4.5).I 4 H3=H3.A6(2)/ALPHA(2)*ENAV S3=S3.R6(2)/ALPHA(2)*ENAV GO TO 4			
125		5 H0=1./ALPHA(3)* (ENAV-CPR(3)*ALC01)*ENAV/CPR(3)) H3=H3.A6(3)*H0 H4=H4-C6(3)*H0 S3=S3.R6(3)*H0 S4=S4-C6(3)*H0			
130		6 H0=H1*H2-JPH3*.JPKTDTIC(L)*KTDTIC)*H4*X(1) SG=S1*S2-JPH3*.JPKTDTIC(K(1)/TC(1)*S4*Y(1) C CALCULATE "NEW" AND "SEW" HF=H0-HFG SF=SG-SFG RETURN			
135		C PRINT ERROR MESSAGE IF C NR NOT EQUAL TO 12.22.502 C IF IS LESS THAN OR EQUAL TO ZERO DEGREE R C IF IS GREATER THAN THE CRITICAL TEMPERATURE 999 PRINT 1000 1000 FORMAT(3RH ERROR IN CALLING SUBROUTINE -SATPRP-) RETURN END			
140					

SURROUTINE VAPOR		73/172 OPT=1	FIN 4.7.470	79/04/02. 10.47.06	PAGE 1
1	C	SURROUTINE VAPOR (NR,TF,PPSIA,VVAP,HVAP,SVAP)			
	C	PURPOSE			
5	C	TO EVALUATE THE THERMODYNAMIC PROPERTIES			
	C	OF THE SUPERHEATED VAPOR PHASE			
	C	OF REFRIGERANT 12.22.504			
	C	GIVEN THE TEMPERATURE AND PRESSURE			
10	C	DESCRIPTIONS OF PARAMETERS			
	C	INPUT			
	C	NR - REFRIGERANT NUMBER (12.22.502)			
	C	TF - TEMPERATURE (F)			
	C	PPSIA - PRESSURE (PSIA)			
	C	OUTPUT			
15	C	VVAP - SPECIFIC VOLUME OF VAPOR (CU FT/LB)			
	C	HVAP - ENTHALPY OF VAPOR (BTU/LB)			
	C	SVAP - ENTHALPY OF VAPOR (BTU/LB R)			
20	C	REMARKS			
	C	FUNCTION SURPROGRAM SPVOL CALLED BY THIS SURROUTINE			
	C	FUNCTION SURPROGRAM TSAT CALLED BY THIS SURROUTINE			
	C	DIMENSION AND TYPE STATEMENTS			
25	C	1 DIMENSION NR(3),R(3),A2(3),B2(3),C2(3),A3(3),R3(3),C3(3),A4(3),			
	C	B4(3),C4(3),A5(3),R5(3),C5(3),A6(3),R6(3),C6(3),K(3),			
	C	ALPHA(3),CPR(3),TC(3),TFR(3)			
	C	2 DIMENSION ACV(3),RCV(3),CCV(3),DCV(3),FCV(3),FCV(3)			
	C	DIMENSION X(3),Y(3)			
	C	REAL J,K,KINIC,LF(0.1,10E			
30	C	CONSTANTS			
	C	EQUATION OF STATE CONSTANTS			
	C	DATA R,H,A2,B2,C2,A3,R3,C3,A4,B4,C4,A5,B5,C5,A6,R6,C6,K,ALPHA,CPR/			
35	C	1 0.008734,0.124098,0.096125,0.0065093886,0.002,0.00167,			
	C	-3.4097273,4.353547,-3.261334,0.001594348,0.002407252,			
	C	0.0020576287,-56.7627671,-44.066688,-24.24879,0.00023944654,			
	C	-0.017464,0.074866748,-1.879612431E-05,7.62789E-05,			
	C	-0.8619131E-05,1.311399084,1.483763,0.33274779,			
	C	-0.00548737007,0.002310142,-8.5765677E-04,0.0003,0.005723E-06,			
40	C	7.0240549E-07,0.0002412368,0.0003,0.00044E-05,			
	C	A.8368667E-06,3.468834E-05,5.35565E-06,-7.9168095E-09,			
	C	-2.54900678E-05,-1.845051E-04,-3.7167231E-04,0.0001,0.363787E08,			
	C	1.5370377E09,5.475,4.244,2.000548,2609.0,0.0007,0.0007,TC/			
	C	693.31664,5.619,56/			
45	C	SPECIFIC HEAT AT CONSTANT VOLUME CONSTANTS			
	C	DATA ACV,HV,CCV,OCV,FCV,FCV/0.000945,0.0212036,0.020419,			
	C	1 3.32602E-04,2.25440E-04,2.996802E-04,-2.413896E-07,			
	C	2 -6.509607E-08,-1.409043E-07,6.72363E-11,0.000210661E-11,			
	C	3 0.000,0.000,0.000,0.000,0.000,0.000,0.000,0.000,			
50	C	ENTHALPY AND ENTROPY OF VAPOR CONSTANTS			
	C	DATA X,Y,Z,5545512.62,4009.35,308,-0.016537936,-0.0053335,			
	C	-0.07744/			
	C	MISCELLANEOUS CONSTANTS			
55	C	DATA TFR,J01E10,1.0E/459.7,459.69,459.67,0.185053,2.307585093,			
	C	1 0.4362944819/			
	C	ASSIGN "I" ACCORDING TO "NR"			

SURGEUYNF VAPOR		73/172 NP1=1	79/04/02. 18.47.86	PAGE 2
60		I=0 IF (NR.FO. 12) I=1 IF (NR.FO. 22) I=2 IF (NR.FO. 502) I=3 IF (I.FO.0) GO TO 999		
65		C C CONVERT "TFM" TO "TM" AND CHECK VALUE T=TF+TFR(I) IF (I.E.0.0) GO TO 999		
70		C C CALCULATE "TFSAT" AND COMPARE WITH "TFM" TFSAT=TSAT(MH,PPSTA) IF (TF.LT.TFSAT) GO TO 999		
75		C C CHECK "PPSTIA" IF (PPSTA.LE.0.0) GO TO 999		
80		C C CALCULATE "VVAP" VVAP=SPVOL (NR,TF,PPSTA)		
85		C C CALCULATE "MVAP" AND "MSVAP" T2=T0+2 T3=T0+3 T4=T0+4 VR=VVAP-R(I) VR2=2.*VR+2 VR3=3.*VR+3 VR4=4.*VR+4 KTDTIC=K(I)*T/TC(I) EKTDIC=EXP(-KTDTIC) EMV=EXP(-ALPHA(I)*VVAP) H1=ACV(I)*1+RCV(I)*T2/2+CCV(I)*T3/3+OCV(I)*T4/4+FCV(I)/T H2=JPPSTIA*VVAP H3=A2(I)/VR+A3(I)/VR2+A4(I)/VR3+A5(I)/VR4 H4=C2(I)/VP+C3(I)/VR2+C4(I)/VR3+C5(I)/VR4 S1=ACV(I)*A1+OG(I)*RCV(I)*T+CCV(I)*T2/2+OCV(I)*T3/3+FCV(I)/T2+T2 S2=JPH(I)*ALOG(VR) S3=B2(I)/VR+B3(I)/VR2+B4(I)/VR3+P5(I)/VR4 S4=H4		
90		C C GO TO 6		
95		C C GO TO 6		
100		C C GO TO 6		
105		C C GO TO 6		
110		C C GO TO 6		

SURROUINF VAPOR		73/172	NP1=1	FIN 4.7.476	79/04/02. 18.47.66	PAGE 3
115	C	PPSIA IS LESS THAN OR EQUAL TO ZERO				
		999 PRINT 1000				
		1000 FORMAT(37H ERROR IN CALLING SURROUINF -VAPOR--)				
		RETURN				
		END 6				

CURRICULUM SPRT		73/1/2 OPT=1	FIN 4.7.470	79/06/02. 18.47.06	PAGE 2
60	C	T=TF*TFRI(1) IF (T.LF.0.0) GO TO 999 CALCULATE "IFSAT" AND COMPARE WITH MTFM IFSAT=TSAT(MR,PPSIA) IF (TF.LT.TF*CAT) GO TO 999 C CHECK MPPSIA IF (PPSIA.LE.0.0) GO TO 999 C CALCULATE "VVAP" VVAP=SPVOL(MR,TF,PPSIA) CALCULATION OF DERIVATIVES V1=VVAP-B(1) V2=V1*V1 V3=V2*V1 V4=V3*V1 V5=V4*V1 V6=V5*V1 ERTTC=EXP(-K(1)*T/TC(1)) GO TO (1,2,3),I 1 FOPDV=0. FOPDT=0. GO TO 4 2 FOPDV=-ALPHA(1)*EXP(-ALPHA(1)*VVAP)/(A6(1)*RA(1)*T) FOPDT=H6(1)*EXP(-ALPHA(1)*VVAP) GO TO 4 3 FOPDV=-ALPHA(1)*(EXP(-3.*ALPHA(1)*VVAP)+2.*CPR(1)*EXP(-2.* ALPHA(1)*VVAP))/EXP(-2.*ALPHA(1)*VVAP)+2.*CPR(1)*EXP(- -ALPHA(1)*VVAP)+CPR(1)*2*(A6(1)*B6(1)*T*CA(1)*ERTTC)/ FOPDT=(A6(1)-K(1)*C6(1)*ERTTC/TC(1))*EXP(-2.*ALPHA(1)*VVAP)/ (EXP(-ALPHA(1)*VVAP)+CPR(1)) 4 DPNV=-R(1)*V2+2.*(A2(1)*B2(1)*T+C2(1)*ERTTC)/V3-3.*(A3(1)*B3(1)* T+C3(1)*ERTTC)/V4-4.*(A4(1)*B4(1)*T+CA(1)*ERTTC)/V5-5.*(A5(1)* R5(1)*V6+C5(1)*ERTTC)/V6+FOPDV DPN1=P(1)/V6*(R2(1)-K(1)*C2(1)*ERTTC/TC(1))/V2+R3(1)-K(1)*C3(1)* ERTTC/TC(1))/V3+(R4(1)-R(1)*CA(1)*ERTTC/TC(1))/V4+(R5(1)-R(1)* C5(1)*ERTTC/TC(1))/V5+FOPDT GO TO (5,5,10),I 5 FCCV=0. GO TO 15 10 FCCV=C6(1)*EXP(-ALPHA(1)*VVAP)/ALPHA(1)-(C6(1)*CPR(1)/ALPHA(1))* ALOG(1)*EXP(-ALPHA(1)*VVAP)/CPR(1)) C CALCULATE "CM" 15 CM=ACV(1)*HCV(1)*T+C6V(1)*T+2*OCV(1)*T+3*FCV(1)/T+2-(10.185053* K(1)+2*T*ERTTC/TC(1)+2)*(C2(1)/V1+C3(1)/V2+V21*CA(1)/V3+V3) C CALCULATE "CP" 20 CP=CV-0.185053*(FOPDT+2*DPNV) C CALCULATE "GAMMA" GAPMA=CP/CM C CALCULATE "SONIC" SONIC=VVAP*SONIC*1857.3609)*T*DPDT+2*(CM-4633.056*DPDV) RETURN PRINT ERROR MESSAGE IF MR NOT EQUAL TO 12.22 OR 502 IF TS LESS THAN OR EQUAL TO ZERO NEGREE R IF TS LESS THAN TSAT CORRESPONDING TO PSAT=PPSIA PPSIA IS LESS THAN OR EQUAL TO ZERO 999 PRINT 1000			
65	C				
70	C				
75	C				
80	C				
85	C				
90	C				
95	C				
100	C				
105	C				
110	C				

SUBROUTINE SPHT	13212 OPT=1	FIN 4.1-476	19/04/02. 18.47.06	PAGE 3
115	1000 FORMAT(37H ERROR IN CALLING SUBROUTINE -SPHT-)			
	RETURN			
	END			

APPENDIX II

MODIFIED REFRIGERATION SYSTEM

BODY TYPE 'K'



-106-

THERMAL PRESTCOLD LTD.

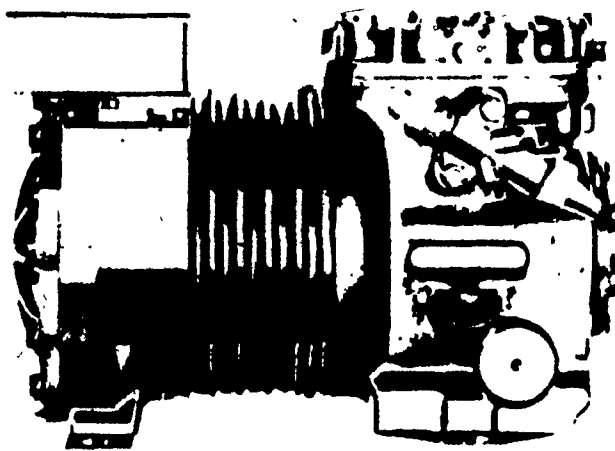
60 Hz

REFRIGERANT R12 R22 & R502

MODEL C-200/K376-G

Compressor data

Speed	1750 rev/min
Bore	1 $\frac{1}{8}$ in
Stroke	1 $\frac{1}{8}$ in
No. of cylinders	2
Displacement	376 ft ³ /hr
Suction valve	$\frac{7}{8}$ in o.d. sweat
Discharge valve	$\frac{1}{2}$ in o.d. flare
Oil charge (USA)	1.8 pints (29 oz)
Net weight	100 lbs



Application

Evaporating temperature range:

R12 -10 °F to + 60°F

R22 -40°F to + 20°F

R502 -40°F to + 20°F

within the limits of condensing temperature and motor limiting conditions indicated on the performance chart.

Compressor cooling

AIR - Minimum flow of 152 m/min (500 ft/min) on discharge side of body.

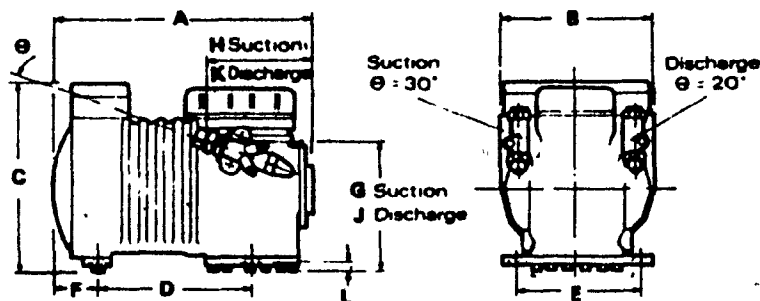
WATER - $\frac{3}{8}$ in o.d. water coil wound on body.

Motor protection

FORM A Temperature and current sensitive self resetting overload cut-out. No external current sensing protection required.

FORM B Temperature and current sensitive self resetting overload cut-out connected at the star point of the motor windings. No external current sensing protection required.

DIMENSIONS



Standard compressor

	A	B	C	D	E	F	G	H	J	K	L	M
mm	360	208	254	208	162	56	181	149	193	137	9	20
in	14 $\frac{1}{16}$	8 $\frac{1}{8}$	10	8 $\frac{1}{16}$	6 $\frac{3}{8}$	2 $\frac{1}{8}$	7 $\frac{1}{8}$	5 $\frac{7}{8}$	7 $\frac{13}{32}$	5 $\frac{13}{32}$	$\frac{11}{32}$	$\frac{23}{32}$

RESILIENT MOUNTINGS (optional) increase height by dimension M

Description	Part No.	No. off
Springs, red, motor end	17/2/1239	2
Springs, red, compressor end	17/2/1239	2
Rubbers, upper	17/2/1055	4
Rubbers, lower	17/2/1056	4

ELECTRICAL DATA

	single phase	three phase		
Voltage	220/240	200/220	440/480	550/600
Phase	1	3	3	3
Frequency, Hz	60	60	60	60
Locked rotor current A	54	44.5	24	15.5
Max. run current A	11.0	7.9	4	3
Start capacitance μ F	120			
Run capacitance μ F	20			
Motor protection	A	B	B	B

OCS
1-26-79

R-502 (85 PSIG GAS CHARGE)

#1 73 PSIG

1/23/79

73 PSIG

BULB AT ROOM AMBIENT (78°F)

#2 74 PSIG

74

LO SIDE PRESSURE INCREASED TO TRIP

R-12 (CROSS AMBIENT FILL)

#1 71 PSIG

1/24/79 71 PSIG

BULB AT ROOM AMBIENT (78°F)

#2 70

70

LOW SIDE PRESSURE INCREASED TO TRIP

#3 71

71

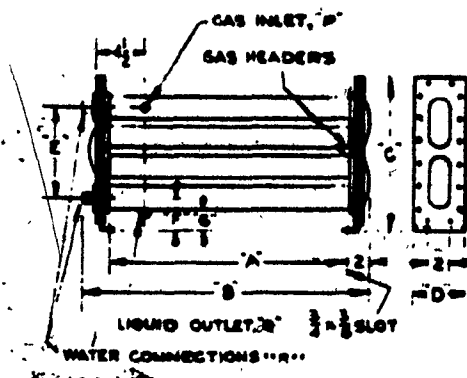
CHARTS BELOW: LO SIDE PSIG HELD, BULB TEMP DECREASING
R-502

#1			#2		
HI SIDE		LO SIDE	HI SIDE		LO SIDE
BULB TEMP.	VAPOR PRESS.	PSIG	BULB TEMP.	VAPOR PRESS.	PSIG
32°F	68 PSIG	60	32.5°F	69 PSIG	60
21	54	45	20.5	53	45
12	43	35	12	43	35
2	33	25	2	33	25

R-12

#1			#2			#3		
HI SIDE		LO SIDE	HI SIDE		LO SIDE	HI SIDE		LO SIDE
BULB TEMP.	VAPOR PRESS.	PSIG	BULB TEMP.	VAPOR PRESS.	PSIG	BULB TEMP.	VAPOR PRESS.	PSIG
51	47 PSIG	40	51	47 PSIG	40	52	48 PSIG	40
41	37	30	41	37	30	42	38	30
35	31	25	35	32	25	35	32	25
23	23	17	25	24	17	25	24	17
14	17	10	12.5	16	10	12.5	16	10

Table 2. Test results of differential pressure controls



SPECIFICATIONS															
Model No.	Nom'l HP	Dimensions, Inches							Connections			Water Pressure Drop psi		Fig.	Ship. Wt. Lbs.
									P	G	R				
		A	B	C	D	E	F	G	O.D. Sweat	O.D. Sweat	F.P.T.	1-1/2 GPM	3 GPM		
K-1 1/2 X	1-1/2	21-3/8	26-1/2	13-1/8	4-3/8	8	3	2	1/2	3/8	1/2	.2	.8	15	42
K-2 X	2	21-3/8	26-1/2	13-1/8	4-3/8	8	3	2	1/2	3/8	3/4	.2	.8	15	45
K-3 X	3	28-5/8	35	13-1/8	4-3/8	8	3	2	5/8	1/2	3/4	.5	2.0	15	55
K-5 X	5	28-5/8	35-1/2	15-3/4	5	9-3/8	4-1/8	3	7/8	5/8	1	.5	1.8	15	75
K-7-1/2 X	7-1/2	28-5/8	35-3/4	17-3/4	5-1/2	10-1/2	4-3/8	3	7/8	7/8	1-1/4	.7	2.5	15	95
K-10 X	10	34-3/4	42-1/4	17-3/4	5-1/2	10-1/2	4-3/8	3	1-1/8	7/8	1-1/4	1.4	4.2	15	113

Table 3. Test unit chiller specifications

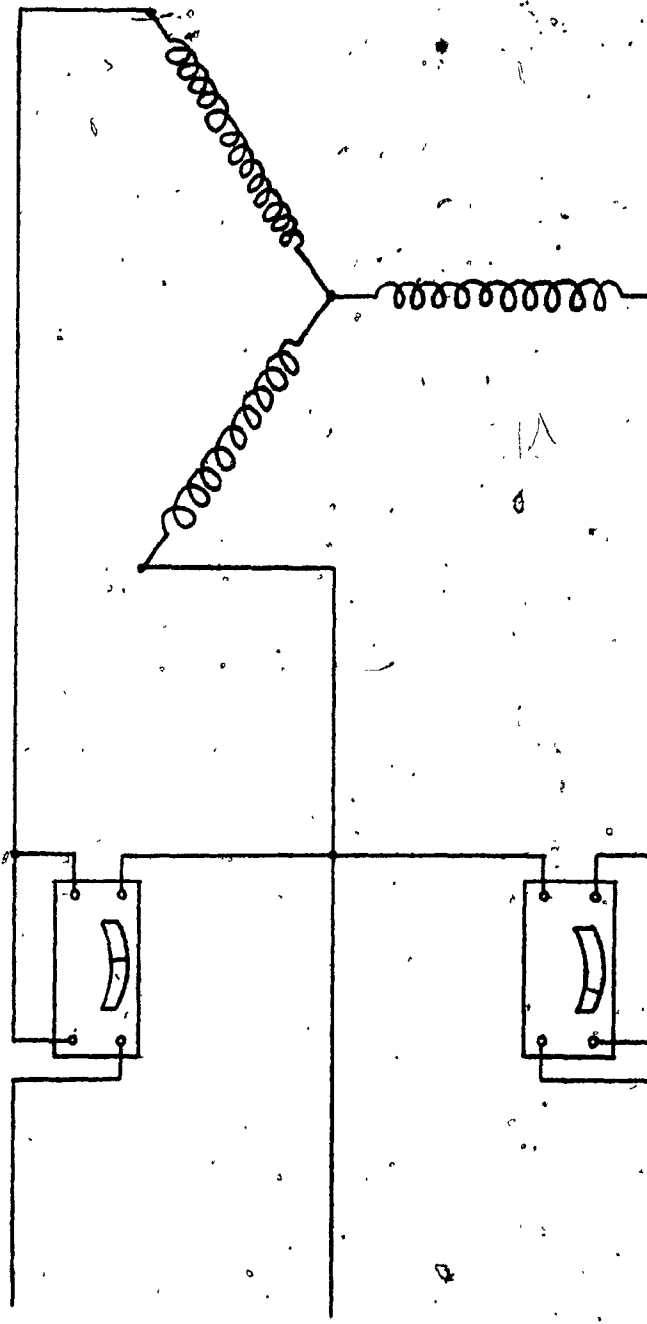
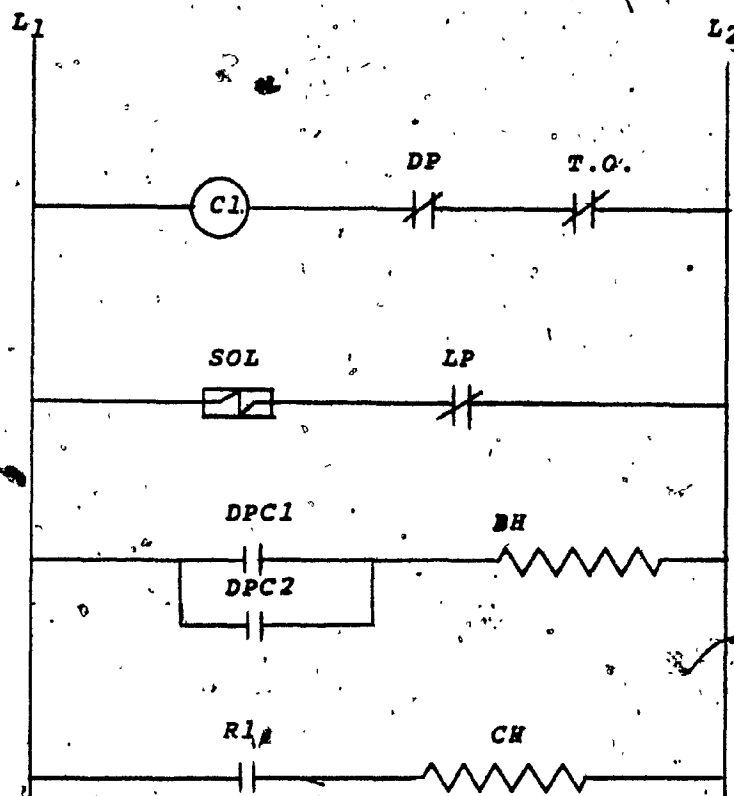


FIG. A1 Test unit watt meter connection



C1=coil of compressor contactor
 DP=dual pressure safety control (high-low pressure control)
 T.O.= thermal overload
 SOL=pump down solenoid
 LP=low pressure control (operating control)
 DPC1=differential pressure control 1
 DPC2=differential pressure control 2
 BH=condensing pressure control bulb heater
 R1=auxiliary contact of compressor contactor
 CH=crankcase heater

FIG. A2 Wiring diagram schematic of modified test unit

APPENDIX III

CHAMBER COOLING SYSTEM DESIGN

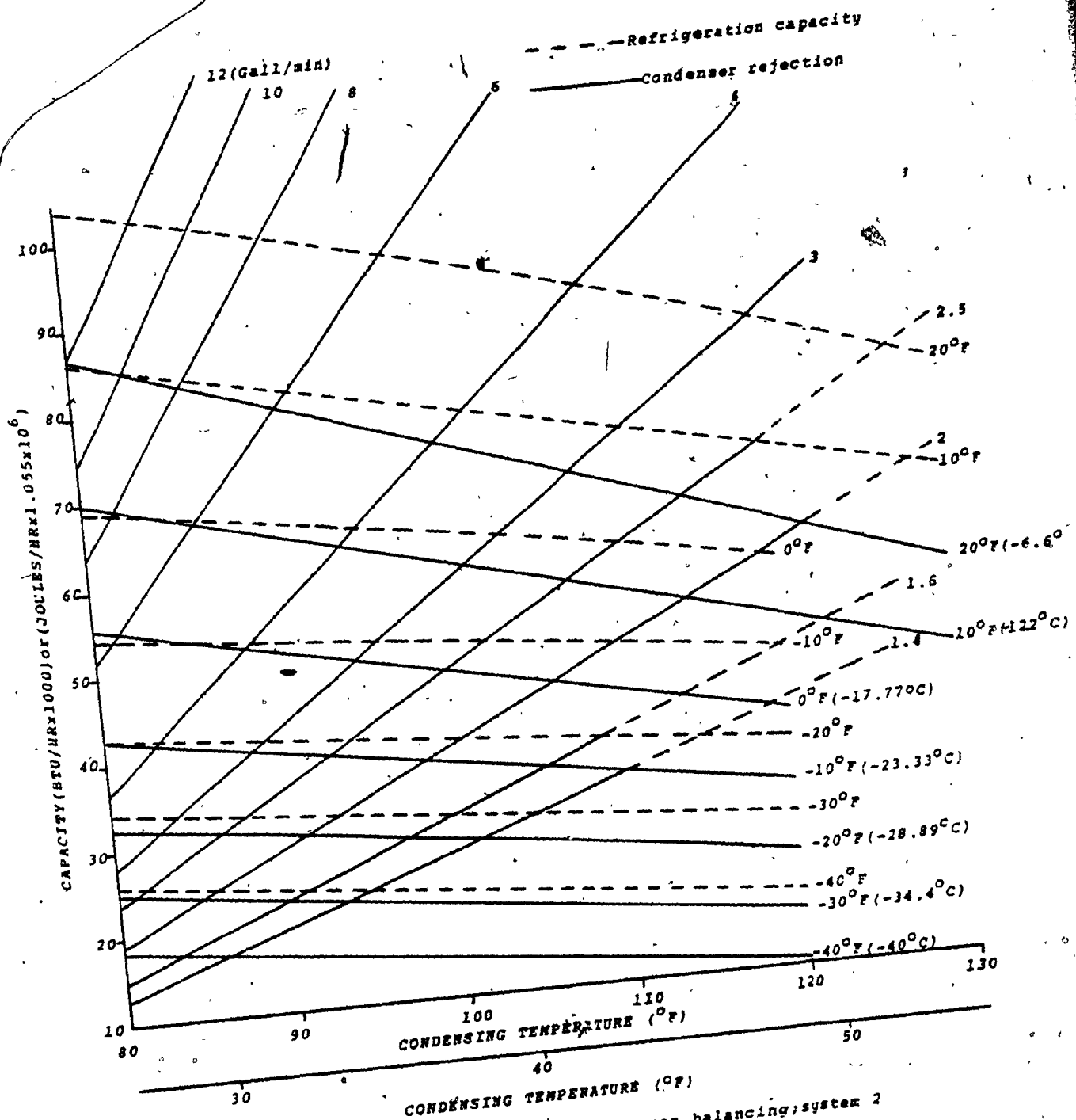


FIG.A3 Chamber cooling system compressor-condenser balancing; system 2

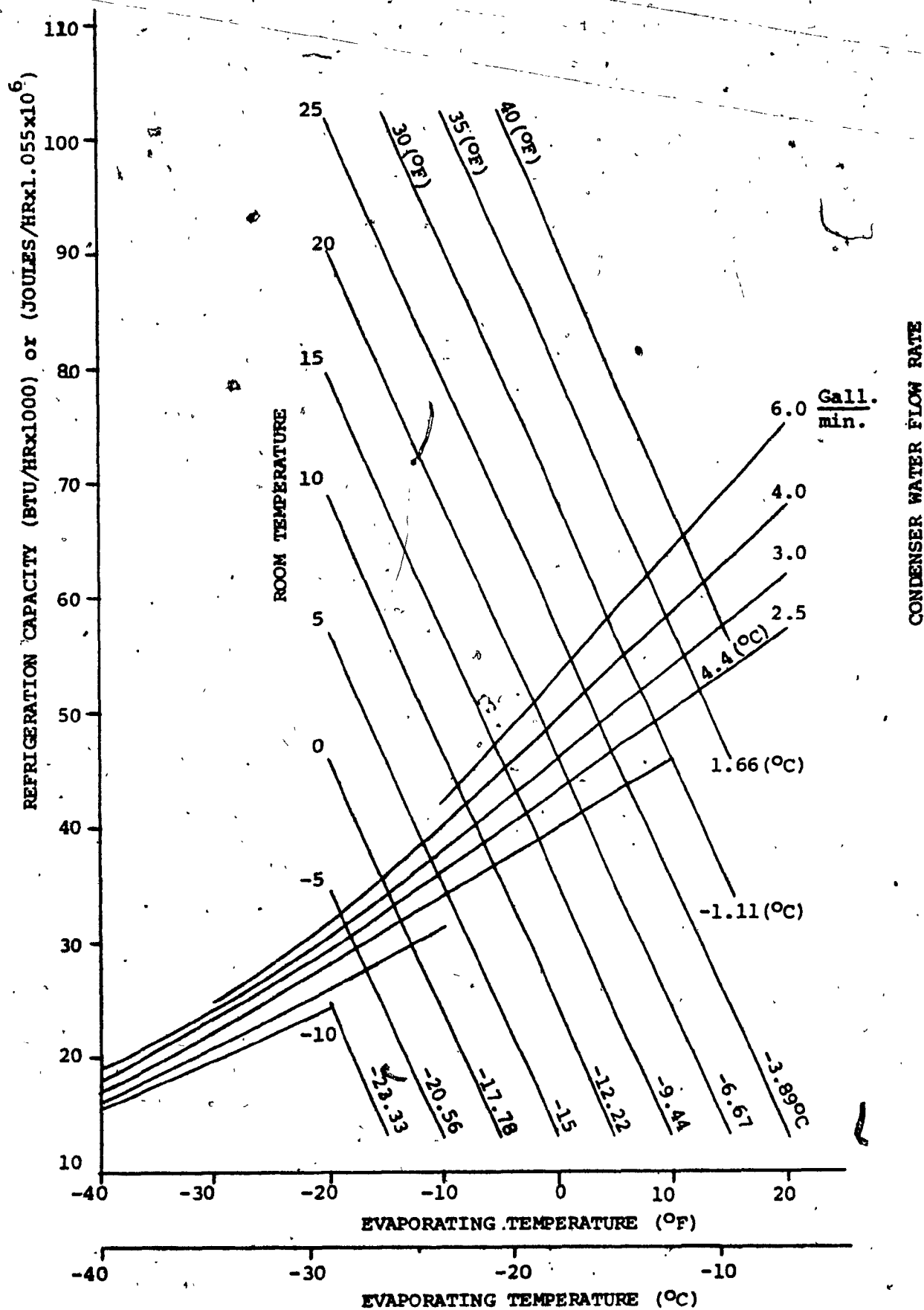


FIG A4 Chamber cooling system compressor-condenser-evaporator.

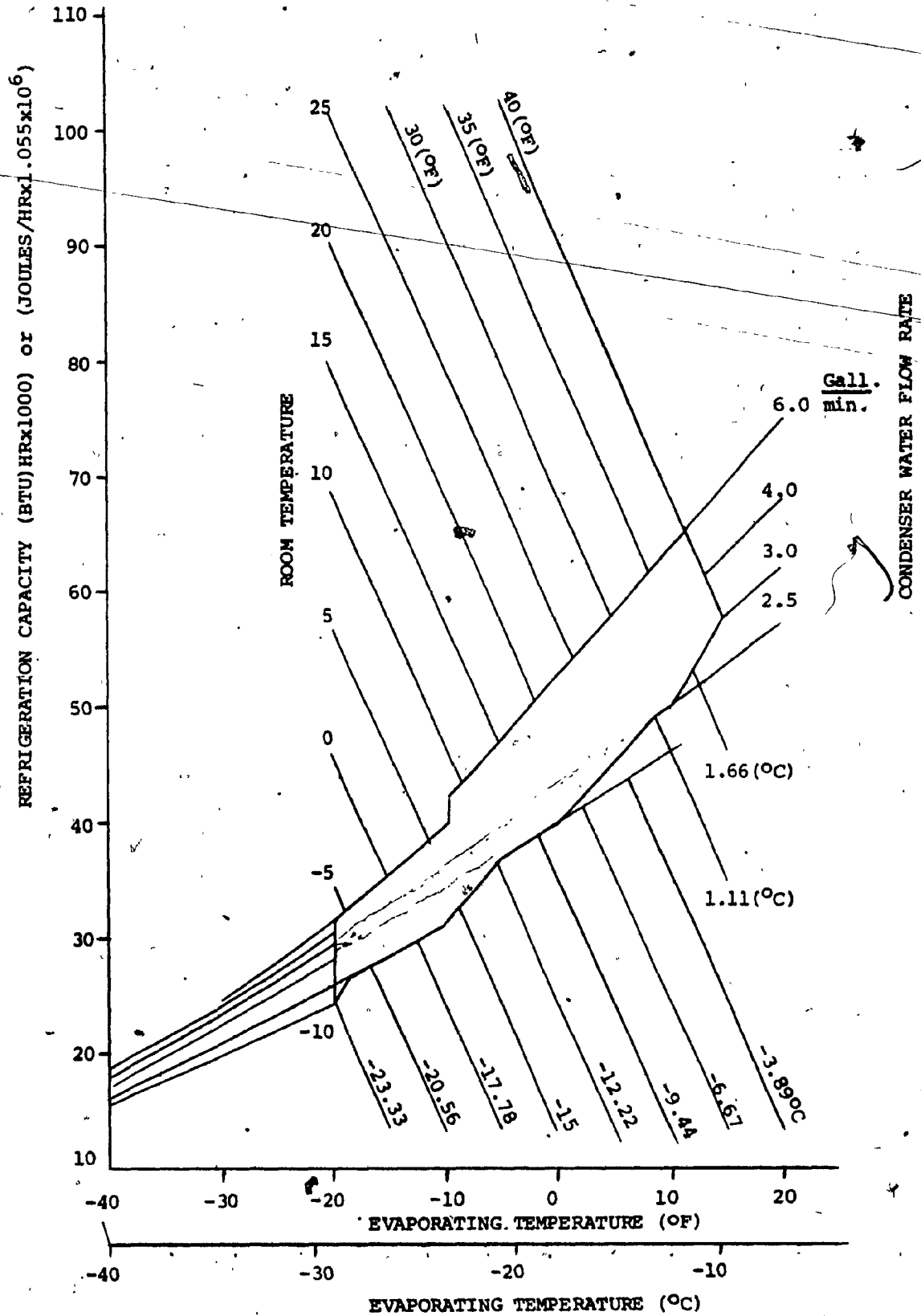


FIG A5 Chamber cooling system operation envelope; system 2.

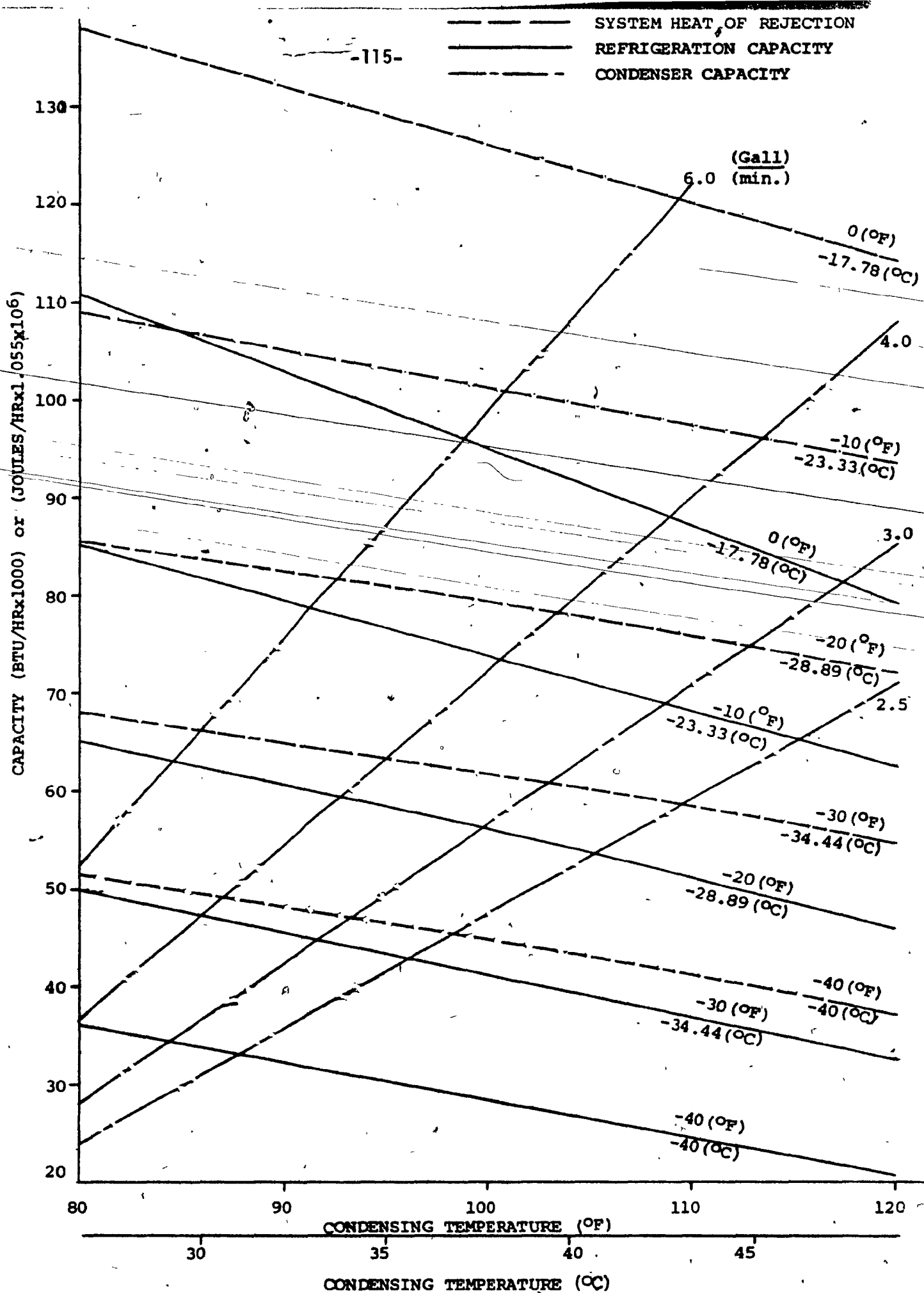


FIG A6 Chamber cooling system compressor-condenser balancing; system 1.

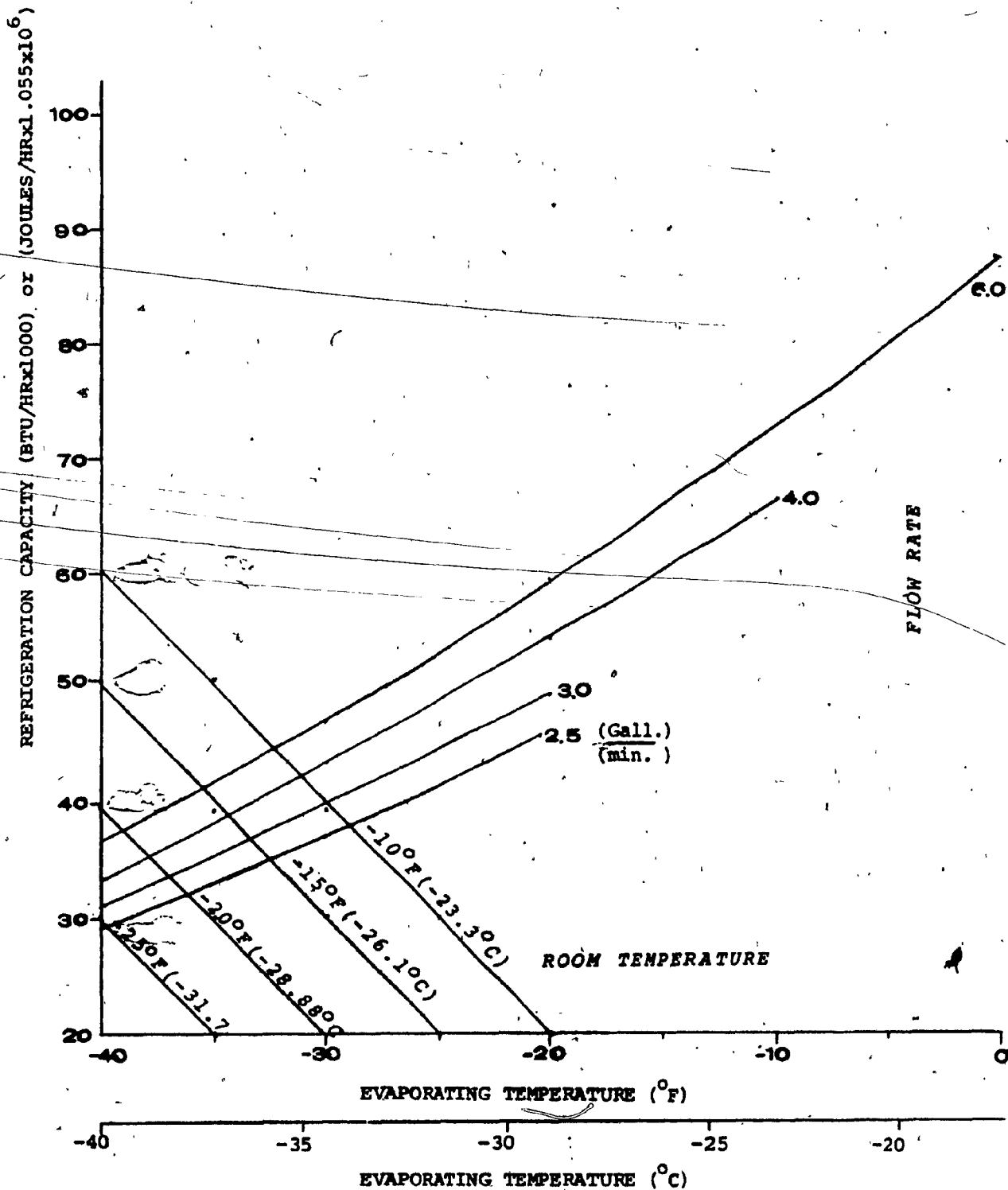


FIG A7. Chamber cooling system compressor-condenser-evaporator balancing; system 1.

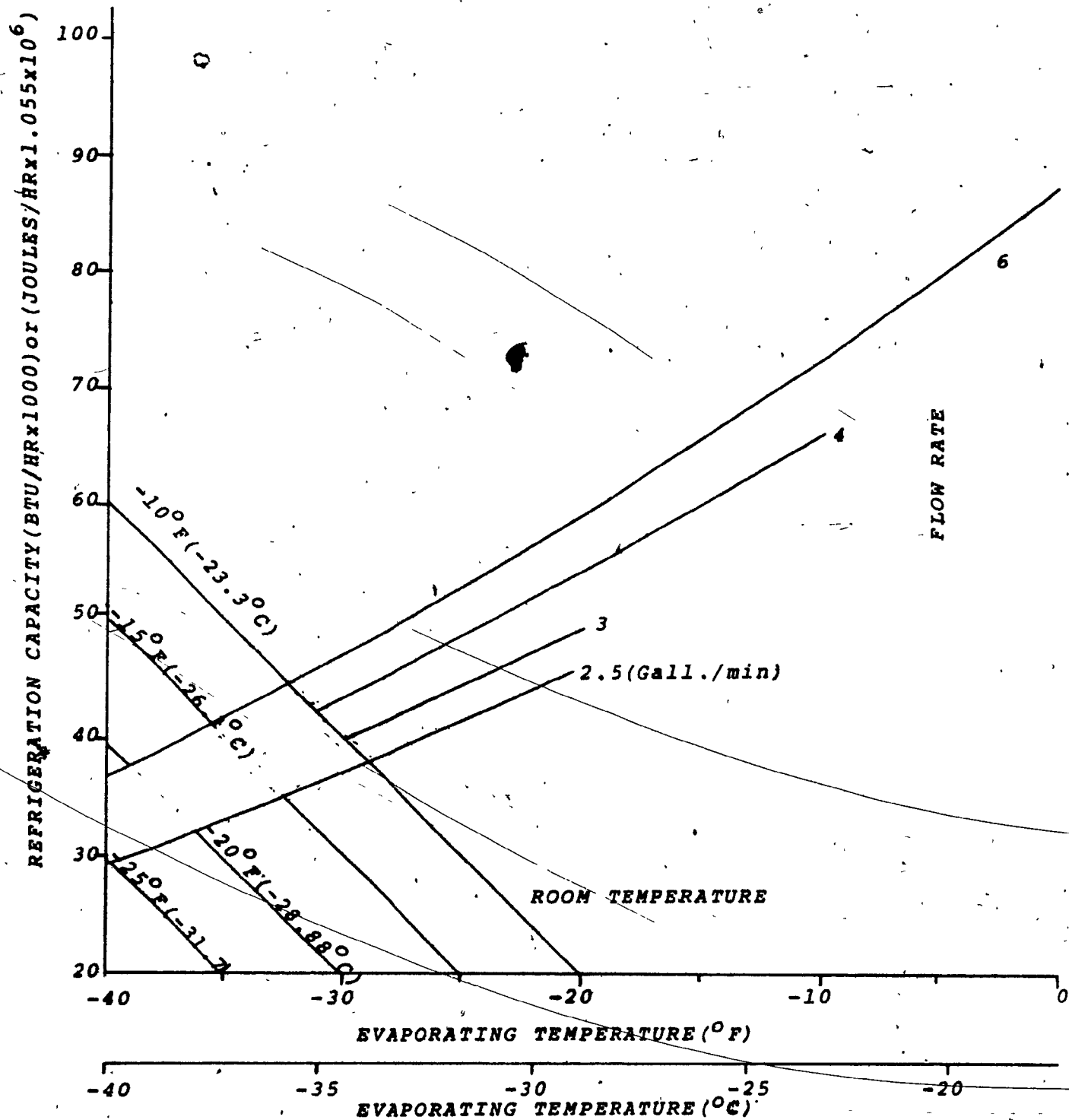
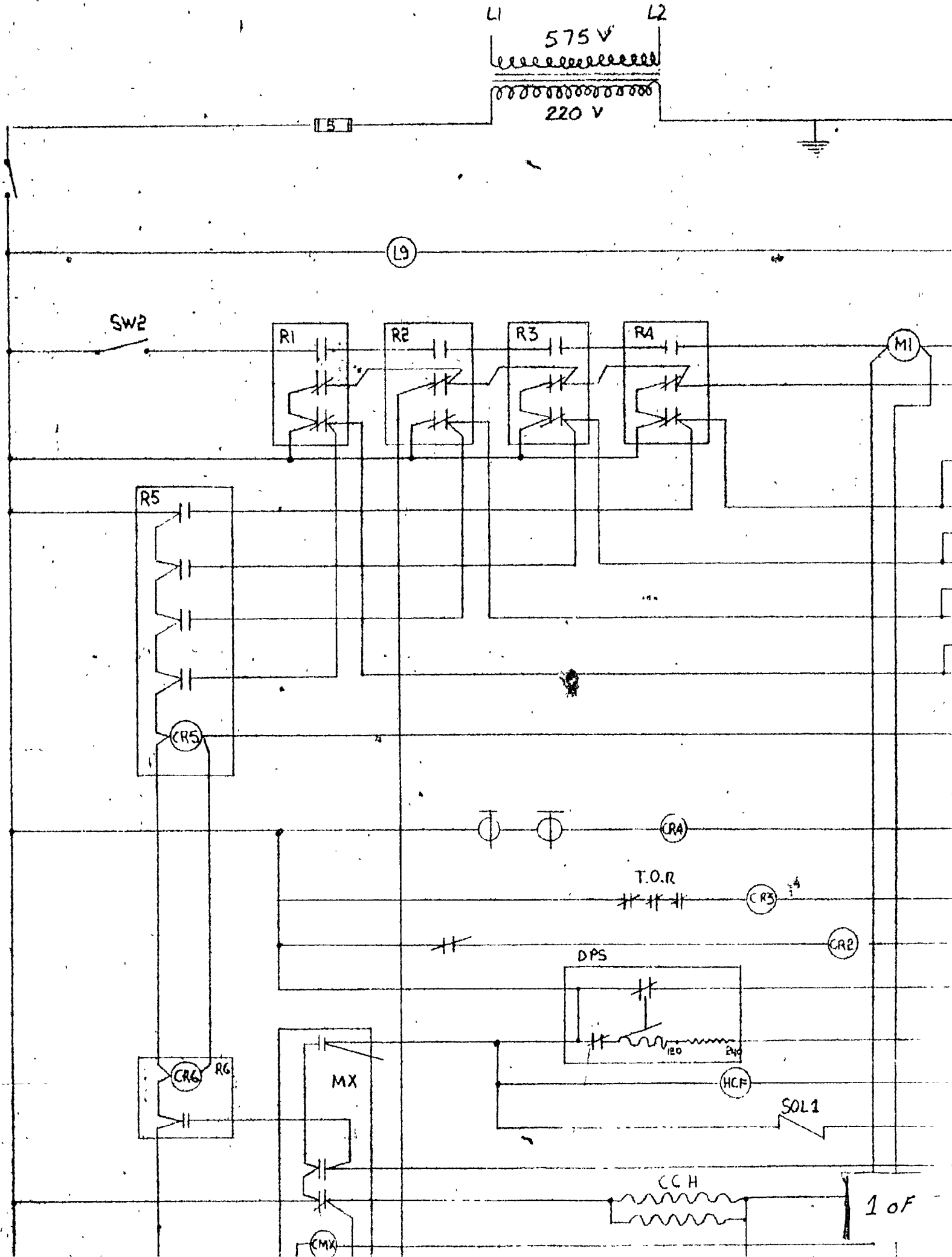
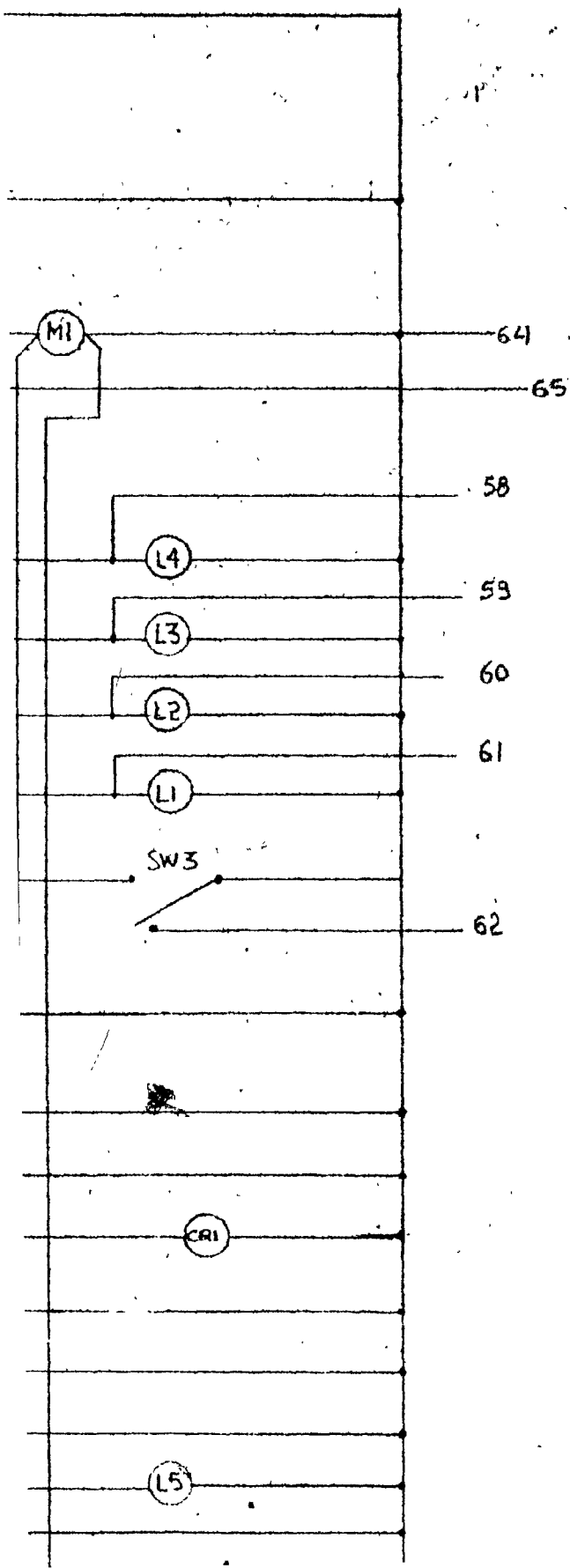


FIG. A8 Chamber cooling system operation envelope, system 1

VI

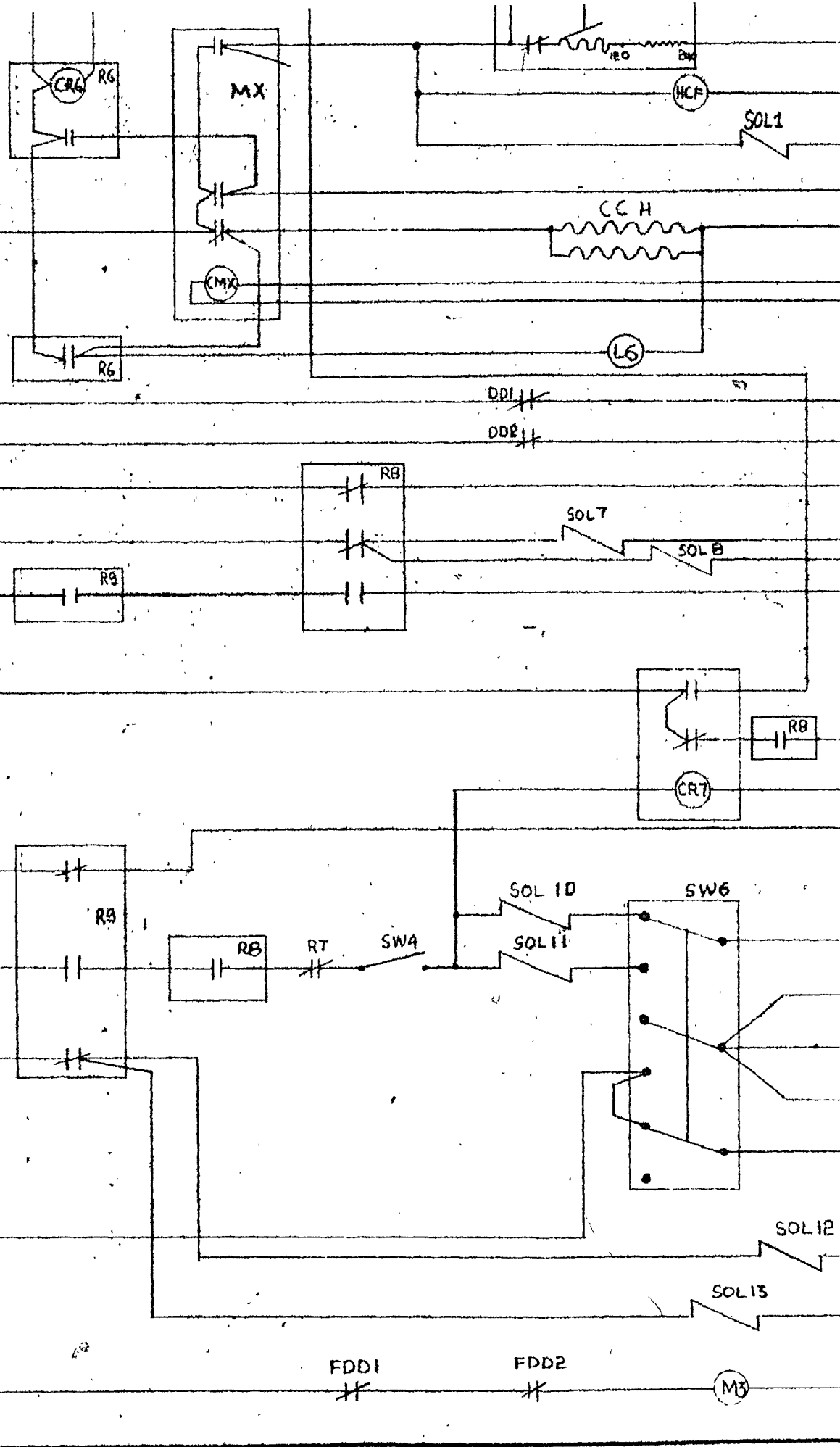


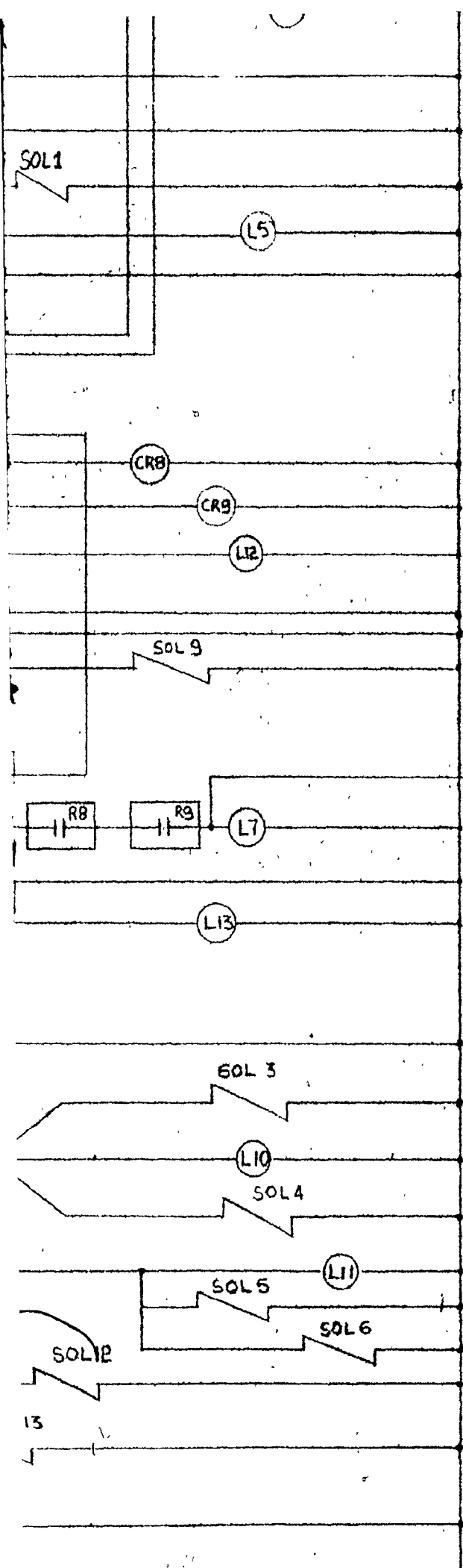


ITEM NO.	CODE
1	A
2	OCN
3	OCN
4	OCN
5	OCN
6	OCN
7	OCN
8	OCN
9	OCN
10	OCN
11	OCN
12	C. 2
13	11
14	1101
15	1101
16	1101
17	1101
18	11
19	11
20	11
21	11
22	11
23	11
24	11
25	11
26	110
27	111
28	111
29	111
30	11
31	11
32	11
33	11
34	OPK
35	PC
36	R1
37	R2
38	R3
39	R4
40	
41	

CODE	DESCRIPTION
A	Alarm remote
CCM	Crankcase heaters
CR1	Coil, oil pressure control
CR2	Coil, pressure control relay
CR3	Coil, thermal overload relay
CR4	Coil, head thermostat relay
CR5	Coil, indicator light test relay
CR6	Coil, indicator light test relay
CR7	Coil, remote alarm relay
CR8	Coil, defrost relay system 1
CR9	Coil, defrost relay system 2
C.T.	Control transformer
F1	Fuse, control circuit
DD1	Fan delay defrost unit 1
DD2	Fan delay defrost unit 2
C.F.	Head cooling fan
TI, 2	Head temperature thermostat
IL1	Indicator light, oil pressure control
IL2	Indicator light, pressure control
IL3	Indicator light, thermal overload relay
IL4	Indicator light, head thermostat
IL5	Indicator light, compressor fan
IL6	Indicator light, crankcase heaters
IL7	Indicator light, pumpdown cycle
IL8	Indicator light, control circuit
IL10	Indicator light, system No. 1
IL11	Indicator light, system No. 2
IL12	Indicator light, defrost system 1
IL13	Indicator light, defrost system 2
M1	Coil, compressor starter
M3	Coil, evaporator fan contactor
MX	Coil, auxiliary condenser compressor starter
OP2	Oil pressure control
PC	Pressure control (high-low)
R1	Relay, oil pressure control
R2	Relay, pressure control
R3	Relay, thermal overload
R4	Relay, head temperature thermostat
R5	Relay, indicator light test
167	Relay, indicator light test

L





15
36
37
38
39
40
41
42
43
44
45
46
47
48
49
50
51
52
53
54
55
56
57
58
59
60
61
62
63
64
65

34	OPS	Oil pressure control
35	PC	Pressure control valve
36	R1	Relay, oil pressure control
37	R2	Relay, pressure control
38	R3	Relay, thermal control
39	R4	Relay, tank level control
40	R5	Relay, control line
41	R6	Relay, control line
42	R7	Relay, control line
43	R8	Relay, control line
44	R9	Relay, control line
45	R10	Relay, control line
46	SW1	Switch, control circuit
47	SW2	Switch, control circuit
48	SW3	Switch, indicator light
49	SW4	Switch, control circuit
50	SW5	Switch, alarm system
51	SW6	Switch, system selector
52	SOL1	Solenoid, oil return line
53		
54	SOL2	Solenoid, capacity control
55	SOL3	Solenoid, capacity control
56	SOL4	Solenoid, capacity control
57	SOL5	Solenoid, capacity control
58	SOL6	Solenoid, liquid line to refrigerant
59	SOL7	Solenoid, hot gas system
60	SOL8	Solenoid, discharge line
61	SOL9	Solenoid, liquid line system
62	SOL10	Solenoid, liquid line system
63	SOL11	Solenoid, hot gas system
64	SOL12	Solenoid, liquid line to refrigerant
65	TOR	Thermal overload relay

8 of 8

REV	DATE	DESCRIPTION	APPROVAL
01	10/1/78	INITIAL DESIGN	
02	10/1/78	CONCEPT DESIGN	
03	10/1/78	WIRING SCHEMATIC	
04	10/1/78	FINAL DESIGN	
05	10/1/78	CONSTRUCTION	
06	10/1/78	TESTING	
07	10/1/78	REVISIONS	
08	10/1/78	FINAL REVIEW	
09	10/1/78	ASSEMBLY	
10	10/1/78	DELIVERY	